UNCLASSIFIED
SECURITY CLASSIFICATION OF THIS PAGE (When Data Entered)

REPORT DOCUMENTATION PAGE		READ INSTRUCTIONS BEFORE COMPLETING FORM
1. REPORT NUMBER AFFDL-TR-74-54	2. GOVT ACCESSION NO.	3. RECIPIENT'S CATALOG NUMBER
4. TITLE (and Subtitle) Final Report On Program to Improve MIL-F-83300		5. TYPE OF REPORT & PERIOD COVERED Final Report for Period January 1972 to March 1974 6. PERFORMING ORG. REPORT NUMBER AD-5013-F-2
7. AUTHOR(s) Chalk, Charles R. Radford, Robert C. Wasserman, Richard		8. CONTRACT OR GRANT NUMBER(s) F33615-71-C-1722
9. PERFORMING ORGANIZATION NAME AND ADDRESS Calspan Corporation P. O. Box 235 Buffalo, New York 14221		10. PROGRAM ELEMENT, PROJECT, TASK AREA & WORK UNIT NUMBERS Project 643A
11. CONTROLLING OFFICE NAME AND ADDRESS Air Force Flight Dynamics Laboratory Air Force Systems Command Wright-Patterson Air Force Base, Ohio 45433		12. REPORT DATE June 1974 13. NUMBER OF PAGES 160
14. MONITORING AGENCY NAME & ADDRESS(if different from Controlling Office)		15. SECURITY CLASS. (of this report) Unclassified 15a. DECLASSIFICATION/DOWNGRADING SCHEDULE

16. DISTRIBUTION STATEMENT (of this Report)

Approved for public release: distribution unlimited

17. DISTRIBUTION STATEMENT (of the abstract entered in Block 20, if different from Report)

18. SUPPLEMENTARY NOTES

19. KEY WORDS (Continue on reverse side if necessary and identify by block number)

Flying Qualities	Longitudinal Characteristics	Landing Approach
MIL-F-83300	Control Power	Pilot in the Loop
MIL-F-8785B(ASG)	Hover	
VTOL Aircraft	Low Speed Flight	

20. ABSTRACT (Continue on reverse side if necessary and identify by block number)

MIL-F-83300, Military Specification for Flying Qualities of Piloted V/STOL Aircraft, was adopted by the Air Force and Navy in December 1970. This report documents an effort to generate new data for substantiation of parts of the specification. Two experimental programs were performed under subcontract to Calspan: an in-flight simulation to examine STOL longitudinal characteristics, and a fixed-base simulation to study control power and control usage in hover and low-speed flight. The former experiment was accomplished

DD FORM 1 JAN 73 1473 EDITION OF 1 NOV 65 IS OBSOLETE

SECURITY CLASSIFICATION OF THIS PAGE (When Data Entered)

20. Abstract (continued)

by the National Research Council of Canada, and the latter by United Aircraft Research Laboratory. A limited analysis of the data obtained was performed by Calspan and recommendations were made for future experiments to expand the data base for existing and additional requirements.

FOREWORD

This report was prepared for the United States Air Force by Calspan Corporation, Buffalo, New York in partial fulfillment of Contract F33615-71-C-1722. This report is the final report to be prepared under this contract. Two other Air Force reports were published during performance of this contract by subcontractors to Calspan Corporation. The first was prepared by United Aircraft Research Laboratories:

> Vinje, E.W. and D.P. Miller: "Flight Simulator Experiments and Analysis in Support of Further Development of MIL-F-83300-V/STOL Flying Qualities Specification," AFFDL-TR-73-74, July 1973.

The second was prepared by the National Research Council of Canada:

> Doetsch, K-H. and D.W. Laurie-Lean: "The Flight Investigation and Analysis of Longitudinal Handling Qualities of STOL Aircraft on Landing Approach," AFFDL-TR-74-18, March 1974.

The work reported here was performed during the period January 1972 through March 1974 by the Flight Research Department of Calspan Corporation under sponsorship of the Air Force Flight Dynamics Laboratory, Wright-Patterson Air Force Base, Ohio as part of Project 643A.

The Air Force Project Engineer was Mr. Terry Neighbor (FGC).

This report was submitted by the authors in April 1974.

TABLE OF CONTENTS

LIST OF ILLUSTRATIONS

List of Illustrations (cont.)

List of Illustrations (Cont.)

SECTION I

INTRODUCTION

A fully coordinated V/STOL flying qualities specification was adopted by the Air Force and Navy as MIL-F-83300 (Reference 1) in December 1970. The specification was accompanied by a technical report (Reference 2) giving background and substantiation of the requirements. Both of these were results of Part III of the Air Force Advanced Development Program called VTOL Integrated Flight Control System (VIFCS).

Although MIL-F-83300 was accepted as a specification, further work was needed to refine and further substantiate the existing requirements and to develop new requirements. In July 1971, the Air Force Flight Dynamics Laboratory (AFFDL) awarded a three-year contract to Calspan Corporation for an experimental and analytical program to generate flying qualities data and to make recommendations for revision of MIL-F-83300.

As part of this three-year program, Calspan planned three experimental programs:

(1) A moving-base ground simulation was to be performed by Calspan using the facilities at AFFDL. The objective was to investigate the parameters, and determine criteria, for the control of speed and flight path angle during STOL landing approach. This was intended to be a broad survey study that would help design the in-flight experiment to be performed by the National Research Council of Canada (NRC). Efforts to

---

[1] Anon.: "Military Specification -- Flying Qualities of Piloted V/STOL Aircraft" MIL-F-83300, December 1970.

[2] Chalk, C.R., D.L. Key, J.Kroll, Jr., R.Wasserman, R.C.Radford: "Background Information and User Guide for MIL-F-83300 -- Military Specification Flying Qualities of Piloted V/STOL Aircraft," AFFDL-TR-70-88, February 1971.

perform the ground simulation program at AFFDL were unsuccessful because of unacceptable equipment performance and the experiment was not completed. The experiment plan is documented in Reference 3.

(2) An in-flight simulation was performed in the NRC variable stability Bell 47G3B1 helicopter. This experiment was intended to follow the ground simulation experiment at AFFDL and to benefit from the results of that project; however, because the ground simulation experiment could not be performed, it was necessary to proceed independently. An in-flight experiment was designed by Calspan (References 4 and 5) and performed by NRC on subcontract. The NRC final report was published as Reference 6.

---

[3] Key, D.L. and R.C. Radford: "CAL Test Plan for STOL Landing Approach Simulation at AFFDL". Calspan VTOL H.Q. TM No. 31, 11 February 1971.

[4] Key, D.L. and J. Kroll, Jr.: "Calspan Experiment Design for NRC In-Flight Simulation of STOL Longitudinal Characteristics in Landing Approach." Calspan VTOL H.Q. TM No. 35, 22 January 1973.

[5] Kroll, John Jr.: "Calspan Experimental Design for NRC In-Flight Simulation of STOL Longitudinal Characteristics in Landing Approach." Calspan VTOL H.Q. TM No. 35, Addendum A, 8 March 1973.

[6] Doetsch, K-H and D.W. Laurie-Lean: "The Flight Investigation and Analysis of Longitudinal Handling Qualities of STOL Aircraft on Landing Approach." AFFDL-TR-74-18, March 1974.

(3) A ground simulator experiment was performed, under subcontract, by United Aircraft Research Laboratory (UARL). The objective of this experiment was to study control power and control usage in hover and low speed flight. Calspan guided and participated in this program. The final report was published as Reference 7.

An interim report on the program to improve MIL-F-83300 was published as Reference 8. This report described the simulation experiment plans and discussed the topics of MIL-F-83300 which would be given the most attention during the specification revision effort. It also documented the results of and analysis of STOL data which was performed to establish a baseline model and ranges of stability and control characteristics to be used in the simulation experiments. An analysis of pilot-STOL dynamics in the landing approach is also contained in Reference 8.

Air Force Project 643A was terminated in 1972 and the specification revision work being performed by Calspan Corporation was reduced in scope. The revised program provided for completion of the subcontracts by NRC and UARL, publication of the subcontractors' reports documenting the experiments performed, effort by Calspan to monitor this contract activity and effort by Calspan to analyze portions of the experimental results. The effort to prepare recommended revisions to MIL-F-83300 was eliminated from the contract.

The purpose of this report is to summarize the overall contract activity and to document the analysis performed by Calspan of part of the data generated in the experiments performed by NRC and UARL.

---

[7] Vinje, E.W. and D.P. Miller: "Flight Simulator Experiments and Analysis in Support of Further Development of MIL-F-83300 - V/STOL Flying Qualities Specification." AFFDL-TR-73-74, July 1973.

[8] Key, D.L., R.C. Radford and R.T.N. Chen: "First Interim Report On Program to Improve MIL-F-83300." Calspan Report No. AD-5013-F-1, May 1972.

SECTION II

FORWARD FLIGHT EXPERIMENT

2.1 BACKGROUND

This program resulted from an evaluation of the need for modification and formulation of additions to the existing V/STOL specification longitudinal handling qualities requirements. The experiment was planned in the context of the handling qualities problems of STOL aircraft in the landing approach (PA) Flight Phase. This emphasis reflects both the current Air Force interest in advancing STOL technology and the state of our understanding of the problems of this complex flight regime.

A review of the sections of the Background Information and User Guide (BIUG), Reference 2, appropriate to low speed flight (35 knots $< V < V_{con}$) revealed that most of the substantiating data is based on extrapolations from the higher speed flight regimes. At the same time there are qualitative requirements which are essential to the landing approach task that could not be quantified due to a lack of any appropriate data.

2.2 EXPERIMENT DESIGN CONSIDERATIONS

The longitudinal landing approach Flight Phase comprises many subtasks such as navigation and guidance (ILS intercept), precision tracking (glide slope and localizer), and maneuvering (flare and touchdown). There are a myriad of factors which influence the ease with which these tasks can be accomplished, some of which are:

- short and long term attitude dynamics
- speed and flight path coupling characteristics
- thrust control configuration (i.e., thrust angle and response characteristics)
- "frontside" or "backside" of power curve
- task variables, glide slope angle, speed, VFR or IFR
- winds and turbulence.

It has been postulated that, in the landing approach, the pilot continuously closes an inner attitude control loop to regulate either airspeed or glide path angle. The selection of control mode (i.e., attitude to control airspeed or attitude to control glide path) appears to be strongly related to the effective inclination of the thrust magnitude control.

The pilot-adapted control loop structure illustrated in Figure 1 is thought to be most applicable when the thrust inclination is low and manipulation of the thrust lever or collective control results primarily in modulation of the X-force. In this situation the pilot will probably use the thrust magnitude control for large corrections to altitude and rate of climb and to establish the trim airspeed. During tracking of the ILS he will probably attempt to use the elevator stick to control pitch attitude and, through pitch attitude, make corrections to the flight path. This control technique will work when the approach is made on the front side of the thrust required curve or when the low frequency factor of the altitude to elevator transfer function numerator, $1/T_{h_1}$, is in the left half plane. If the approach is made on the back side with $1/T_{h_1}$ in the right half plane, an unstable system will result and the airspeed will diverge from the trim speed. This divergence can be prevented by the using the thrust magnitude control to restrain airspeed errors. Under these assumptions we see that the value of $1/T_{h_1}$ is an open-loop parameter that is a good indicator of whether or not control difficulties will be encountered. Based on considerations such as these, a requirement limiting $d\gamma/dV$ was introduced in MIL-F-8785B (Reference 9) for airplanes. This requirement was not included in MIL-F-83300 because it was felt that the basic control loop structure described above probably would not be applicable for V/STOL designs.

The control loop structure illustrated in Figure 2 is thought to be most applicable when manipulation of the thrust lever results in modulation of

---

[9] Anon.: "Military Specification - Flying Qualities of Piloted Airplanes" MIL-F-8785B(ASG) August 1969.

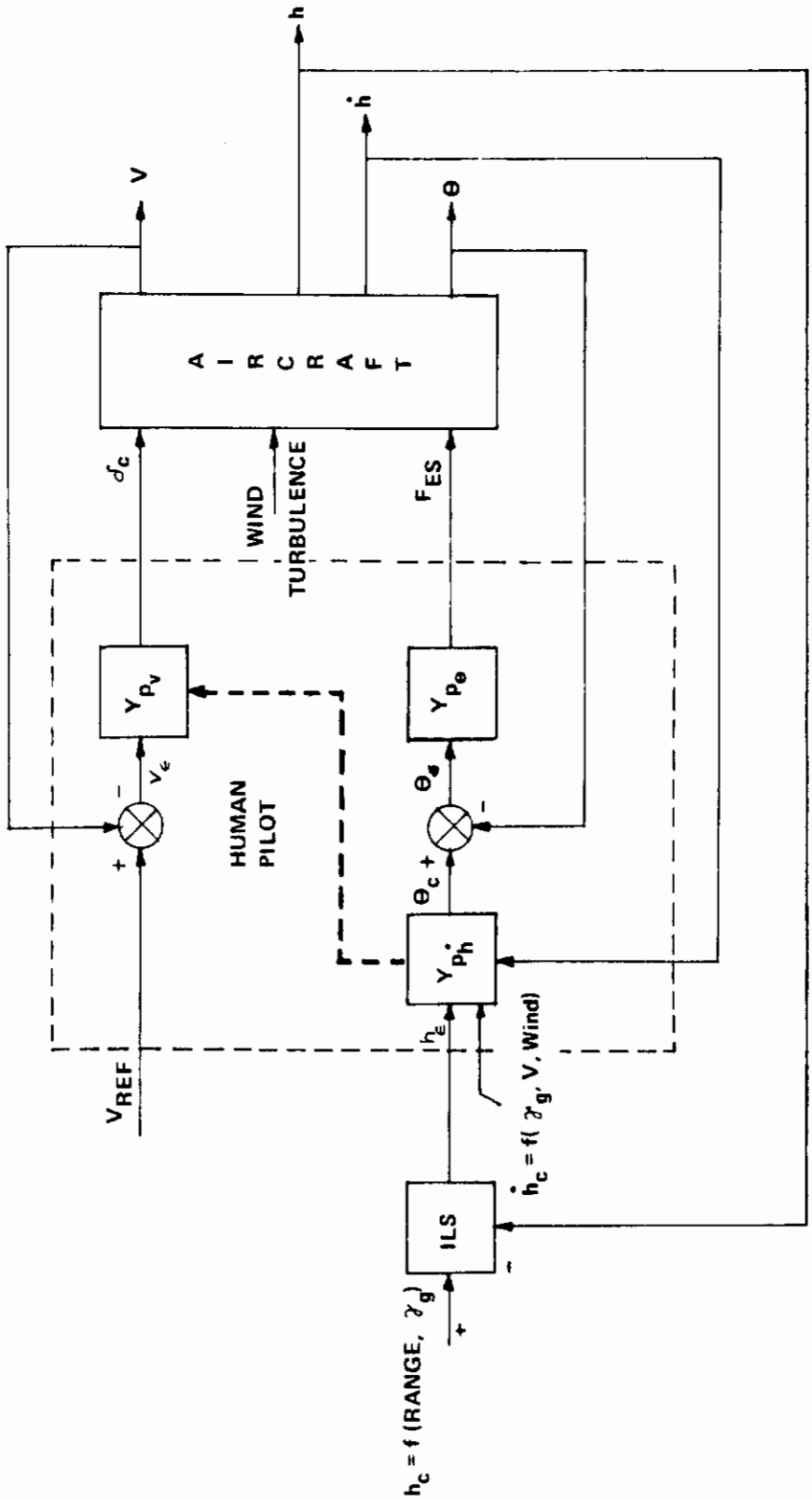

Figure 1 HYPOTHESIZED CONTROL LOOP STRUCTURE FOR PRECISION ILS APPROACH (LOW THRUST INCLINATION)

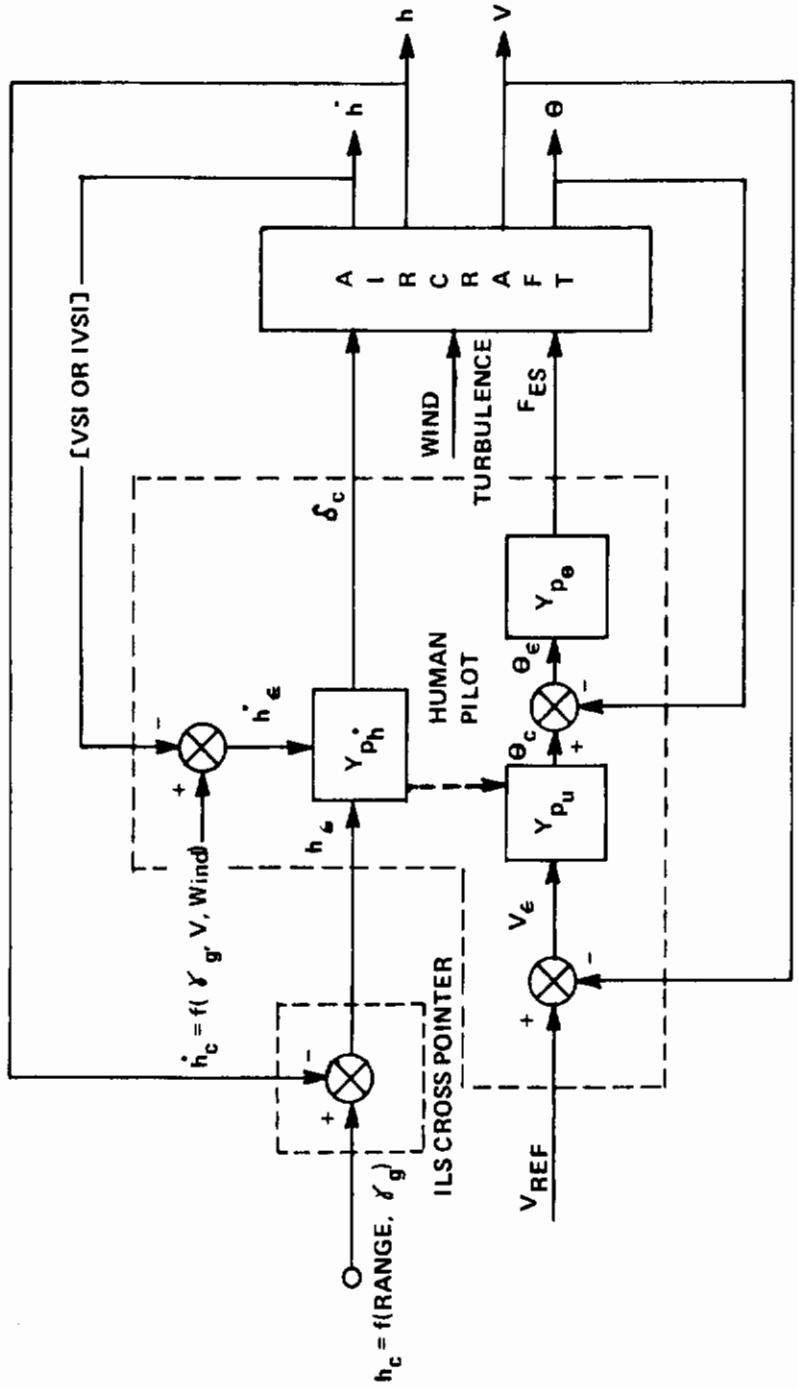

Figure 2 HYPOTHESIZED CONTROL LOOP STRUCTURE FOR PRECISION ILS APPROACH (HIGH THRUST INCLINATION)

a force vector which has a high inclination to the horizontal, i.e., nearly vertical. Consideration of probable STOL configurations indicates that their low-speed lift augmentation systems will generally result in a highly inclined thrust vector. In this situation the pilot will probably use the elevator stick to constrain the pitch attitude of the vehicle during the ILS approach and will modulate the thrust vector magnitude to make corrections to the flight path. Because the pitch attitude to elevator loop will always to closed, it is improbable that open-loop transfer function factors in the altitude to collective transfer function can be used as indicators of control difficulty. This is because the nearly continuous closure of the pitch attitude to elevator loop will modify the situation. The two basically different control situations described above may not occur in practice, i.e., combinations of these situations are likely to be encountered. For example, the thrust vector may have various inclination angles and modulation of the thrust vector may be accompanied by coupled longitudinal and vertical accelerations.

In both control loop structures described above, it is assumed that the pilot actively closes an attitude stabilization control loop. It can be seen, then, that satisfactory control of pitch attitude is likely to be a necessary (albeit not sufficient) condition for satisfactory control of speed and flight path in the landing approach. Factors which influence the attitude response are the roots (eigenvalues) of the aircraft characteristic equation together with the attenuation and phasing introduced by the θ/δ_{es} transfer function numerator zeros. The Ref. 1 requirement quoted below is directed to the character of the longitudinal eigenvalues.

> 3.2.2 Longitudinal dynamic response. The following requirements shall apply to the dynamic response of the aircraft with the pitch control free and with it fixed. These requirements apply following a disturbance in smooth air, and following abrupt pitch control inputs in each direction, for responses of any magnitude that might be experienced in operational use. If the oscillations are nonlinear with amplitude, the requirements shall apply to each cycle of the oscillation.

Level 1: The response of the aircraft shall not be divergent (i.e., all roots of the longitudinal characteristic equation of the aircraft shall be stable). In addition, the undamped natural frequency, ω_n , and damping ratio, ζ , of the second-order pair of roots (real or complex) that primarily determine the short-term response of angle of attack following an abrupt pitch control input shall meet the Level 1 requirements of figure 1.

Level 2: For those Flight Phases of the operational missions of 3.1.1 for which IFR operation is required, the Level 2 requirement is the same as for Level 1. In all other cases, for Level 2, divergent modes of aperiodic response shall not double amplitude in less than 12 seconds. Oscillatory modes may be unstable provided their frequency is less than or equal to 0.84 radians per second and their time to double amplitude is greater than 12 seconds. In addition, the undamped natural frequency and damping ratio of the second-order pair of roots (real or complex) that primarily determine the short-term response of angle of attack following an abrupt pitch control input shall meet the Level 2 requirements of figure 1.

Level 3: Divergent modes of aperiodic response shall not double amplitude in less than 5 seconds. Oscillatory responses shall be stable; however, an instability will be permitted provided its frequency is less than 1.25 radians per second and its time to double amplitude is greater than 5 seconds.

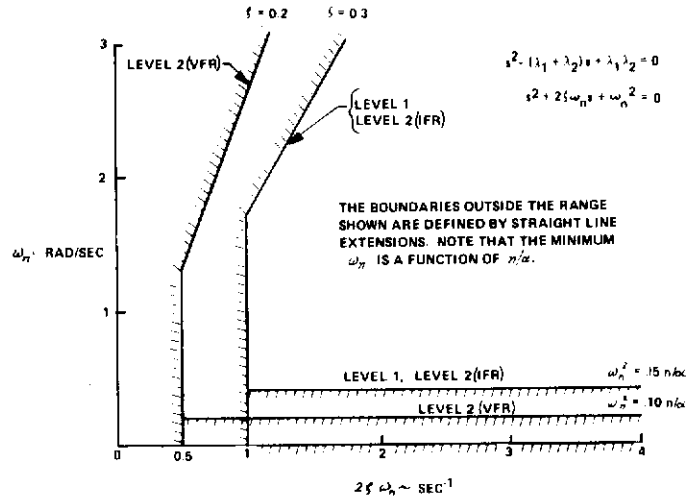

Figure 1 SHORT-TERM LONGITUDINAL RESPONSE REQUIREMENTS (FROM REFERENCE 1)

The Level 1 and 2 limits on total damping and damping ratio in Figure 1 of MIL-F-83300 were tested in the X-22A experiment reported in Reference 10. The results of Reference 10 seemed to confirm these damping limits at least for VFR conditions. The experiment of Reference 10 did not contain data at low enough frequency to test the minimum frequency requirement for $\omega_n^2 = f(n/\alpha)$. This was primarily because it is difficult to accurately set up and maintain very low frequency configurations with a response-feedback variable stability airplane. Thus one of the primary objectives of the NRC experiment was to use the model-following system to set up and evaluate configurations that would test the low-frequency limit in Figure 1 of MIL-F-83300. The tests were performed at one approach speed (60 knots) but because the NRC helicopter has independent control of vertical force, it was possible to vary Z_w independently and thus set up various values of n/α at the single approach speed. The configurations were designed to have values of $2\zeta\omega_n$ within the Level 1 region of MIL-F-83300. In addition, by making the coupling derivatives Z_u and M_u zero, the phugoid mode was reduced essentially to a pole at X_u and one very near the origin (see equations in Reference 2). By setting $Z_u = M_u = 0$, the parameter $d\sigma/dV$ was made negative, i.e., operation on the front side of the power required curve. To further eliminate coupling effects, Z_{δ_e} and M_{δ_c} were also set to zero. Because the NRC helicopter does not have independent control of X-forces, it was not possible to make independent variations of the derivatives X_w and X_u. Because the X-forces were not independently controllable, the steady-state value of airspeed change with altitude for elevator inputs was not independently variable. The generally high value of steady-state u/θ was a limitation of the simulator which may have had the effect of requiring high precision in attitude control to maintain speed.

Through the above described constraints it was hoped that configurations could be designed and evaluated that would test the validity of the

---

10 Smith, R.E., J.V. Lebacqz, and J.M. Schuler: "Flight Investigation of Various Longitudinal Short-Term Dynamics for STOL Landing Approach Using the X-22A Variable Stability Airplane." Calspan Report No. TB-3011-F-2, January 1973.

requirement in Figure 1 of MIL-F-83300. Other parts of the experiment were designed to evaluate the effects of the constraints $Z_u = M_u = 0$ and $Z_{\delta_e} = M_{\delta_T} = 0$, by evaluating configurations with realistic values of these coupling derivatives. The effect of nonzero values of Z_u and M_u is to cause the low-frequency roots associated with the phugoid mode to migrate from their locations at the origin and at X_u. In some cases the characteristic equation factors into four real roots and it is quite arbitrary as to which two roots should be grouped to compare with Figure 1 of MIL-F-83300. Nonzero values of Z_u and M_u also cause positive values of $d\gamma/dV$ and couple the Z-force and the pitching moments with variations in forward speed.

A third part of the experiment was designed to explore whether or not attitude stabilization could ameliorate the unfavorable effects on speed and flight path control resulting from nonzero values of Z_u.

In summary, the objectives of the NRC experiment were first to explore the problem of attitude control with speed and flight path coupling problems suppressed to the greatest extent possible, and then to examine the effects of variations of the coupling parameter Z_u for configurations with augmented pitch attitude dynamics such as pitch rate command-attitude hold and attitude command configurations. The effects of the coupling parameters Z_u, M_u, Z_{δ_e} and M_{δ_T} were also examined for typical unaugmented pitch dynamics. The complete configuration matrix explored in the NRC experiment is shown in Figure 3; the reader is also referred to Reference 6.

The following sections present a summary of the results of an analysis by Calspan of the configurations identified as Group I in the NRC experimental data. This Group was directed at exploring the requirements for pitch attitude control with good speed and flight path characteristics.

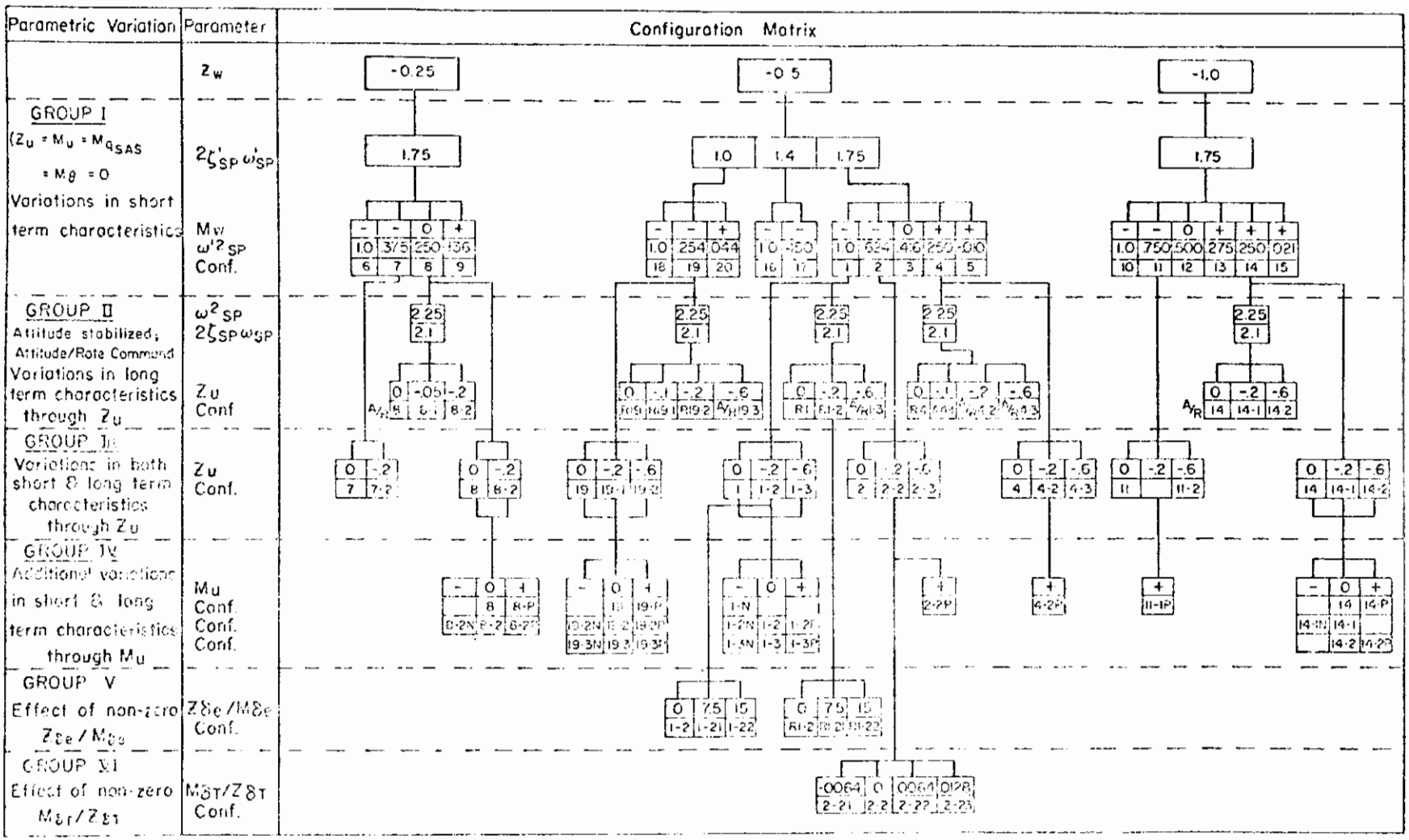

Figure 3 CONFIGURATION MATRIX EVALUATED

2.3 ANALYSIS OF PITCH ATTITUDE CONTROL

The initial phase of the experiment was directed to exploring the effects of various attitude to pitch control transfer function configurations on handling qualities in the landing approach. Details of the task, pilot commentary and ratings are documented fully in Reference 6 and are not repeated here. For these configurations (designated Group I), the coupling derivatives M_u , Z_u , Z_{δ_e} and M_{δ_c} were set to zero to allow concentration on the characteristics of the attitude dynamics. With M_u , Z_u and Z_{δ_e} equal to zero, the attitude transfer function has the form:

$$\frac{\theta_M}{\delta_{ES}} = M_{\delta_{ES}} \frac{(s - X_u)(s - Z_w)}{(s - X_u)(s + \delta)(s^2 + 2\zeta\omega_n s + \omega_n^2)} \tag{1}$$

$$= M_{\delta_{ES}} \frac{s - Z_w}{(s + \delta)(s^2 + 2\zeta\omega_n s + \omega_n^2)} \tag{2}$$

The parameters varied were the short period frequency and damping (ω_n , $2\zeta\omega_n$) and numerator zero (Z_w). The root ($-\delta$) varied in a dependent fashion and was always in the range $-.03 \leq \delta \leq .09$. The control derivative $M_{\delta_{ES}}$ could be selected by the pilot if he didn't like the value presented by the experimenter.

The variations in short-period frequency and damping together with the ratings of the four participating pilots are plotted in Figures 4a and 4b. For comparison, the requirement boundaries of MIL-F-83300 with respect to short-term frequency and damping are plotted as well. At the lowest values of "ω_n", the third-order characteristic equation factored into three real roots. The identification of two of the roots with the "short-period" mode is somewhat arbitrary, but for the purpose of these summary plots, the "short-period" mode has been characterized by the two highest-frequency stable roots. It should be recognized that this facet is a primary deficiency of this requirement.

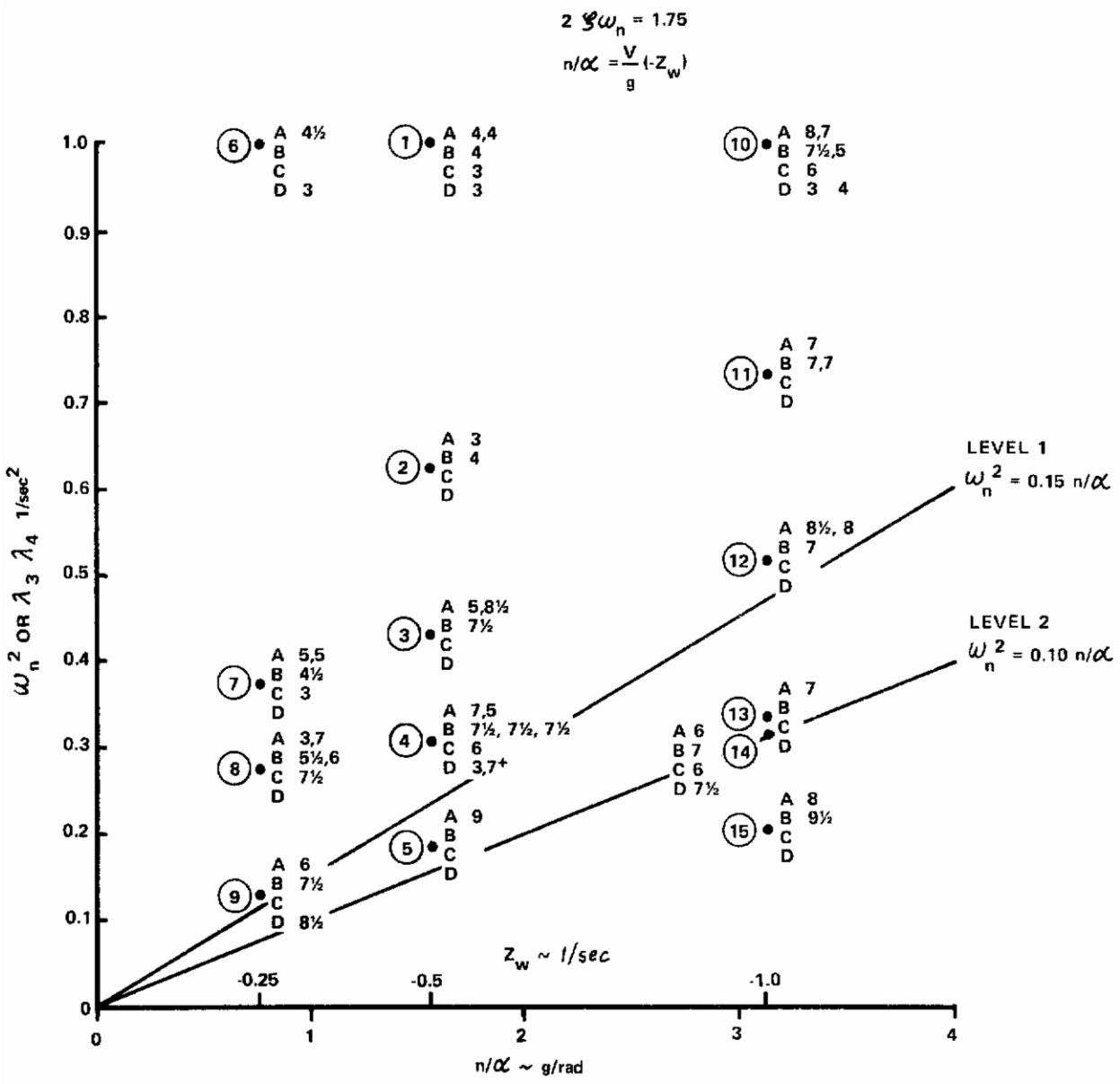

Figure 4(a) COMPARISON OF NRC DATA FROM GROUP I TO $\omega_n^2 = f(n/\alpha)$ REQUIREMENT OF MIL-F-83300

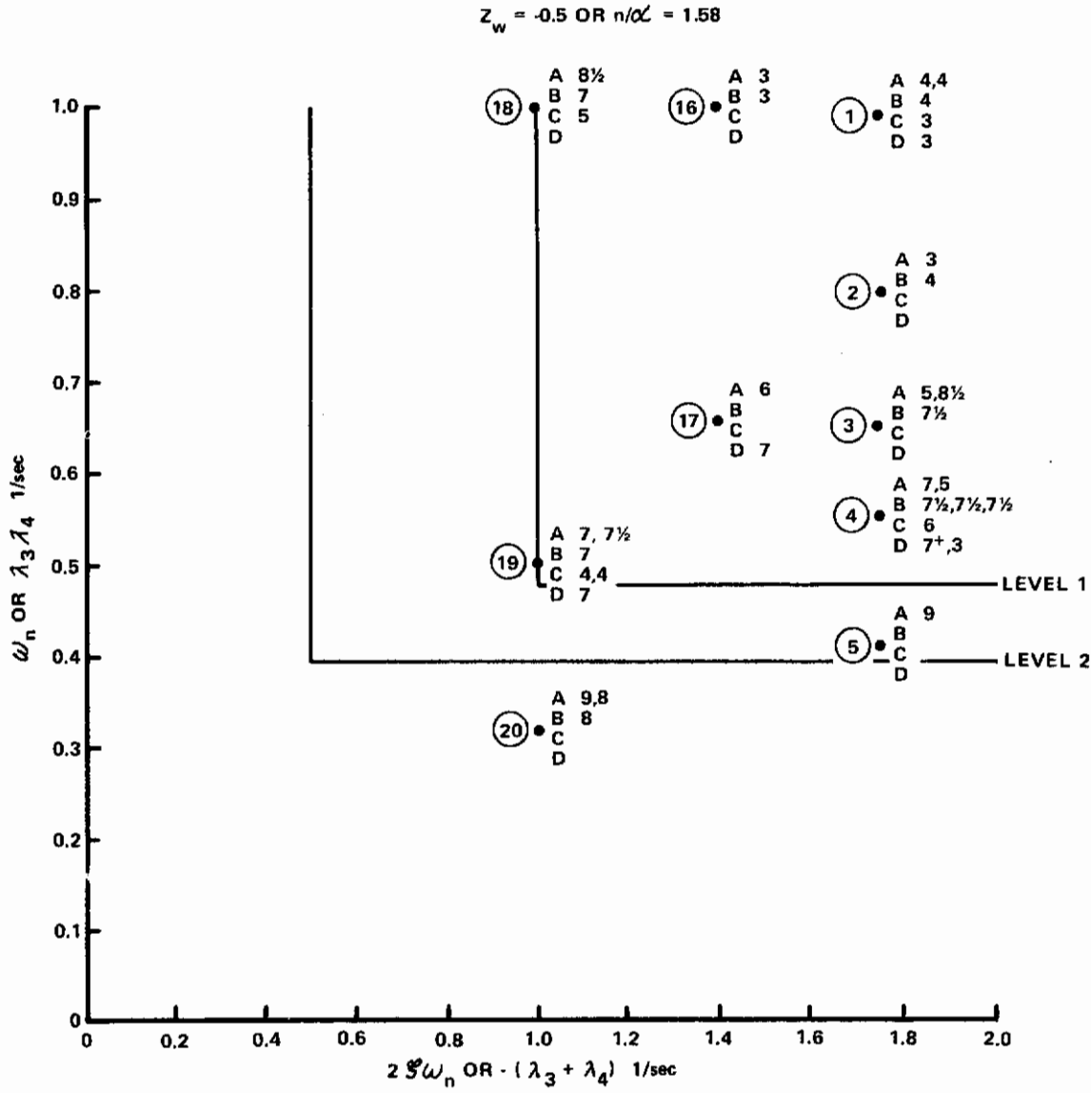

Figure 4(b) COMPARISON OF NRC DATA FOR Z_w = -.5 WITH SHORT-TERM LONGITUDINAL RESPONSE REQUIREMENTS OF MIL-F-83300

Several anomalies of the pilot rating trends with respect to the specification Level 1 boundaries are indicated by Figures 4a and 4b. In Figure 4a, configurations 3, 4, 7, 8, 9, 10, 11 and 12 are in disagreement with the Level 1 minimum frequency boundary. In Figure 4b, configurations 3, 4, 17, 18 and 19 are in disagreement with the Level 1 minimum frequency and minimum damping boundaries. The pilot comments for the configurations listed above contain many references to difficulties in controlling pitch attitude and to the fact that too much attention was required to control pitch attitude to the accuracy required to keep airspeed constant. In several cases, reference is made to pitch overcontrol and PIO resulting from the pilot's efforts to maneuver abruptly or in trying to counter upsets resulting from turbulence.

Because the poor pilot ratings and control difficulties experienced in this phase of the NRC experiment were associated with problems in pitch attitude control, it was decided to perform the closed-loop analysis described in the following sections.

Closed-Loop Analysis

Simple pilot-in-the-loop analysis of the control of pitch attitude was applied to selected configurations to gain insight into the aforementioned anomalies in the pilot rating data and the requirements of MIL-F-83300. The following sections describe the pilot-aircraft model utilized, the closure rules adopted and discusses the correlation of the resulting closed-loop characteristics with the pilot commentary and ratings.

Pilot-Aircraft Model

The model selected was the single loop compensatory tracking model illustrated in Figure 5. This model is considered to be representative of pilot-vehicle characteristics during the ILS tracking portion of the landing approach task.

The NRC Bell 47G3B1 variable stability helicopter employs a model-following system. Thus the controlled element, Y_c , of Figure 5 includes, in addition to the force feel system dynamics and pitch transfer function, an element representing the model following dynamics, θ/θ_M . Reference 6 indicates that the following transfer function is representative of the model-following dynamics over the frequency range of interest to the pilot:

$$\frac{\theta}{\theta_M} = \frac{6^2}{s^2 + 2(.5)(6)s + 6^2} \tag{3}$$

The linear aspects of the force feel system dynamics are described as follows in Reference 6:

$$\frac{\delta_{ES}}{F_{ES}} = \frac{8.2^2}{s^2 + 2(.3)(8.2)s + 8.2^2} \tag{4}$$

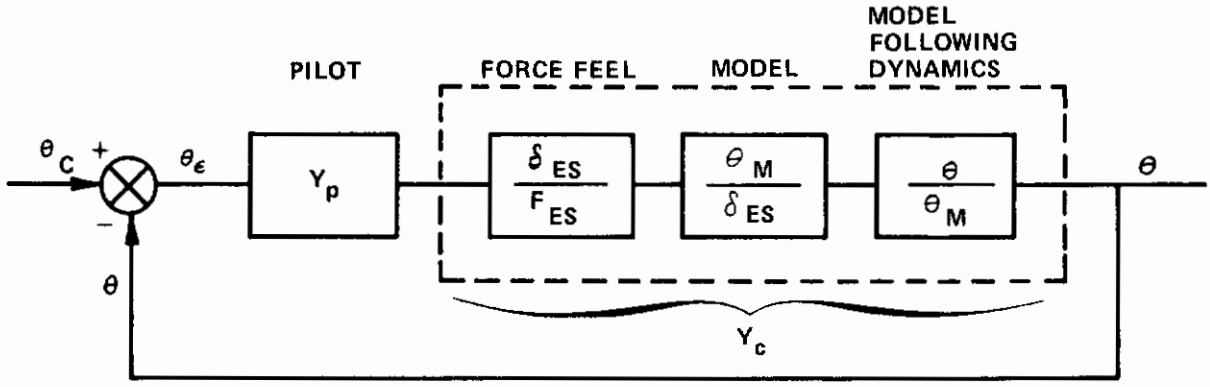

Figure 5 COMPENSATORY TRACKING MODEL

The combination of these two transfer functions produces the frequency response characteristics illustrated in Figure 6. To simplify the model of the controlled element, the feel system and model-following dynamics were approximated by a pure time delay, $e^{-.25s}$. This approximation is plotted for comparison on Figure 6. Thus, the controlled element model, Y_c, is given by

$$Y_c = e^{-.25s}\left(\frac{\theta_M}{\delta_{ES}}\right) \tag{5}$$

This approximation is considered to be sufficiently accurate up to frequencies of the order of 3 to 4 radians per second.

The pilot's control characteristics were represented by the crossover model

$$Y_p = K_p \frac{(1+T_L s)}{(1+T_I s)} e^{-\tau_p s} \tag{6}$$

There is a considerable body of evidence that this transfer function is a reasonable description of the pilot's behavior as a linear regulator in the region of crossover frequency (References 11 through 13).

---

[11] McDonnell, J.D.: "Pilot Rating Techniques for the Estimation and Evaluation of Handling Qualities." AFFDL-TR-68-76, Dcemmber 1968.

[12] McRuer, D. and D. Graham: "Human Pilot Dynamics in Compensatory Systems." AFFDL-TR-65-15, July 1965.

[13] McRuer, D.T. and H.R. Jex: Effects of Task Variables on Pilot Models for Manually Controlled Vehicles." Paper presented at AGARD Meeting, Cambridge, England, September 1966.

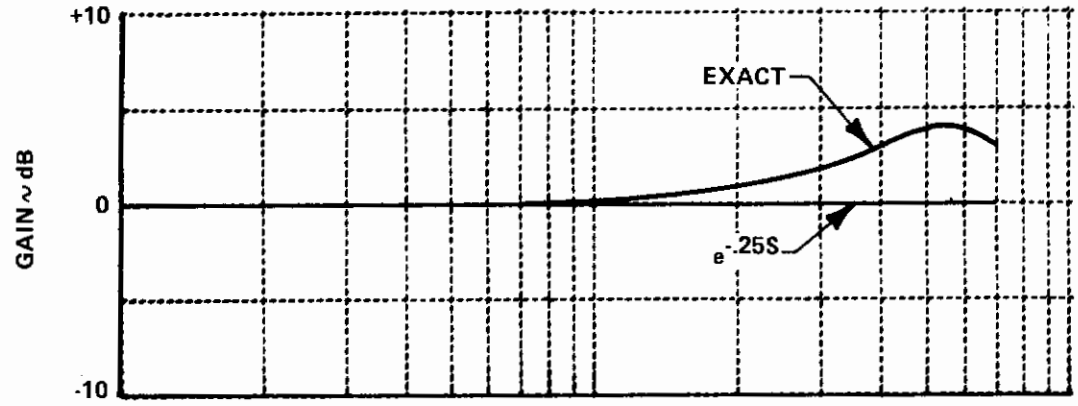

$$\frac{\delta_{ES}(s)}{F_{ES}(s)} \cdot \frac{\theta(s)}{\theta_M(s)} = \frac{(6)^2 \cdot (8.2)^2}{(s^2 + 2(.5)6s + 6^2)(s^2 + 2(.3)8.2s + 8.2^2)} \qquad (7)$$

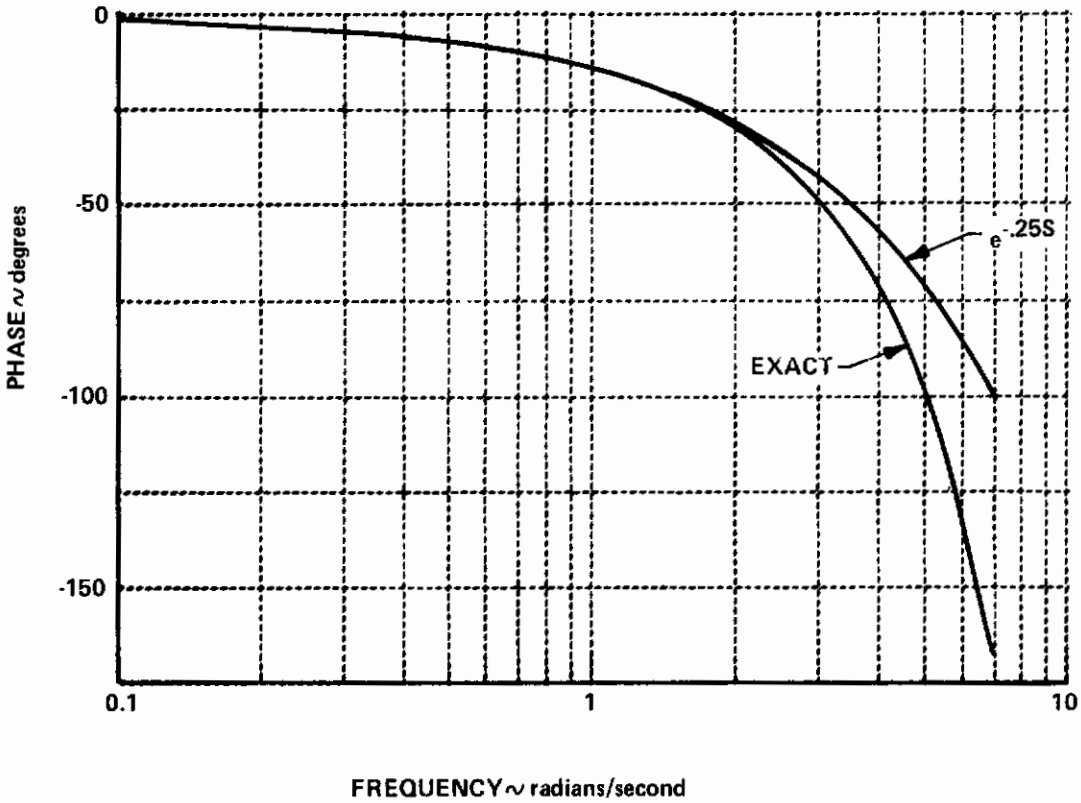

Figure 6 COMPARISON OF THE FREQUENCY RESPONSE OF COMBINED FORCE FEEL AND MODEL–FOLLOWING SYSTEM DYNAMICS WITH $e^{-.25S}$

Closure Rules

In analyzing pilot-vehicle systems, closure rules have been formulated in terms of open-loop transfer characteristics $Y_p Y_c$ as presented, for example, in References 12 and 13. Experimental measurements indicate that the pilot attempts to construct a closure by adjusting his lead T_L, lag T_I, and gain K_p, to create a broad region of $|Y_p Y_c| = K/s$ in the neighborhood of the crossover frequency ω_c. The magnitude of the crossover frequency is somewhat ill-defined, but appears to be a function of factors such as input noise bandwidth, controlled element characteristics, etc.

For simple controlled elements (i.e., $Y_c = K_c/s$, $K_c/s(s+\alpha)$) the pilot should be able to provide open-loop $|Y_p Y_c| = K/s$ effectively over an infinite frequency range as follows:

$$\text{For} \quad Y_c = \frac{K}{s}: \quad T_L = T_I = 0$$

$$\text{For} \quad Y = \frac{K}{s(s+\alpha)}: \quad T_L = \frac{1}{\alpha}, \; T_I = 0$$

However, even for these simple systems the pilot gain K_p and thus the resulting closed-loop performance (bandwidth, magnitude of resonance peak) is highly sensitive to the magnitude of the crossover frequency. For more complex controlled elements, pilot lead and lag become dependent on crossover frequency as well.

In analyzing the results of a recent investigation of fighter handling qualities in up-and-away tracking tasks, Neal and Smith (Reference 14) developed an alternate set of closure rules based on closed-loop system

---

[14] Neal, T.P. and R.E. Smith: "An In-Flight Investigation to Develop Control System Design Criteria for Fighter Airplanes." AFFDL-TR-70-74, June 1970.

performance ($Y_p Y_c / (1 + Y_p Y_c)$). Stated briefly, the rules require that the pilot develop gain, lead and lag such that the closed-loop system exhibits a specified bandwidth, ω_B (defined as the frequency at which the closed-loop phase angle is $-\pi/2$). In addition the closure must minimize any resonance, subject to the constraint that low-frequency "droop" shall not exceed -3dB. For the aircraft pitch attitude transfer functions investigated, the minimum resonance achievable tended to be limited by the "droop" criterion. Thus, application of the closure rules tended to determine a unique set of pilot compensation parameters (T_I, T_L, K_p) for each configuration. The correlation of pilot commentary and ratings with the compensation required and the magnitude of the closed-loop resonance was found to be excellent.

For continuity with the work of Neal and Smith, it was decided to apply their closure rules to the configurations of this experiment. It was anticipated, however, that because of Flight Phase differences (i.e., high-speed up-and-away flight versus low-speed STOL landing approach), the bandwidth frequency of Reference 14, (nominally 3 radians/second) would not be applicable to this experiment. In fact, Reference 15 indicates that ω_B = 1.2 radians/second is more appropriate. In light of the sensitivity of the pilot closure parameters to the assumed bandwidth, and in the absence of pilot compensation measurements, the following approach was taken to estimate a nominal bandwidth for the analyses of the pitch attitude configurations of this experiment.

Estimation of Bandwidth Frequency

In the present experiment, a group of configurations was evaluated for which the effective attitude transfer function was

---

15. Chalk, C.R., D.A. Di Franco, J.V. Lebacqz and T.P. Neal: "Revisions to MIL-F-8785B(ASG) Proposed by Cornell Aeronautical Laboratory Under Contract F33615-71-C-1254" AFFDL-TR-72-41, April 1973.

$$\frac{\theta_M}{\delta_{ES}} = \frac{M_{\delta_{ES}}}{s(s-M_q)} \tag{8}$$

Experimental evidence (Reference 11) suggests that for a simple controlled element of this form, the pilot will develop lead $T_L \doteq -1/M_q$ so as to cancel the pole $(s-M_q)$ resulting in the desired K/s open-loop transfer function form

$$Y_p Y_c = K_p T_L M_{\delta_{ES}} \frac{e^{-(\tau_p+.25)s}}{s} = \frac{K}{s} e^{-\tau_E s} \tag{9}$$

If it is assumed that the pilots in this experiment adapted a similar compensation, it is possible to estimate the degradation in pilot rating with increased lead compensation. Figure 7 is a plot of pilot rating versus $T_L = -1/M_q$ for the configurations of this experiment. Also plotted are the results of a NASA helicopter experiment (Reference 16) under the same assumption that $T_L = -1/M_q$. In addition, lead compensation and the corresponding pilot ratings from Reference 11 are plotted. It can be seen that the results of this experiment indicate a more severe degradation of rating with lead compensation than do the other two experiments cited. This trend is possibly attributable to task differences: the NASA helicopter experiment did not involve an acutal landing approach, while the experiment of Reference 11 consisted primarily of fixed-base compensatory tracking of a displayed error signal.

The differences could also be related to the other lags or time delays in the system, i.e., feel system and model-following for the two flight

---

16. Di Carlo, Daniel J., James R. Kelly and Robert W. Sommer: "Flight Investigation to Determine the Effect of Longitudinal Characteristics on Low-Speed Instrument Operation." NASA TN D-4364, March 1968.

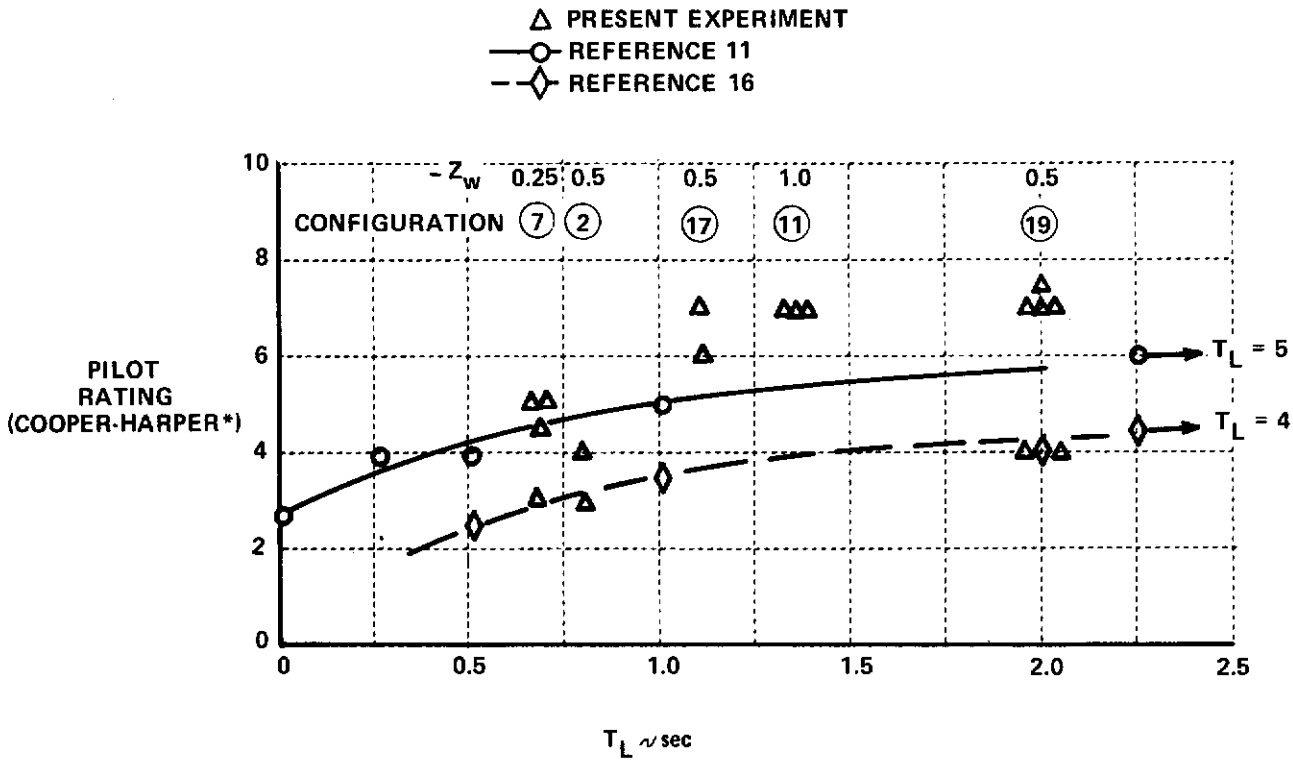

Figure 7 PILOT RATING VARIATION WITH LEAD COMPENSATION FOR CONTROL ELEMENT FORM $Y_c = \frac{\theta(s)}{F_E(s)} = \frac{K_c}{s(s+\alpha)}$ ASSUMING $T_L = 1/\alpha$

*REFERENCE 16 USED EXPANDED NASA PILOT RATING SYSTEM

experiments. It is also possible that the degradation in rating is only partially related to the lead compensation requirements. Although the root $s - Z_w$ does not appear in the attitude transfer function for these configurations, Z_w does manifest itself in the turbulence sensitivity of the configurations and response to collective control. The value of Z_w corresponding to each of these configurations is indicated on Figure 7.

In Equation 9 a nominal value of the pilot delay time of $\tau_p = 0.3$ seconds has been assumed, consistent with the analyses of Reference 14. A net delay time $\tau_E = .25 + .30$ is used in the analysis to account for the feel system plus the model-following system and the pilot.

Invoking the closed-loop bandwidth condition $\angle \left(\frac{Y_p Y_c}{1 + Y_p Y_c} \right) = -\frac{\pi}{2}$ Equation 9 yields

$$-\frac{\pi}{2} = -\omega_B \tau_E - \tan^{-1} \left(\frac{\omega_B - K \sin \omega_B \tau_E}{K \cos \omega_B \tau_E} \right) \tag{10}$$

Rearranging terms, the required gain is given by:

$$K = \omega_B \sin \omega_B \tau_E \tag{11}$$

It is noted that from this equation we can relate the open-loop crossover frequency ω_c (where $|Y_p Y_c| = 0$ dB, or 1) to the bandwidth frequency ω_B. Since $\left| K e^{-\tau_E s}/s \right| = K/\omega$, its amplitude is 1 when

$$\omega_c = K = \omega_B \sin \omega_B \tau_E \tag{12}$$

Thus for a given τ_E and $\omega_B \tau_E < \frac{\pi}{2}$ there is a unique relationship between open-loop crossover frequency and closed-loop bandwidth frequency. This relationship implies that if pilot compensation (i.e., T_L, T_I) can generate a $|Y_p Y_c| = K/s$ relationship over a sufficiently broad frequency range, satisfaction of either a bandwidth criterion or the equivalent crossover frequency criterion should result in effectively the same closed-loop system.

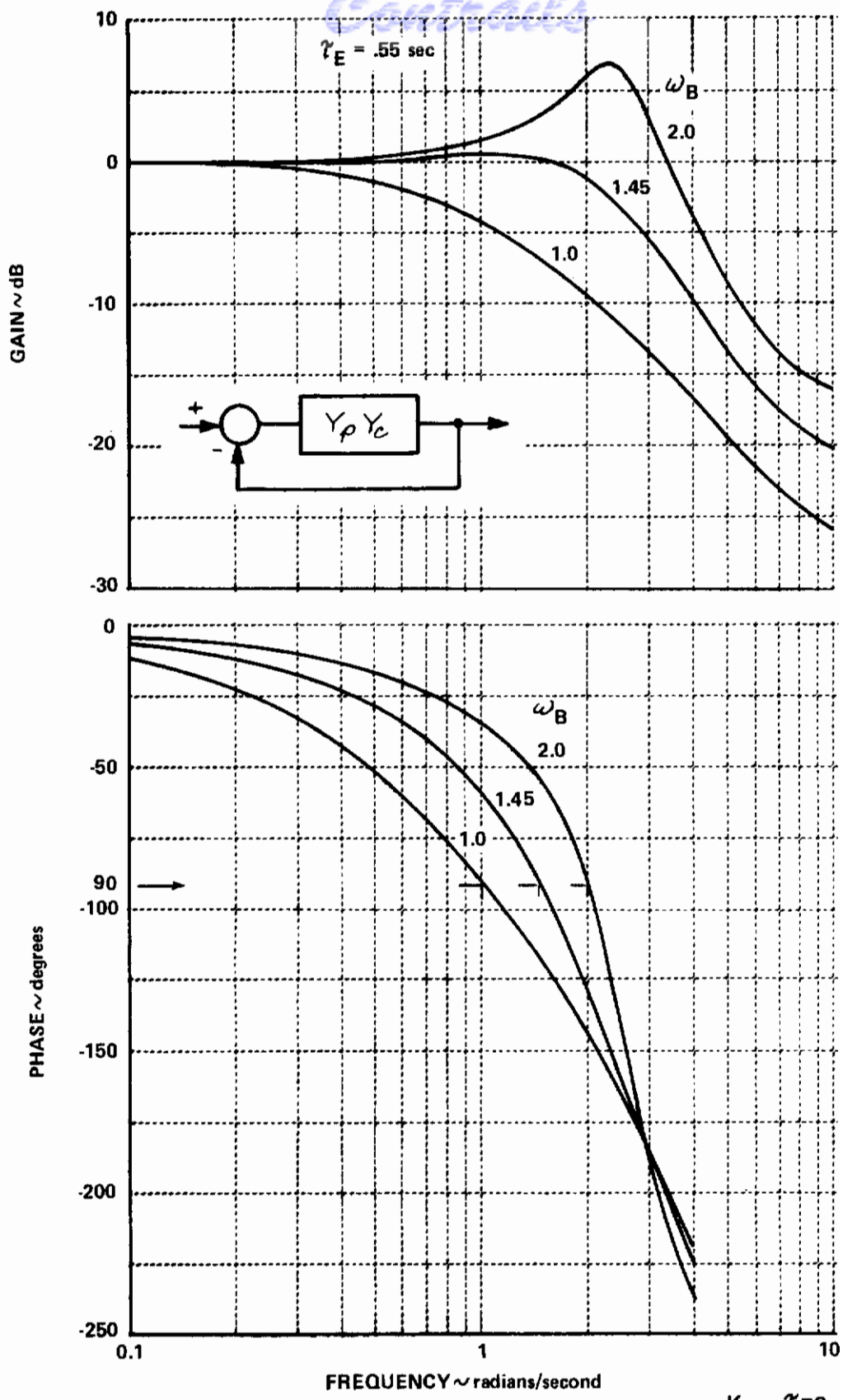

Figure 8 CLOSED-LOOP FREQUENCY RESPONSE FOR $Y_p Y_c = \frac{K}{S} e^{-\tau_E S}$

It can be seen from Equation 11 that as open-loop gain K increases, the closed-loop bandwidth ω_B also increases. Figure 8 illustrates the variation in the character of the closed-loop frequency response as a function of bandwidth frequency. At a bandwidth frequency of 2 the frequency response resembles that of a lightly damped second-order system, while for $\omega_B = 1$, the response is more like that of an overdamped system. A bandwidth frequency of 1.45 appeared to be a reasonable compromise between these extremes and produced a closed-loop frequency response which has an amplitude greater than -3 dB to about 2.5 radians/second.

To provide insight into the implications of pilot lead generation and bandwidth frequency on closed-loop performance, closed-loop frequency responses were calculated for a pilot/controlled element of the form $Y_p Y_c = e^{-.55s} K_p(1+T_L s)/s(s+1)$ for bandwidths between 1 and 2 radians/second. Figure 9a summarizes these frequency responses in terms of magnitude of closed-loop resonance as a function of lead, bandwidth and pilot gain K_p.

It can be observed that at a given level of $(\theta/\theta_c)_{MAX}$, the pilot must increase lead to increase bandwidth. Figure 9b, crossplotted from Figure 9a, indicates, that for low values of $(\theta/\theta_c)_{MAX}$, ω_B in the neighborhood of 1.45 reflects a limiting condition beyond which further increments in T_L produce very little increase in ω_B. Further, for $(\theta/\theta_c)_{MAX} < 4$, $\omega_B = 1.45$ tends to minimize pilot gain required for a given resonance and at zero resonance results in pilot lead sufficient to cancel the controlled element pole. In addition, the gradient of resonance magnitude with lead and gain is approximately zero. It appears that this choice of ω_B, for the controlled element form assumed, produces a closed-loop system with minimum sensitivity to changes in pilot compensation. It is noted that the magnitude of the bandwidth producing these characteristics is related to the equivalent time delay in that, for smaller time delays, a higher bandwidth would be achievable.

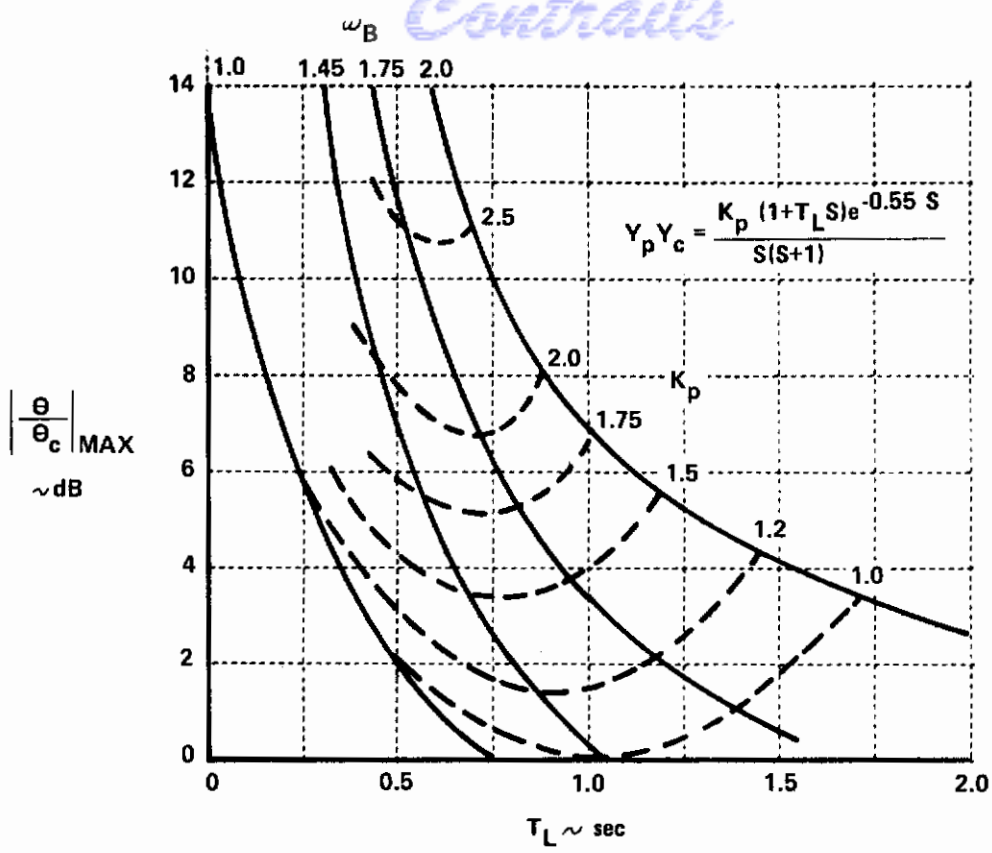

Figure 9 (a) RESONANCE MAGNITUDE AS A FUNCTION OF PILOT LEAD, GAIN AND BANDWIDTH FREQUENCY, $Y_c = \frac{1}{S(S+1)}$

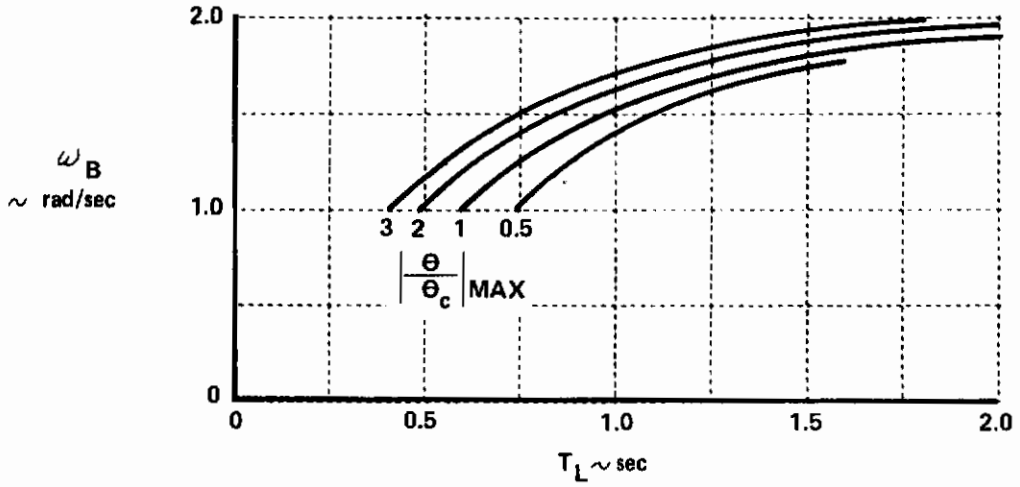

Figure 9 (b) BANDWIDTH FREQUENCY AS A FUNCTION OF PILOT LEAD FOR CONSTANT RESONANCE MAGNITUDE

In summary, ω_B = 1.45 may be thought of as the maximum closed-loop bandwidth (determined by system characteristics) that the pilot would be likely to try to achieve unless task and input noise characteristics forced him higher. Higher bandwidths could also be realized, if necessary, but for low resonance, large increments in lead would be required.

From the standpoint of input noise effects, the artificial turbulence simulated in the NRC experiment, with a break frequency of the order of .2 radians/second, would not likely, of itself, demand high bandwidth. With the exception of Reference 15, little data is available to indicate task related effects on bandwidth. Based on these considerations, ω_B = 1.45 was considered a reasonable criterion for the closed-loop analyses described in the following sections. The value of bandwidth to be used in a specification requirement will have to be established from experimental results and will probably be a function of task and control modes available, i.e. whether or not direct force control is available.

Effect of $Z_w (1/T_{\theta_2})$ at Constant Short Period Frequency

Configurations 6, 1 and 10 were analyzed to determine the variations in pilot closure characteristics as a function of Z_w with constant short term (short period) dynamic characteristics. The following table summarizes the characteristics of the model attitude transfer functions (Equation 2) together with the ratings of the four pilots.

Config.	Z_w	δ	$2\zeta\omega_n$	ω_n	Pilot Ratings			
					A	B	C	D
6	-.25	.03	1.75	1.0	4.5			3
1	-.50	.02	1.75	1.0	4, 4	4	3	3
10	-1.0	.02	1.75	1.0	8, 7	7.5, 5	6	3 → 4

For each of these attitude transfer functions, the closed-loop frequency response characteristics were calculated as a function of pilot lead compensation T_L . The pilot gain, K_p , was adjusted in a dependent fashion to satisfy the bandwidth condition (ω_B = 1.45). In these experiments, the pilot was allowed to adjust the controlled element gain, that is, $M_{\delta_{ES}}$. It is assumed, therefore, that there was no significant influence of pilot gain K_p on the pilot ratings. In other words the loop gain, proportional to $K_p M_{\delta_{ES}}$, could be adjusted to satisfy the bandwidth criterion while maintaining optimum values of K_p through appropriate adjustments to $M_{\delta_{ES}}$.

Figures 10, 11 and 12 illustrate the variation in closed-loop frequency response as a function of the lead compensation, T_L . It is noted that the lead compensation is not limited significantly by low-frequency "droop". The plots tend to indicate, rather, a resonance amplitude and pilot lead trade-off. That is, for a given configuration, as lead increases, the closed-loop resonance is reduced.

This closed-loop resonance and pilot lead trade-off is summarized, for the three configurations, in Figure 13. It can be observed that the pilot rating trends and the closed-loop system measures appear consistent. That is, at a given level of closed-loop resonance $(\theta/\theta_c)_{MAX}$, the pilot ratings tend, on the average, to degrade in proportion to the required lead compensation. In addition, the configuration receiving the worst ratings was the least sensitive to improvement with increased lead. Further, the effect of increasing the magnitude of Z_w appears to be to reduce the effective total damping of the closed-loop system as indicated by the requirement for increased pilot lead compensation.

Further insight into this phenomenon can be gained by considering the effect of Z_w on the root loci of the θ/θ_c transfer function with attitude feedback only. Neglecting the effect of model following and force feel dynamics, a root locus plot for pitch attitude feedback gain for Configuration 10 is shown in Figure 14. At sufficiently high gain, the numerator zero s-Z_w is

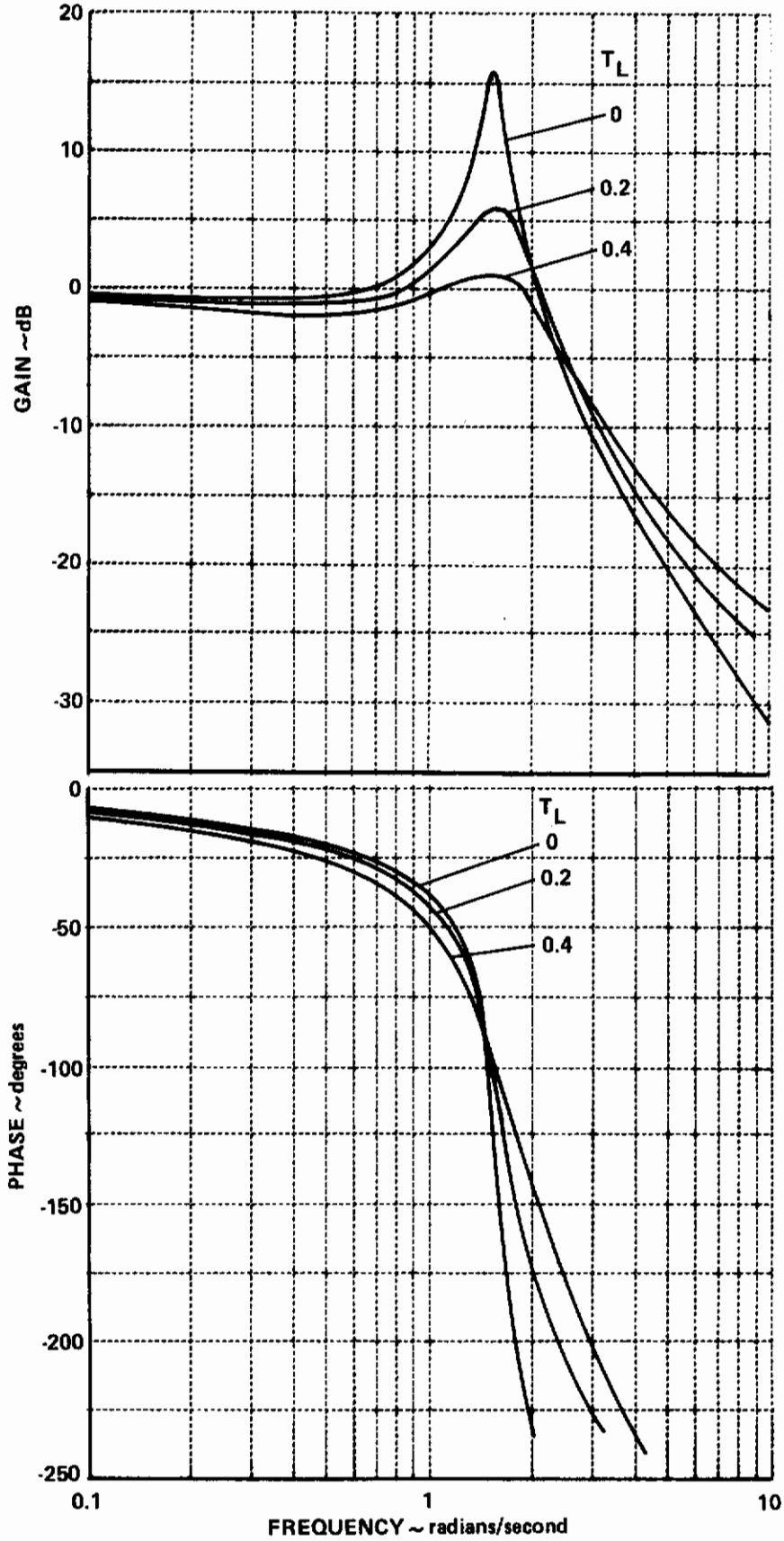

Figure 10 CLOSED-LOOP FREQUENCY RESPONSE AS A FUNCTION OF T_L FOR CONFIGURATION 6

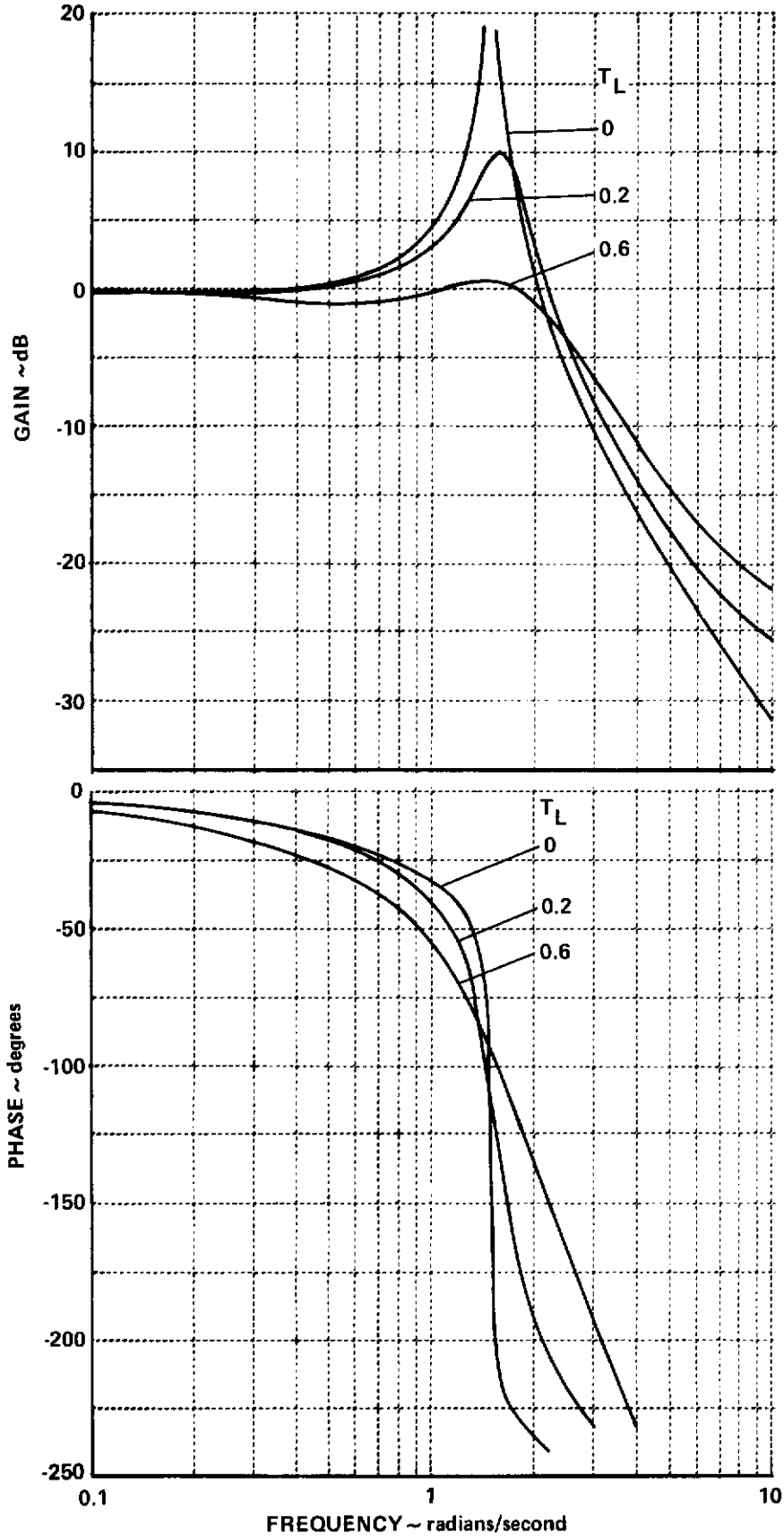

Figure 11 CLOSED-LOOP FREQUENCY RESPONSE AS A FUNCTION OF T_L FOR CONFIGURATION 1

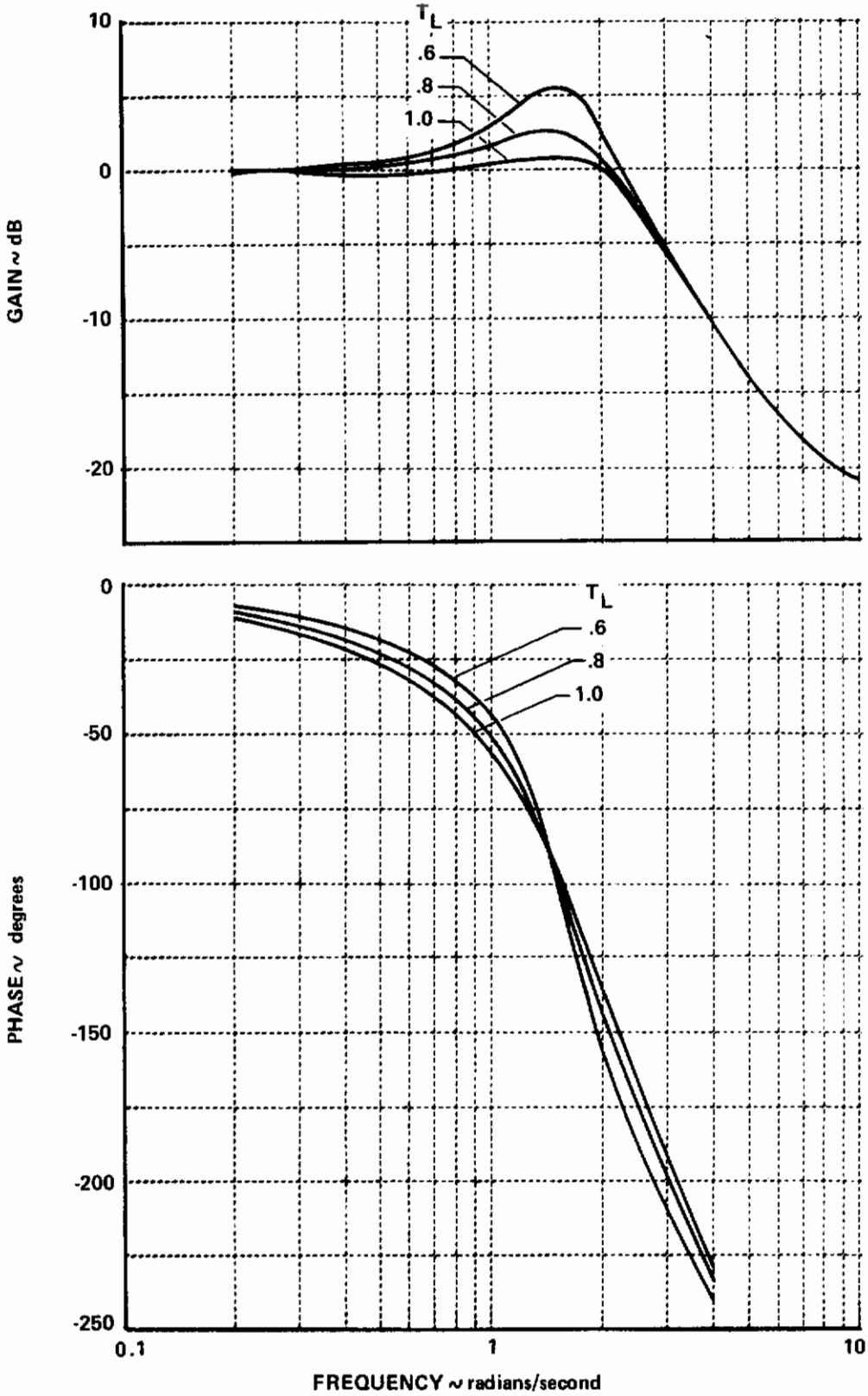

Figure 12 CLOSED-LOOP FREQUENCY RESPONSE AS A FUNCTION OF T_L FOR CONFIGURATION 10

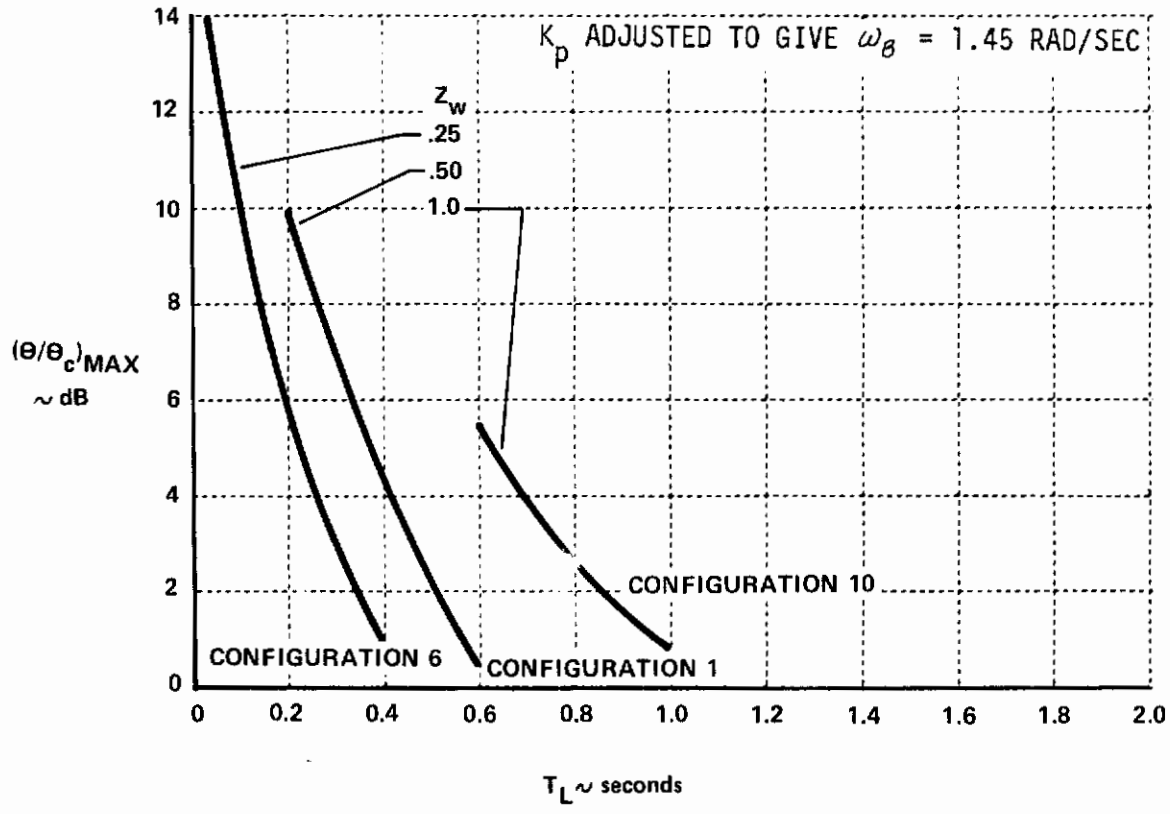

Figure 13 VARIATION IN MAXIMUM RESONANCE PEAK $(\Theta/\Theta_c)_{MAX}$ WITH LEAD COMPENSATION T_L AND Z_w

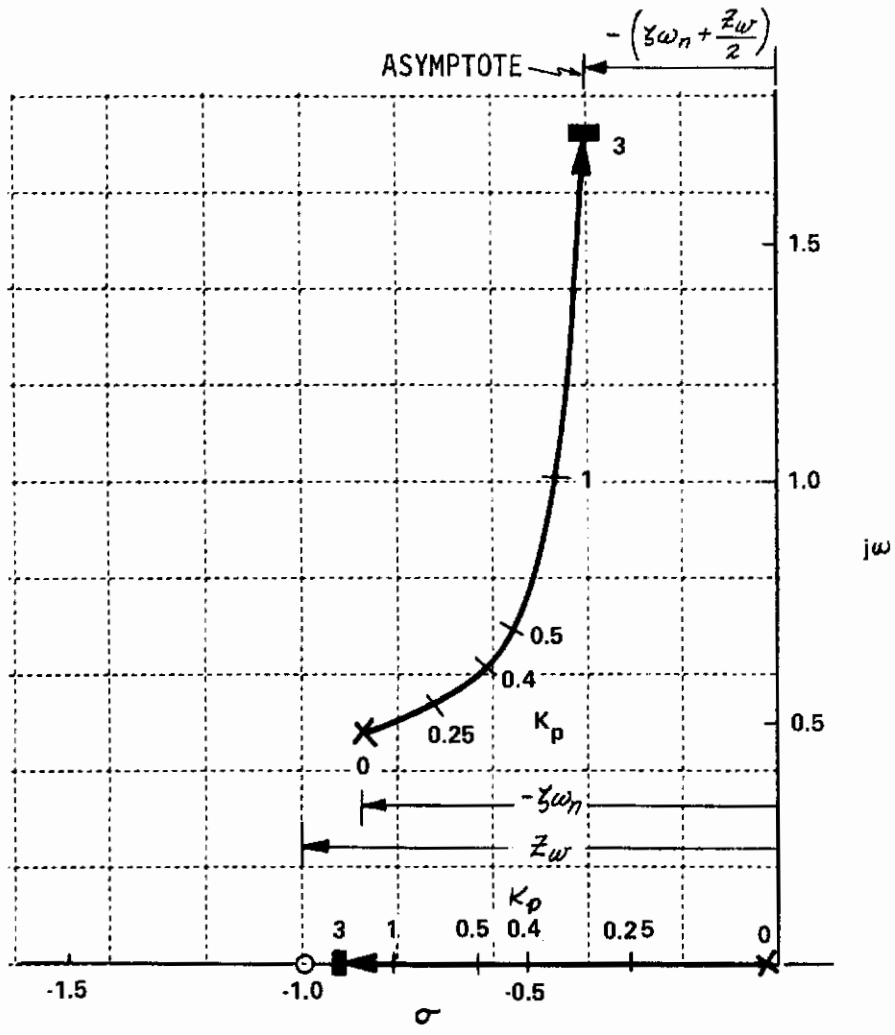

Figure 14 ROOT LOCUS FOR CONFIGURATION 10 WITH ATTITUDE FEEDBACK ONLY, $T_L = \tau_e = 0$

approximately cancelled by a denominator pole and the transfer function is characterized by a second-order lightly damped pair of oscillatory roots. The total damping of this second-order pair of roots asymptotically approaches $2\zeta\omega_n + Z_w$ where $2\zeta\omega_n$ is the total damping of the basic aircraft oscillatory roots. Thus, increasing the magnitude of $-Z_w$ while holding $2\zeta\omega_n$ constant tends to reduce the damping of the closed-loop system. The effect of the feel system and model-following lags is to deflect the root loci toward the right half plane and will cause instability if the gain is high enough.

Pilot commentary for Configuration 10 tends to support the trends indicated by the closed-loop analyses. Difficulties in controlling attitude with attendant airspeed control problems were cited. Specifically, Pilot A complained of pitch oscillations requiring too much attention. Pilot D remarked that for rapid large pitch control inputs, an overcontrolling and PIO tendency was developed which could be alleviated by the pilot reducing his gain.

Effect of Short Period Frequency (ω_n)

The effects of varying short-term frequency at two levels of $-Z_w$ were examined. The coefficients of the attitude transfer functions are tabulated below. At the lowest values of frequency ω_n = .42 and .45 rad/sec, the short-period roots have degenerated into a pair of real roots.

Config.	Z_w 1/sec	δ 1/sec	$-(\lambda_1+\lambda_2)$ $2\zeta\omega_n$ 1/sec	$\lambda_1\lambda_2$ ω_n^2 1/sec^2	Pilot Ratings			
					A	B	C	D
1	-.5	.02	1.75	1.0	4, 4	4	3	3
2	-.5	.01	1.75	.79	3	4	-	-
3	-.5	0	1.75	.66	5, 8.5	7.5	-	-
5	-.5	-.09	1.75	.42	9	-	-	-
10	-1.0	.02	1.75	1.0	8, 7	7.5, 5	6	3→4
11	-1.0	.013	1.75	.86	7	7, 7	-	-
12	-1.0	0	1.75	.71	8.5, 8	7	-	-
15	-1.0	-.09	1.75	.45	8	9.5	-	-

The closed-loop frequency responses for these configurations are shown in Figures 11, 12 and 15 to 18 as functions of lead compensation.

The curves, once again, indicate the trade-off between closed-loop resonance and pilot lead. Low-frequency "droop" does not limit the maximum lead compensation applied. Figure 19 summarizes the variation in $(\theta/\theta_c)_{MAX}$ with T_L . At the lowest short period frequencies (Configurations 5 and 15), increased lead compensation was effective in reducing the resonance above ω = 1.0 rad/sec but a secondary resonance appeared at a lower frequency. Configurations with the poorest ratings are, as before characterized by the greatest lead requirements for a given level of closed-loop resonance and also show a lower rate of improvement with increasing lead.

Figure 20 is a root locus plot for Configuration 5 showing the effect of pure attitude feedback (T_L, pilot and vehicle time delays are neglected). When the short period has degenerated into a pair of real roots, the lowest-frequency root and the root $-\delta$ tend to combine into a lightly damped oscillatory pair at moderate gain levels.

Pilot commentary for Configurations 3 and 5 suggest that the pitch attitude control problems are a combination of closed-loop and open-loop difficulties. Complaints of enormous steady-state responses and attitude divergence suggest that the residue of the low-frequency roots may be the source of trouble.

Only one evaluation of Configuration 5 was made and the pilot commented on a pitch PIO as the aircraft was leveled. This situation could arise if the pilot attempted tight pitch attitude control (high pilot gain) without developing adequate lead. The closed-loop system would be similar to that shown in Figure 20, but with lower damping of the low-frequency roots because of the effects of pilot time delay.

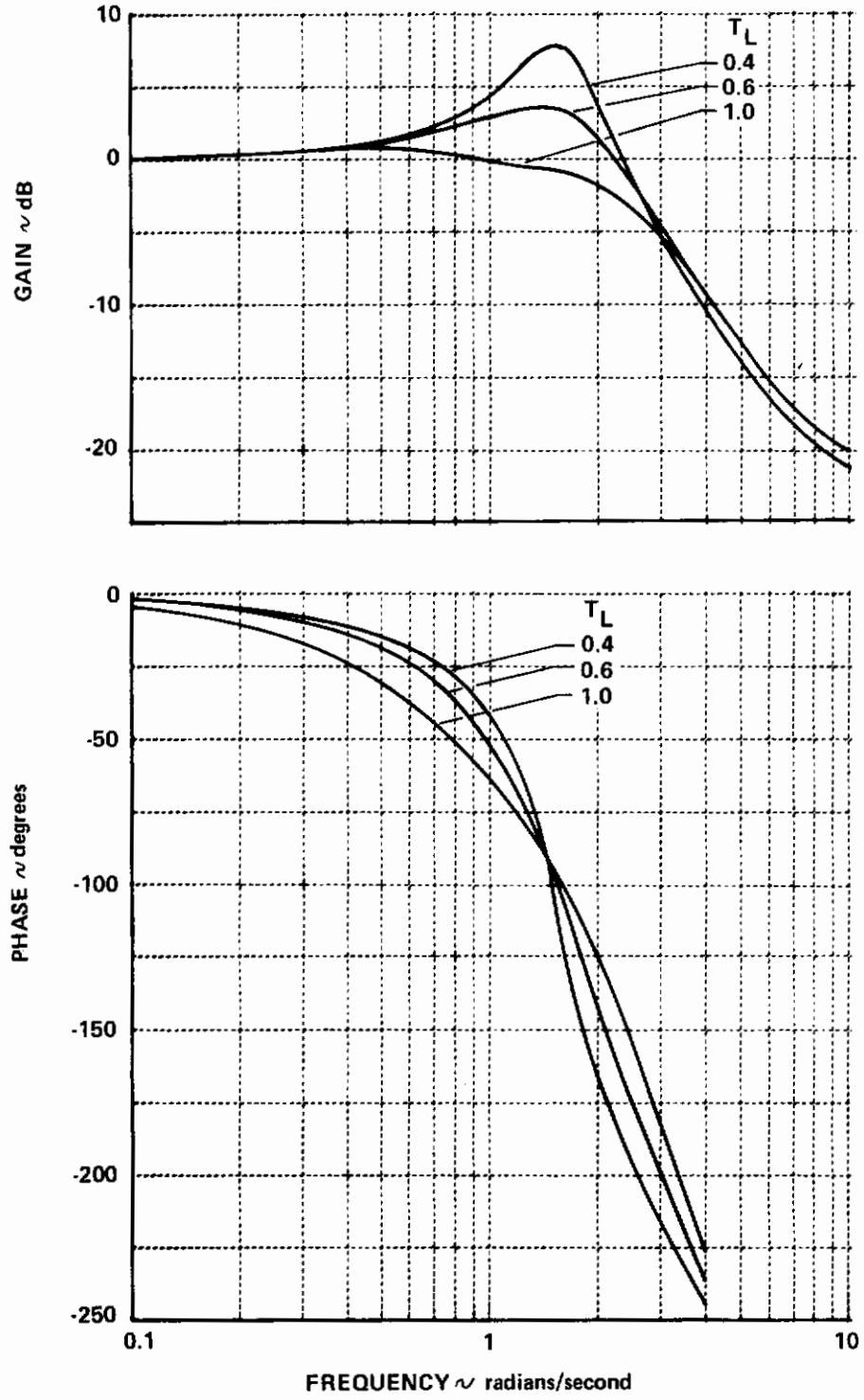

Figure 15 CLOSED-LOOP FREQUENCY RESPONSE AS A FUNCTION OF T_L FOR CONFIGURATION 3

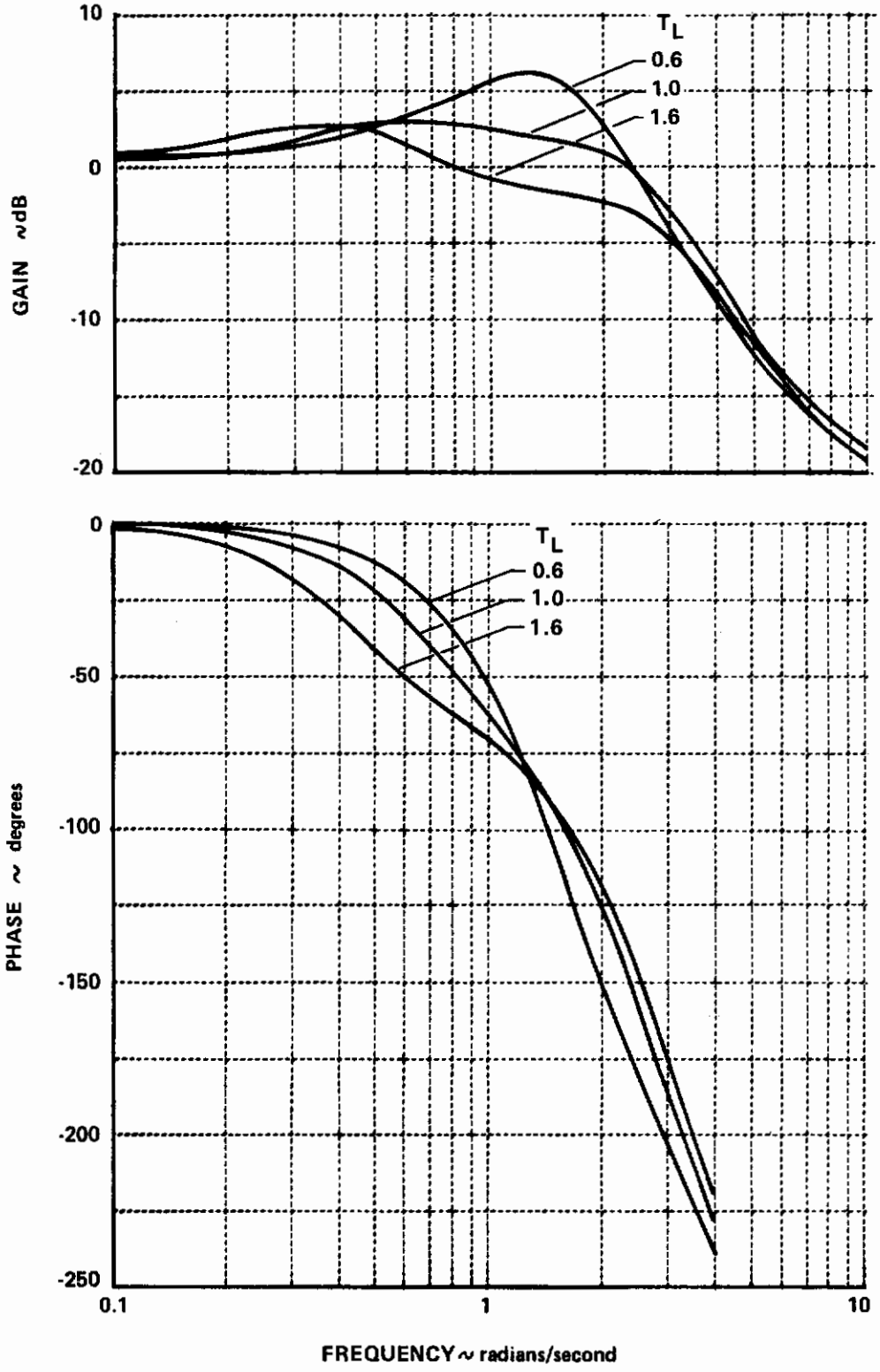

Figure 16 CLOSED-LOOP FREQUENCY RESPONSE AS A FUNCTION OF T_L FOR CONFIGURATION 5

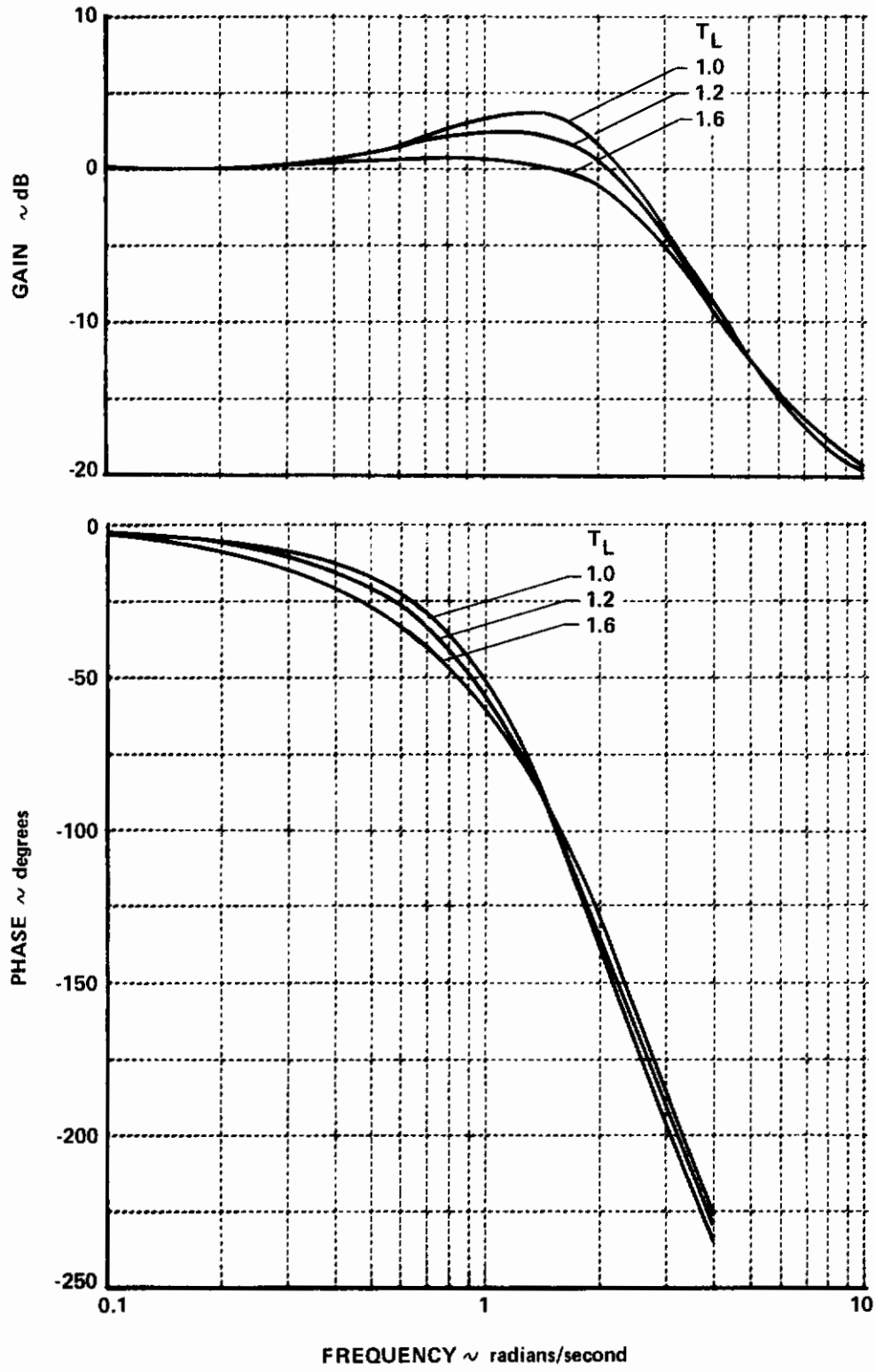

Figure 17 CLOSED-LOOP FREQUENCY RESPONSE AS A FUNCTION OF T_L FOR CONFIGURATION 12

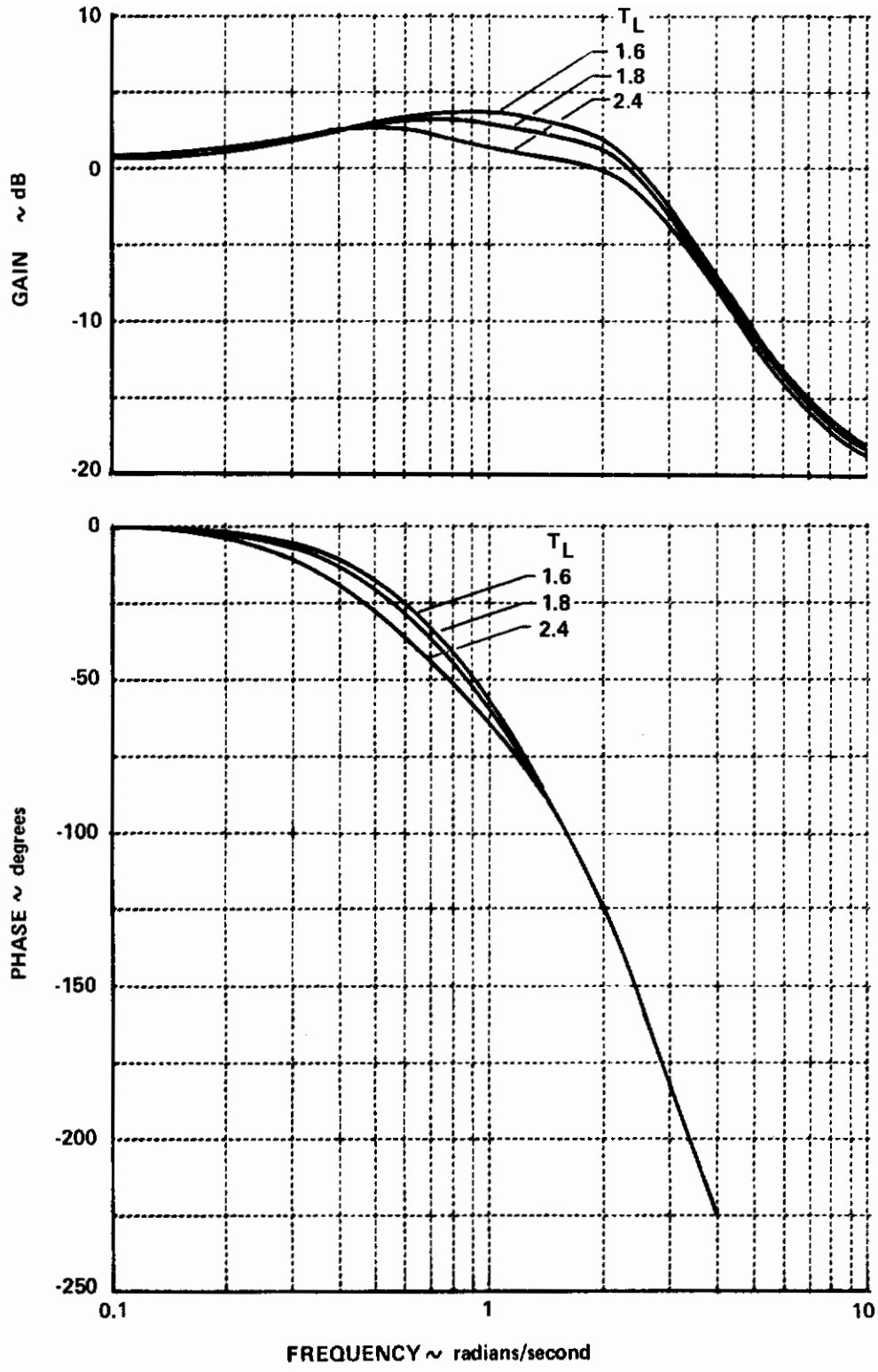

Figure 18 CLOSED-LOOP FREQUENCY RESPONSE AS A FUNCTION OF T_L FOR CONFIGURATION 15

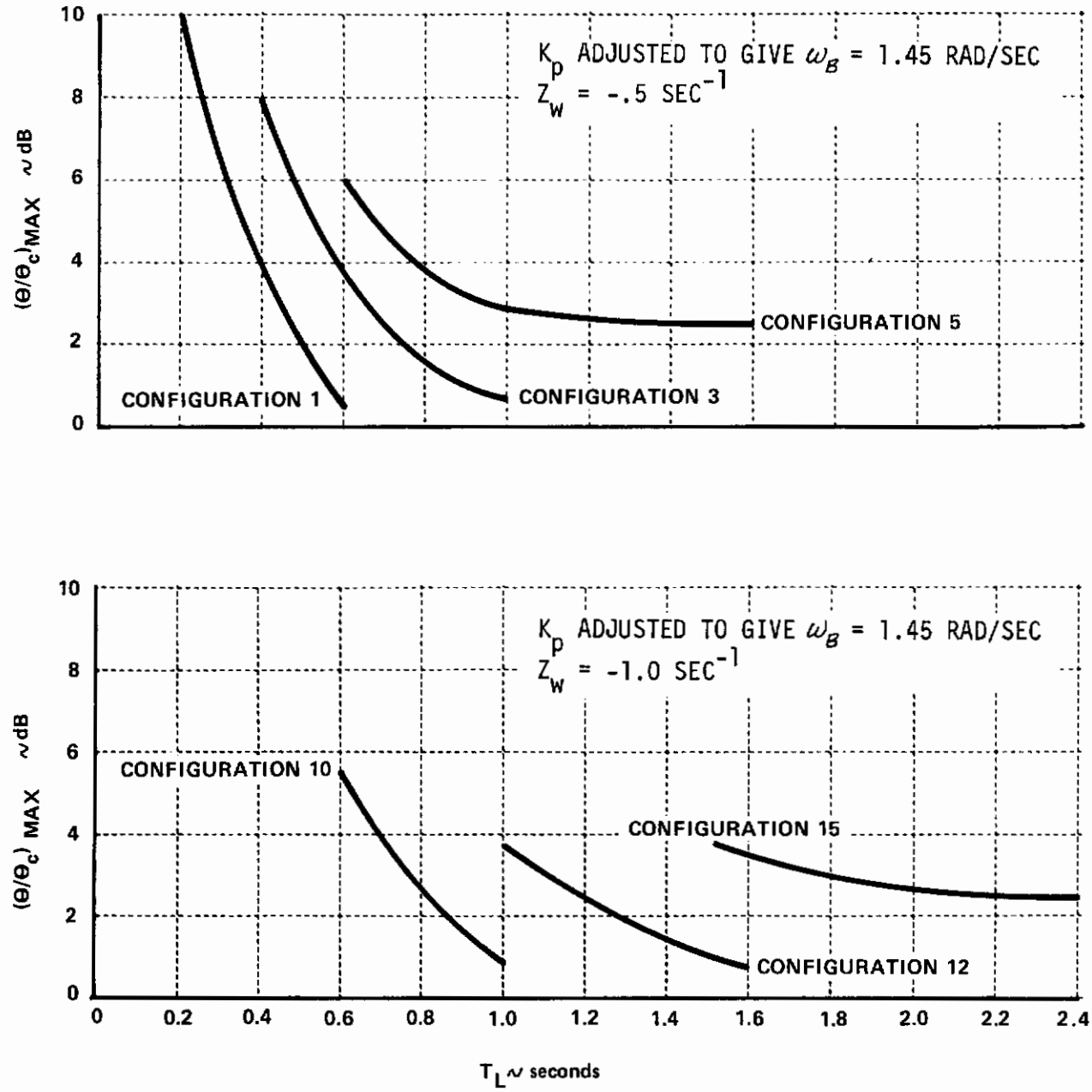

Figure 19 VARIATION IN MAXIMUM RESONANCE PEAK $(\Theta/\Theta_c)_{MAX}$ WITH LEAD COMPENSATION AND SHORT PERIOD FREQUENCY AT TWO VALUES OF Z_w

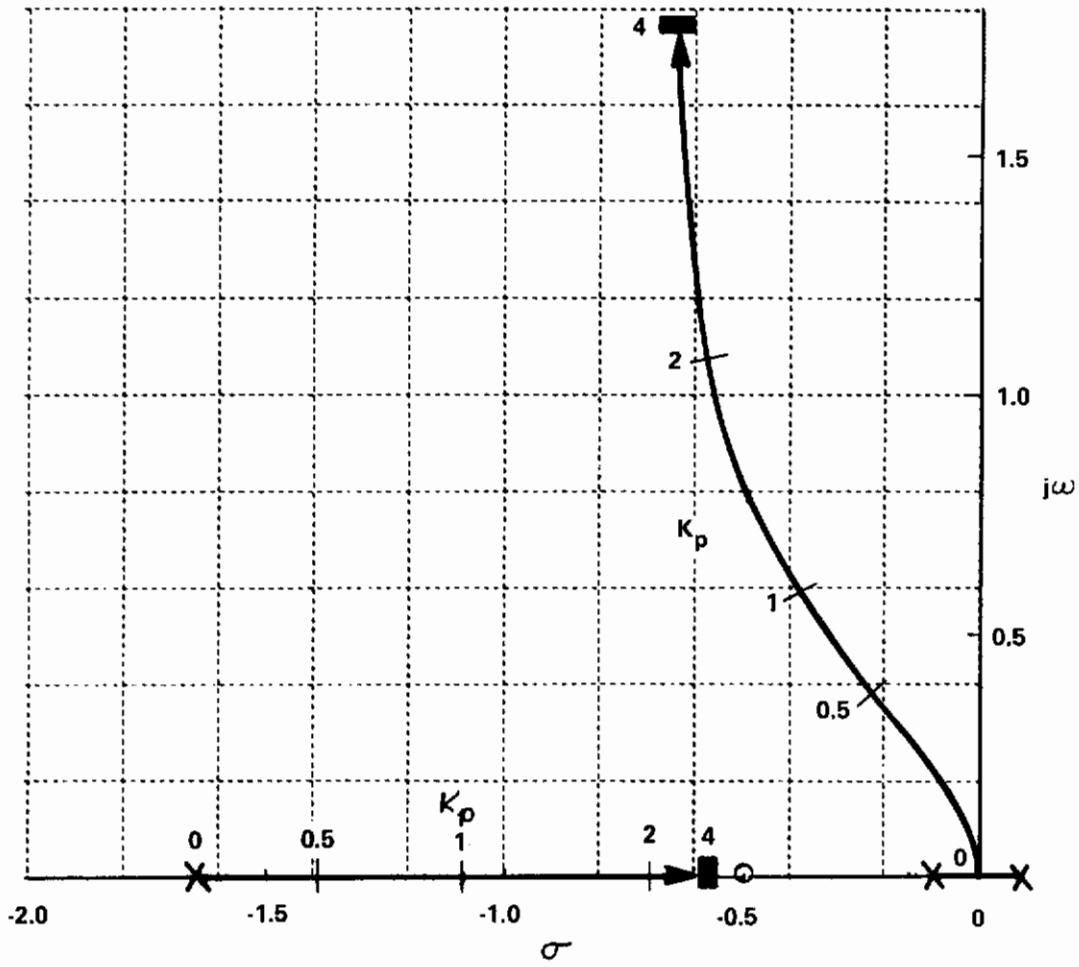

Figure 20 ROOT LOCUS FOR CONFIGURATION 5 WITH ATTITUDE FEEDBACK ONLY, $T_L = \tau_e = 0$

Effect of Short-Period Damping ($2\zeta\omega_n$)

Variations in total damping ($2\zeta\omega_n$) was simulated only at Z_w = -.5. To illustrate the effects of reduced damping, Configurations 1 and 18 are compared. The following table summarizes the pertinent transfer function coefficients.

Config.	Z_w	δ	$2\zeta\omega_n$	ω_n	Pilot Ratings			
					A	B	C	D
1	-.5	.02	1.75	1.0	4, 4	4	3	3
18	-.5	.034	1.0	1.0	8.5	7	5	-

Comparisons of Figures 11 and 21 shows the effect of varying lead compensation on the closed-loop frequency response characteristics. The effect of the reduced damping of Configuration 18 is evidenced by the requirement for increased lead at a given level of closed-loop resonance. In addition, this configuration exhibits a tendency to increased low-frequency "droop" at high values of T_L . Examination of the summary plot (Figure 22) suggests that with the lower damping the pilot is likely to be restricted in the trade-off between resonance and droop that he can make. At high T_L he is able to reduce the resonance peak but only at the expense of increased droop. The converse applies for reduced T_L .

Pilot comments for Configuration 18 are somewhat contradictory, which is likely attributable to the large lead requirement to compensate for inadequate damping, and the difficulty of suppressing a resonance peak without incurring excessive "droop". Pilots A and B both complained of oscillatory tendencies while Pilot C commented that there were no oscillatory tendencies.

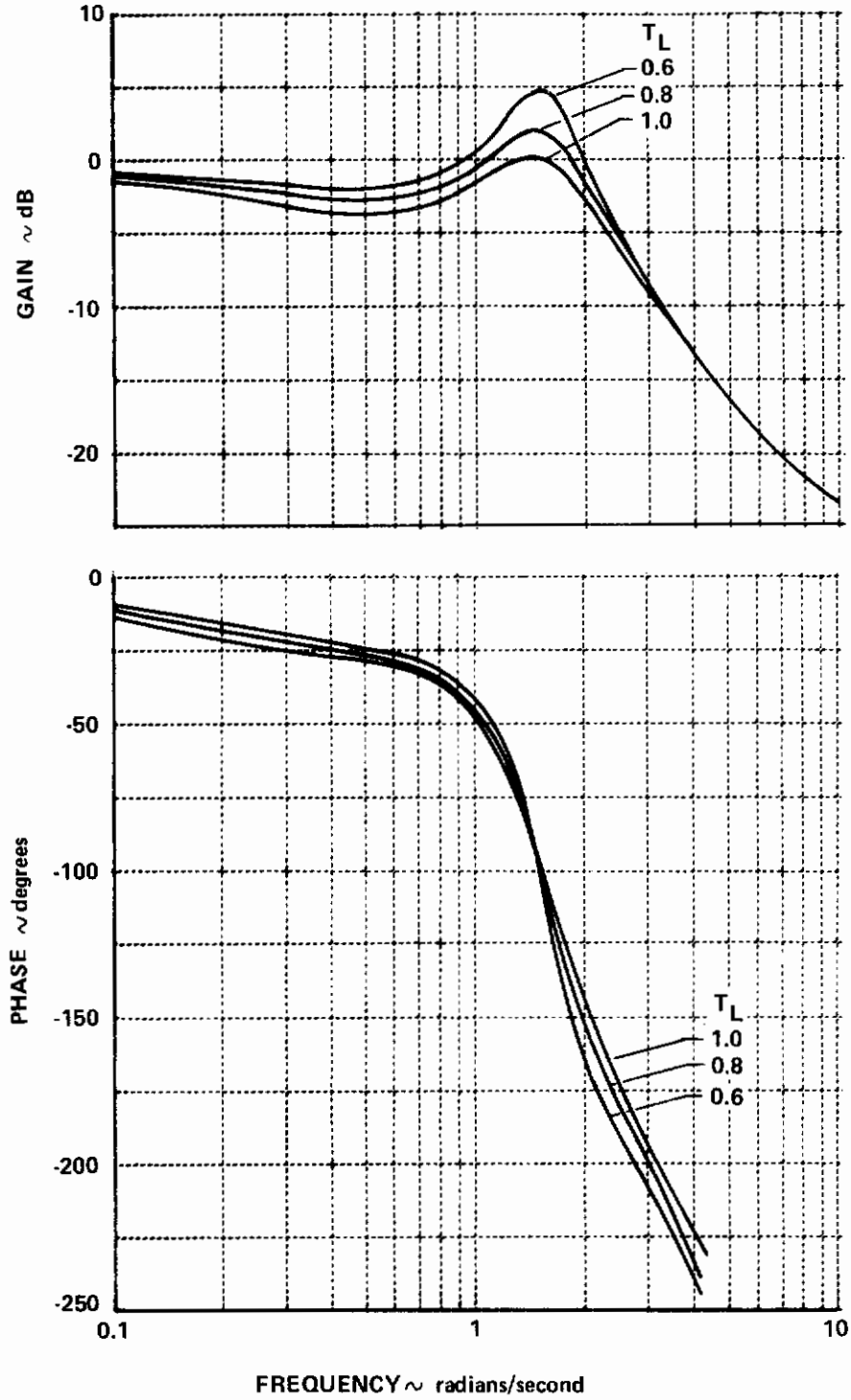

Figure 21 CLOSED-LOOP FREQUENCY RESPONSE AS A FUNCTION OF T_L FOR CONFIGURATION 18

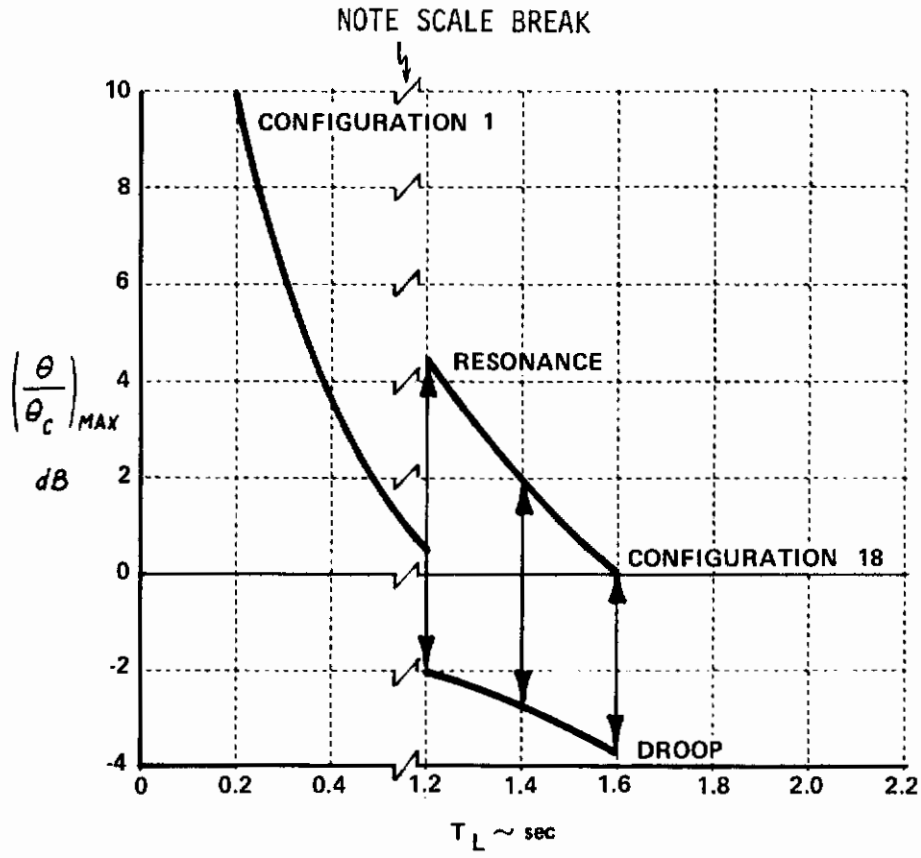

Figure 22 VARIATION IN MAXIMUM RESONANCE PEAK $(\Theta/\Theta_c)_{MAX}$ WITH LEAD COMPENSATION FOR TWO VALUES OF SHORT PERIOD DAMPING

2.4 COMPARISON OF NRC GROUP I DATA TO PITCH MANEUVER RESPONSE REQUIREMENT OF REFERENCE 15

The configurations of Group I of the NRC experiment were compared to the pitch maneuver response requirement recommended in Reference 15. The phase angle increment, $\Delta \angle_\theta$, and the slope parameter $\Delta A/\Delta \angle_\theta$ are defined in Reference 15. These measurements were taken from plots of $|\theta/F_s|$ vs. $\angle\left(\frac{\theta}{F_s} + \tau\omega\right)$ for the combined feel system, model-following system and the model configurations of Group I. The measured data are contained in Figure 23 for ω_θ = 1.2 rad/sec and ω_θ = 1.45 rad/sec. The data for ω_θ = 1.2 rad/sec are plotted in Figure 24. The dashed lines on Figure 24 are the Level 1 and Level 2 requirement boundaries recommended in Reference 15. The solid line indicates adjustment to the Level 2 boundary that would better accomodate the NRC data. Even with this adjustment to the Level 2 boundary, however, there are several configurations in the Level 2 region (Configurations 3, 4, 5, 8, 9, 10, 11, 17 and 18), that received ratings worse than PR = 6.5. The rationalization for including these configurations in the Level 2 region of the pitch maneuver response requirement is that characteristics other than pitch maneuvering may have contributed to the poor ratings. The drag characteristics of the helicopter resulted in a rather high value of $\frac{u}{\theta}\Big|_{ss}$ = -13 (ft/sec)/deg. Because of this characteristic, considerable precision in attitude control was required to maintain the reference airspeed.

Data for the landing approach Flight Phase from References 10 and 17 are presented in Figures 25 and 26. The revised Level 2 boundary would represent a conservative interpretation of the data from Reference 17.

The correlation obtained for the data in Figures 24, 25, and 26 is encouraging and further testing and development of the open-loop pitch maneuver response requirement is recommended.

---

17. Wasserman, R. et al.: "In-Flight Simulation of Minimum Longitudinal Stability for Large Delta-Wing Transports in Landing Approach and Touchdowns." AFFDL-TR-72-143, Vol. I and II, February 1973.

CONF.	Z_w 1/SEC	$2\zeta\omega_n$ 1/SEC	$\Delta\phi_\theta$ ω_θ = 1.2 DEG	$\Delta\phi_\theta$ ω_θ = 1.45 DEG	SLOPE $(\Delta A/\Delta\phi_\theta)$ ω_θ = 1.2 dB/DEG	SLOPE $(\Delta A/\Delta\phi_\theta)$ ω_θ = 1.45 dB/DEG	PR A	PR B	PR C	PR D
1			-71.6	-87.9	.140	.140	4, 4	4	3	3
2			-81.6	-94.6	.178	.161	3	4		
3	-.5	1.75	-85.7	-97.9	.211	.170	5, 8.5	7.5		
4✓			-89.3	-100.4	.240	.174	5, 7	7.5, 7.5, 7.5	6	7, 3
5✓			-94.3	-104.0	.276	.190	9			
6			-78.7	-99.6	.099	.104	4.5	5		3
7	-.25	1.75	-75.8	-89.3	.171	.148	5, 5	4.5	3	
8			-78.4	-91.2	.184	.149	3, 7	5.5, 6	7.5	
9✓			-80.8	-92.9	.200	.153	6	7.5		8.5
10			-89.0	-103.6	.184	.184	8, 7	7.5, 5	6	3-4
11			-95.3	-108.1	.223	.207	7	7, 7		
12			-101.2	-112.3	.258	.228	8.5, 8	7		
13✓	-1.0	1.75	-106.0	-115.7	.318	.242	7			
14✓			-106.6	-116.1	.314	.246	6	7	6	7.5
15✓			-111.0	-119.2	.393	.246	8	9.5		
16			-74.0	-92.6	.102	.112	3	3		
17	-.5	1.4	-90.4	-103.6	.222	.180	6			7
18			-88.6	-110.7	.062	.080	8.5	7	5	
19	-.5	1.0	-103.9	-115.8	.262	.233	7, 7.5	7	4, 4	7
20✓			-108.7	-118.8	.306	.238	9, 8	8		

✓ UNSTABLE REAL ROOT

Figure 23 PITCH DYNAMIC RESPONSE DATA FOR NRC GROUP I

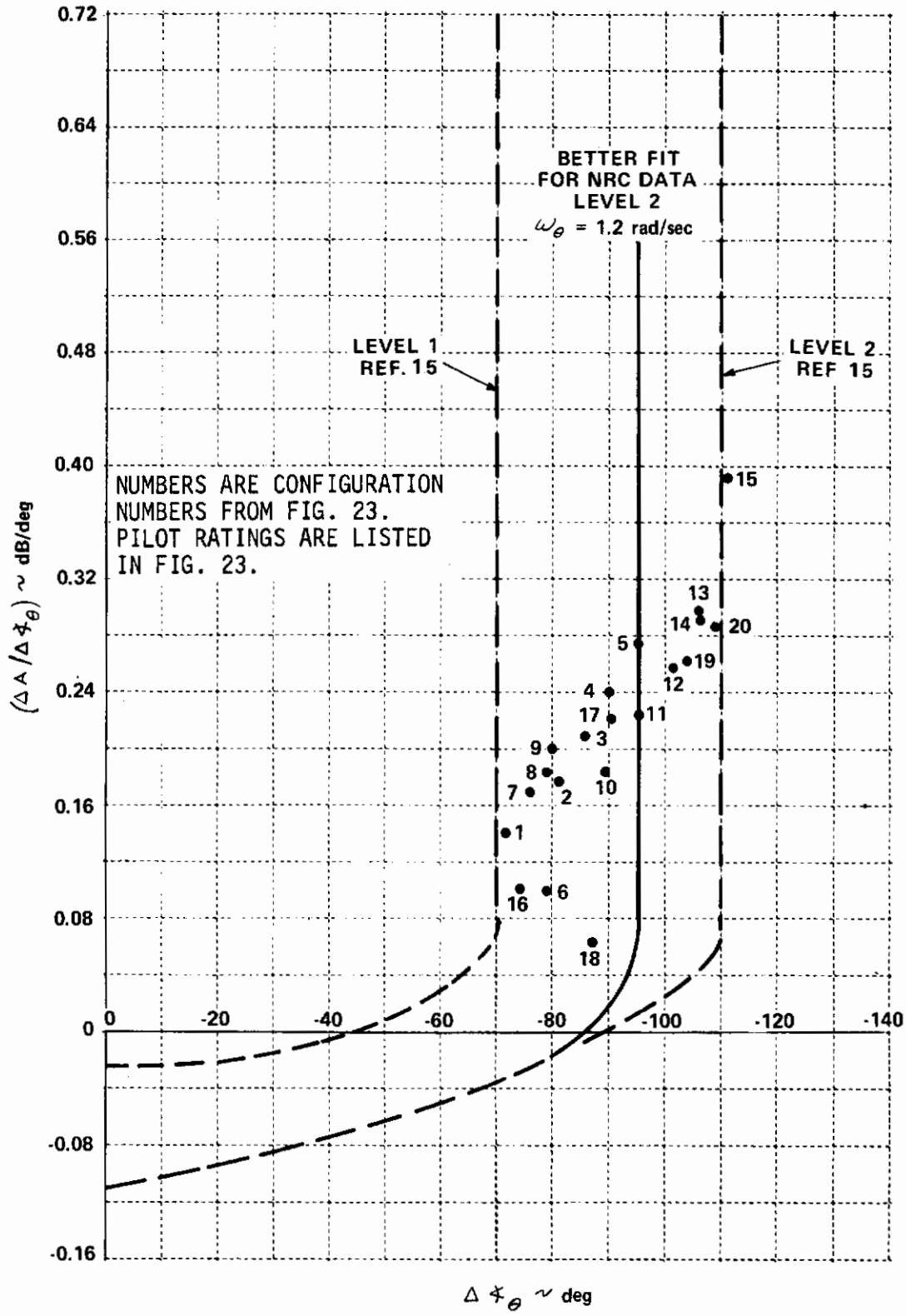

Figure 24 DATA FROM NRC GROUP I COMPARED TO PITCH MANEUVER RESPONSE REQUIREMENT OF REF. 15

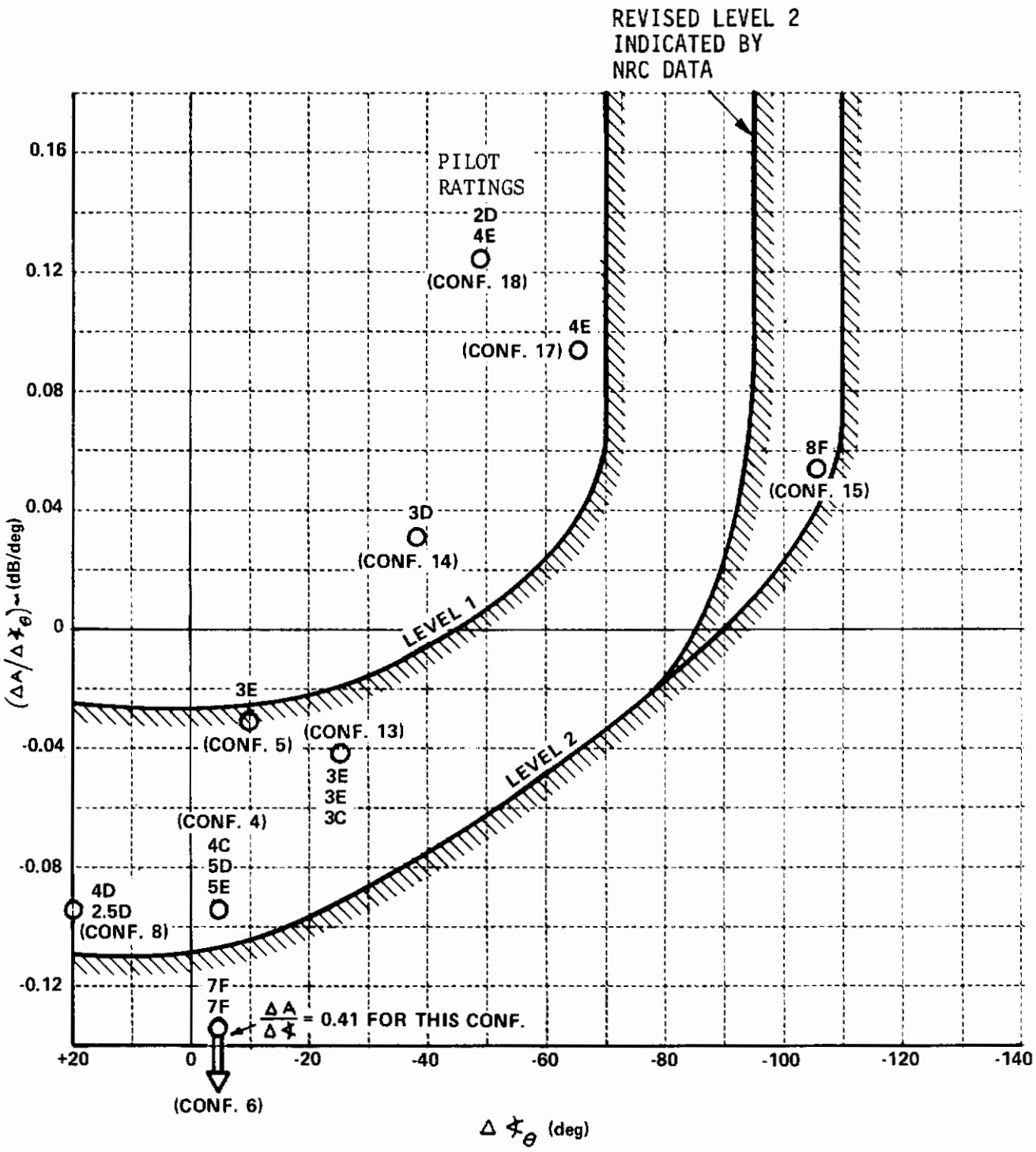

Figure 25 DATA FROM REF. 10 COMPARED TO PITCH MANEUVER RESPONSE REQUIREMENTS OF REF. 15

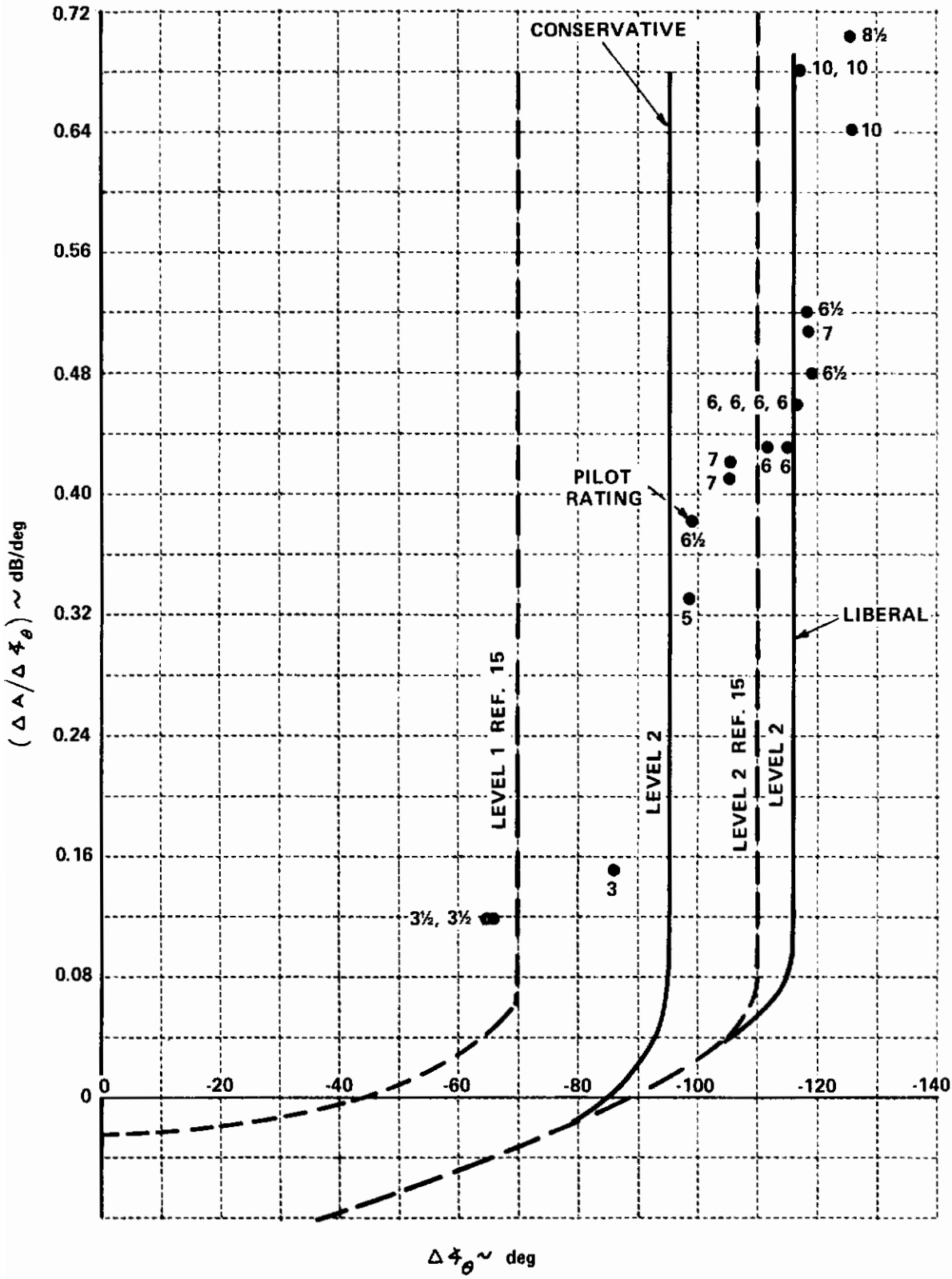

Figure 26 DATA FROM REF. 17 COMPARED TO PITCH MANEUVER RESPONSE REQUIREMENTS OF REF. 15

2.5 CONCLUSIONS AND RECOMMENDATIONS FROM FORWARD FLIGHT EXPERIMENT

1. The experiment described herein has significantly augmented the data base pertinent to the handling qualities of STOL aircraft in the landing approach (PA) Flight Phase.

2. The results have shown that the quality of the pitch attitude control is a dominant factor affecting the ease and precision of speed and flight path control in landing approach. This conclusion is drawn in the context of a STOL aircraft with an effectively vertical thrust magnitude control for which the pilot tends to use attitude as a speed control and thrust magnitude for flight path control.

3. Under conditions of satisfactory pitch attitude control characteristics, the pilots expressed a preference for configurations with little or no coupling of rate of climb response with commanded airspeed changes, i.e., $(\dot{h}/u)_{\delta_{ES}} = 0$. Because the NRC helicopter has no independent control of X-forces, the significance of the other flight-path coupling parameter, $(u/\dot{h})_{\delta_T}$, could not be determined. This parameter should be investigated in a future STOL landing approach simulation.

4. The present formulation of the requirements of MIL-F-83300 relating to longitudinal dynamic characteristics should be modified to reflect characteristics necessary for good pitch attitude control. A major difficulty with paragraph 3.3.2 is the possible ambiguities that may arise from specifying Level 1 and 2 characteristics in terms of the frequency and damping of the second-order pair of roots which primarily shape the angle of attack response. Under conditions of low short-period stiffness (i.e., short period is two real

roots) different frequencies result depending on which low-frequency root is associated with the short period pair. However, even under conditions where the angle of attack response is characterized by a short-period mode well separated from the phugoid, the present paragraph is deficient because it does not account for the effects of control system dynamics.

5. Desirable values of Z_w appear to be bounded by excessive turbulence response at high values and by poor height rate response to thrust magnitude control at low values.

6. Pilot-in-the-loop analysis was a useful analytical tool for gaining insight into the problems of pitch attitude control. Unlike most of the configurations in the Neal-Smith experiment, however, the configurations analyzed in the NRC experiment did not lead to unique closed-loop compensation characteristics. Rather, for each configuration a pilot gain and lead compensation trade-off could be made in meeting the closed-loop bandwidth and resonance limits. The results, however, were consistent in that the configurations receiving the worst pilot ratings required the greatest compensation for a given resonance magnitude and exhibited a reduced gradient of resonance magnitude improvement with increased pilot lead compensation. Pilot-in-the-loop analysis of the results of this experiment should be continued. Specifically, attention should be directed to the attitude configurations of Groups II and III to determine the closed-loop problems introduced by factors such as unstable aperiodic and oscillatory roots of the characteristic equation, and reduced frequency separation of the short period and phugoid modes.

7. Inasmuch as the pilots' attitude closure alters the speed and flight response characteristics, closed-loop analysis should be applied to the outer loop as well. The present data indicates a pilot preference for uncoupled responses. However, additional experimental data and analysis is required for definition of quantitative limits on response coupling.

SECTION III

UARL EXPERIMENT - HOVER & LOW SPEED

3.1 INTRODUCTION

Fixed- and moving-base ground simulator experiments were performed on subcontract by United Aircraft Research Laboratories to obtain additional data for use in the substantiation and refinement of the hover and low speed flight requirements of MIL-F-83300. The results of that investigation, including the documentation of the task and analysis performed by United Aircraft Research Laboratories are reported in Reference 7. In general, the results of the investigation reported in the above reference tend to substantiate the present hover and low speed flight requirements of MIL-F-83300.

It is not the intent of this section to review the experiment reported in Reference 7. Rather, the purpose of this section is the application of recently developed requirements, discussed in detail in Reference 15 to the types of control system dynamics normally associated with hover and low speed flight. In particular, the emphasis will be placed on the application of the format of the recommended revisions to subparagraph 3.2.2 of MIL-F-8785B(ASG), substantiated in Reference 15, to controlled-element transfer functions of the following forms:

a) K/s

b) $K/(s)(s+\lambda)$

c) $K/s\,(s+\lambda)(\tau s+1)$ and

d) K/s^2

These controlled-element transfer functions are essentially of lower order than those used in Reference 15, and to a very large extent tend to typify the form of controlled-element transfer functions associated with VTOL, V/STOL and STOL aircraft for hover and low-speed flight for the height, pitch (roll) attitude, and directional equations of motion.

The following subsections will discuss the application of the "open-loop" requirement of Reference 15 to hover and low speed flight, discuss closed-loop considerations, and review the data presented in several references for comparison of open- and closed-loop parameters for the previously cited transfer function forms.

3.2 OPEN-LOOP EXAMINATION

This subsection will develop a systematic treatment of the low-order transfer functions associated with hover and low speed flight based on the definitions of the parameters described in Reference 15. Once this has been accomplished, correlation studies will be described to relate the results of recent experimental data to the dynamic requirement. In essence, appropriate values of $\Delta\dot{}$ and the corresponding reference frequency (ω_{REF}) will be determined for the various responses of the aircraft for the data base used. These correlation studies should not be interpreted as recommended revisions to MIL-F-83300; rather they represent a direct illustration of the information available from application of the suggested revisions of MIL-F-8785B(ASG) to the hover and low speed flight regime of MIL-F-83300.

3.2.1 Analytical Development of $(\Delta A/\Delta\dot{})_{\omega_{REF}}$ and $\Delta\dot{}$ for Low-Order Transfer Functions

Definitions of $(\Delta A/\Delta\dot{})$ and $(\Delta\dot{})$ for use in the proposed revisions to MIL-F-8785B(ASG) are presented in Reference 15. For the purposes of the following development, slightly different definitions (related to those presented in Reference 15) will be used to develop the "open-loop" parameters for hover, and low speed flight. The term "open-loop" in this discussion indicates that the pilot is not providing any equalization except for gain and therefore can be represented as $K_p e^{-\tau s}$, where K_p represents pilot gain and τ represents time delay introduced by the pilot in the system. The appropriate controlled element transfer function will be represented by Y_c. Thus for the transfer

functions to be considered, the open-loop transfer function has the form ($Y_p Y_c$) where $Y_p = K_p e^{-\tau s}$ and Y_c is selected from the following:

a) $Y_c = K_c / s$

b) $Y_c = \dfrac{K_c}{s(s+\lambda)}$

c) $Y_c = \dfrac{K_c}{s(s+\lambda)(\tau s+1)} = \dfrac{\bar{K}_c}{s(s+\lambda)(s+\gamma)}$

d) $Y_c = K_c / s^2$

3.2.1.1 Simplified Definitions of $(\Delta A/\Delta \measuredangle)_{\omega_{REF}}$ and ($\Delta \measuredangle$) for Use In This Analysis

The parameter $(\Delta A/\Delta \measuredangle)_{\omega_{REF}}$ is defined from the amplitude ratio-phase angle plot of the transfer function $Y_p Y_c$. If the amplitude ratio is plotted versus the phase, then the parameter $(\Delta A/\Delta \measuredangle)_{\omega_{REF}}$ is defined as the local tangent of the amplitude ratio with respect to the phase at the reference frequency. Units are dB/deg.

The parameter ($\Delta \measuredangle$) is defined from the amplitude ratio - phase angle plot of the transfer function $Y_p Y_c$. It is defined as the phase angle at $\omega_{REF} + 90^\circ$, units are degrees.

3.2.1.2 Analytical Determination of $(\Delta A/\Delta \measuredangle)_{\omega_{REF}}$ and ($\Delta \measuredangle$)

Based on the definitions of the "open-loop" parameters presented in 3.2.1.1 for the controlled elements to be investigated in this section, simple analytical expressions can be developed. A sample development is presented in this subsection and a table is obtained that indicates the "open-loop" parameters for low-order systems.

If the controlled element-pilot can be represented by:

$$Y_p Y_c = \frac{K}{s(s+\lambda)(s+\gamma)} e^{-\tau s}$$,then the amplitude ratio can be expressed as

$$G(\omega) = |Y_p Y_c| = \frac{K}{\omega(\omega^2+\lambda^2)^{1/2}(\omega^2+\gamma^2)^{1/2}}$$

and the phase angle by

$$\phi(\omega) = -90^\circ - \tan^{-1}\left(\frac{\omega}{\lambda}\right) - \tan^{-1}\left(\frac{\omega}{\gamma}\right) - \tau_e \omega$$

where $\tau_e = \frac{180}{\pi}\tau$.

Since the parameter $\Delta A/\Delta\phi$ has units of dB/deg, it is necessary to convert the amplitude ratio to dB, thus:

$$20\left[\log_{10} G(\omega)\right] = 20\left[\log_{10} K - \log_{10}\omega - \frac{1}{2}\log_{10}(\omega^2+\lambda^2) - \frac{1}{2}\log_{10}(\omega^2+\gamma^2)\right]$$

From the definition of $\Delta A/\Delta\phi$ it can be shown that

$$\frac{\Delta A}{\Delta\phi} = 20\,\frac{\dfrac{d\left[\log_{10} G(\omega)\right]}{d\left[\log_{10}(\omega)\right]}}{\dfrac{d\left[\phi(\omega)\right]}{d\left[\log_{10}(\omega)\right]}}$$

Application of the chain rule of differentiation, that is,

$$\frac{d\left[\log_{10} G(\omega)\right]}{d\left[\log_{10}(\omega)\right]} = \frac{d\left[\log_{10} G(\omega)\right]}{d\omega} \times \frac{d\omega}{d\left[\log_{10}\omega\right]}$$

for the components of $\log_{10} G(\omega)$ of the form $+\frac{1}{2}\log_{10}(\omega^2+\lambda^2)$ results in the following:

$$20\,\frac{d\left[\frac{1}{2}\log_{10}(\lambda^2+\omega^2)\right]}{d\left[\log_{10}(\omega)\right]} = 20\left[\frac{1}{2}\times\frac{\log_{10}e}{\lambda^2+\omega^2}(2\omega)\times\frac{\omega}{\log_{10}e}\right] = 20\left[\frac{\omega^2}{\lambda^2+\omega^2}\right]$$

$$= 20\left[\frac{1}{1+\left(\frac{\lambda}{\omega}\right)^2}\right]$$

Thus the numerator of $\Delta A/\Delta\phi$ can be written as

$$N\left(\frac{\Delta A}{\Delta\phi}\right) = -20\left[1+\frac{1}{1+\left(\frac{\lambda}{\omega}\right)^2}+\frac{1}{1+\left(\frac{\gamma}{\omega}\right)^2}\right]$$

Similarly,

$$\frac{d\left[\phi(\omega)\right]}{d\left[\log_{10}(\omega)\right]} = \frac{d\phi}{d\omega}\times\frac{d\omega}{\log_{10}\omega} = \frac{d\phi}{d\omega}\times\frac{\omega}{\log_{10}e}$$

For $\phi(\omega) = \tan^{-1}(\omega/\lambda)$, then

$$\frac{d}{d\omega}\tan^{-1}\left(\frac{\omega}{\lambda}\right) = \frac{+\left(\frac{1}{\lambda}\right)}{1+\left(\frac{\omega}{\lambda}\right)^2}$$

and $$\frac{d\left[\phi(\omega)\right]}{d\left[\log_{10}(\omega)\right]} = \frac{+\left(\frac{\omega}{\lambda}\right)}{\left[1+\left(\frac{\omega}{\lambda}\right)^2\right]\log_{10}e}$$

while for the time-delay portion of the phase angle ($\phi = \tau\omega$)

$$\frac{d\left[\phi(\omega)\right]}{d\left[\log_{10}(\omega)\right]} = \frac{+\,180}{\pi\log_{10}e}\left[\tau\omega\right] = \frac{\tau_e\,\omega}{\log_{10}e}$$

Thus the denominator of ($\Delta A/\Delta\phi$) can be expressed as follows (for the transfer function under consideration)

$$D\left(\frac{\Delta A}{\Delta \not\angle}\right) = -\frac{180}{\pi \log_{10} e}\left[\tau\omega + \sum_i \frac{\left(\frac{\omega}{\lambda_i}\right)}{1+\left(\frac{\omega}{\lambda_i}\right)^2}\right]$$

and previously the numerator expression developed was:

$$N\left(\frac{\Delta A}{\Delta \not\angle}\right) = -20\left[\sum_i \left(\frac{1}{1+\left(\frac{\lambda_i}{\omega}\right)^2}\right)\right]$$

Since $\phi(\omega)$ for the transfer function has the form

$$\phi(\omega) = -\sum \tan^{-1}\left(\frac{\omega}{\lambda_i}\right) - \tau_e\omega$$

then from the definition for $\Delta \not\angle$

$$\Delta \not\angle = 90° - \tau_e\omega - \sum_i \tan^{-1}\left(\frac{\omega}{\lambda_i}\right)$$

Table I which follows is a summary of the expressions derived for various controlled elements, when $Y_p = K_p e^{-\tau s}$, for λ and γ real. From the data presented in Table I, it is possible, of course, to establish the expressions for more complex controlled elements. However, this is beyond the scope of the present investigation.

Figure 27 presents the results of the parameter $(\Delta A/\Delta \not\angle)_{\omega_{REF}}$ vs. ($\Delta \not\angle$) for controlled elements and pilot delay with transfer functions of the form

$$e^{-\tau s}\frac{K_c}{s}, \quad e^{-\tau s}\frac{K_c}{s(s+\lambda)} \quad \text{and} \quad e^{-\tau s}\frac{K_c}{s^2}$$

Figure 27 also presents the effects of constant reference frequency. There are several pieces of information that can be obtained from Figure 27. For example when $\Delta \not\angle = -90°$ the Phase Margin (PM) of the system is zero, and the frequency at which this occurs can be obtained from interpolation for any of the transfer functions presented. Thus, for example, for a desired

TABLE I

ANALYTICAL EXPRESSIONS FOR $\Delta\phi$ AND $(\Delta A/\Delta\phi)_{\omega_{REF}}$ FOR SEVERAL CONTROLLED-ELEMENT TRANSFER FUNCTIONS, Y_c

Controlled Element Transfer Function, Y_c	$\Delta\phi$	$N(\Delta A/\Delta\phi)$	$D(\Delta A/\Delta\phi)$
$K_c s$	$180^\circ - \tau_e \omega$	$+20$	$-\dfrac{\tau_e \omega}{\log_{10} e}$
K_c	$90^\circ - \tau_e \omega$	0	$-\dfrac{\tau_e \omega}{\log_{10} e}$
$\dfrac{K_c}{s}$	$-\tau_e \omega$	-20	$-\dfrac{\tau_e \omega}{\log_{10} e}$
$\dfrac{K_c}{s^2}$	$-90^\circ - \tau_e \omega$	-40	$-\dfrac{\tau_e \omega}{\log_{10} e}$
$\dfrac{K_c}{(s+\lambda)}$	$90^\circ - \tau_e \omega - \tan^{-1}\left(\dfrac{\omega}{\lambda}\right)$	$-20\left[\dfrac{1}{1+\left(\frac{\lambda}{\omega}\right)^2}\right]$	$\dfrac{-180}{\pi \log_{10} e}\left[\tau\omega + \dfrac{\left(\frac{\omega}{\lambda}\right)}{1+\left(\frac{\omega}{\lambda}\right)^2}\right]$
$\dfrac{K_c}{s(s+\lambda)}$	$-\tau_e \omega - \tan^{-1}\left(\dfrac{\omega}{\lambda}\right)$	$-20\left[1+\dfrac{1}{1+\left(\frac{\lambda}{\omega}\right)^2}\right]$	$\dfrac{-180}{\pi \log_{10} e}\left[\tau\omega + \dfrac{\left(\frac{\omega}{\lambda}\right)}{1+\left(\frac{\omega}{\lambda}\right)^2}\right]$
$\dfrac{K_c}{(s+\lambda)(s+\gamma)}$	$90^\circ - \tau_e \omega - \tan^{-1}\left(\dfrac{\omega}{\lambda}\right) - \tan^{-1}\left(\dfrac{\omega}{\gamma}\right)$	$-20\left[\dfrac{1}{1+\left(\frac{\lambda}{\omega}\right)^2} + \dfrac{1}{1+\left(\frac{\gamma}{\omega}\right)^2}\right]$	$\dfrac{-180}{\pi \log_{10} e}\left[\tau\omega + \dfrac{\left(\frac{\omega}{\lambda}\right)}{1+\left(\frac{\omega}{\lambda}\right)^2} + \dfrac{\left(\frac{\omega}{\gamma}\right)}{1+\left(\frac{\omega}{\gamma}\right)^2}\right]$
$\dfrac{K_c}{s(s+\lambda)(s+\gamma)}$	$-\tau_e \omega - \tan^{-1}\left(\dfrac{\omega}{\lambda}\right) - \tan^{-1}\left(\dfrac{\omega}{\gamma}\right)$	$-20\left[1+\dfrac{1}{1+\left(\frac{\lambda}{\omega}\right)^2} + \dfrac{1}{1+\left(\frac{\gamma}{\omega}\right)^2}\right]$	$\dfrac{-180}{\pi \log_{10} e}\left[\tau\omega + \dfrac{\left(\frac{\omega}{\lambda}\right)}{1+\left(\frac{\omega}{\lambda}\right)^2} + \dfrac{\left(\frac{\omega}{\gamma}\right)}{1+\left(\frac{\omega}{\gamma}\right)^2}\right]$

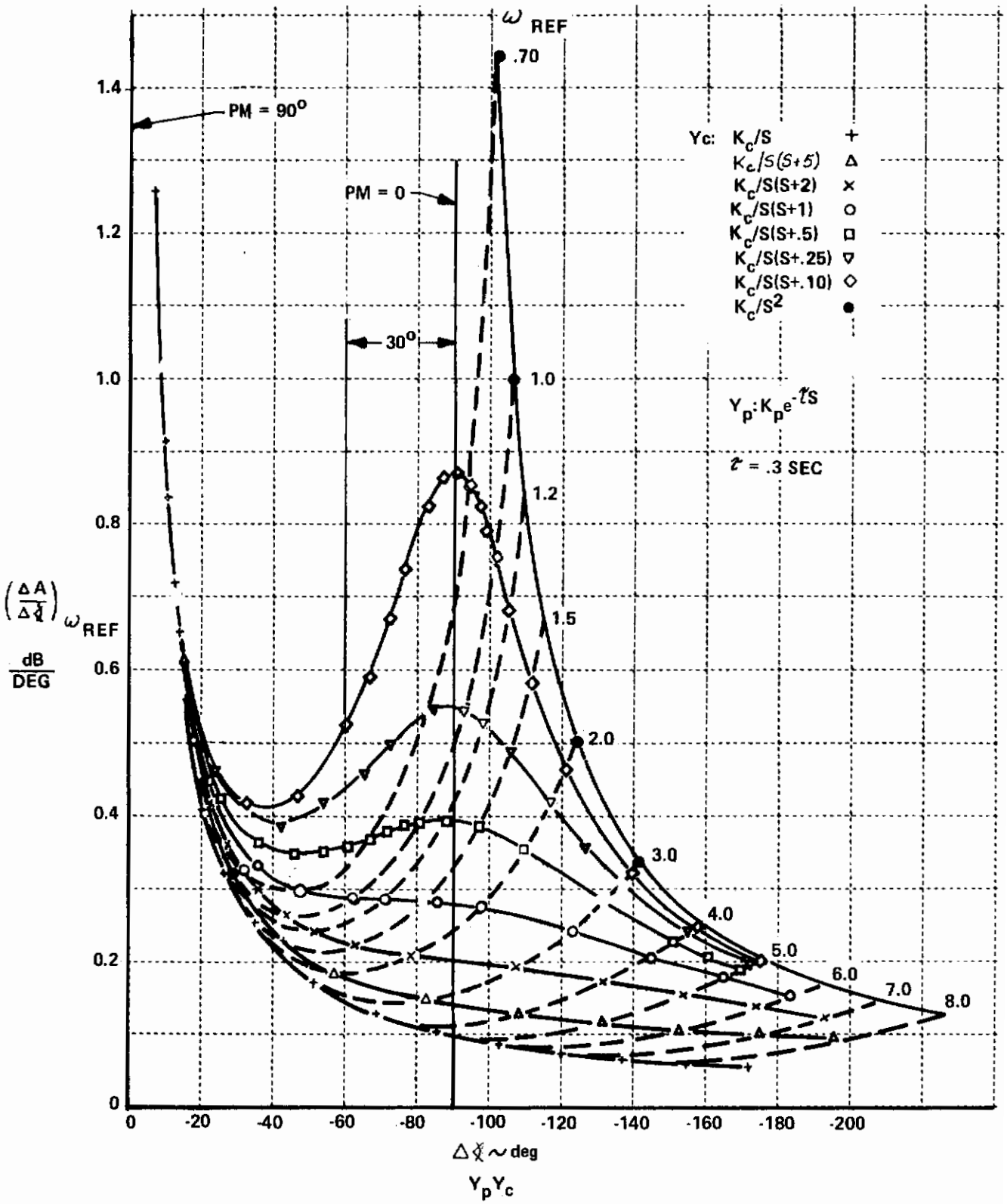

Figure 27 OPEN-LOOP PARAMETERS FOR LOW-ORDER CONTROLLED ELEMENTS

system, the crossover frequency corresponding to a desired phase margin can be obtained directly. In addition, the plot clearly illustrates the change in nature for $K/s(s+\lambda)$ systems as λ varies, from K/s to K/s^2 for $Y_p = K_p e^{-\tau s}$. In addition, it is possible to reconstruct the Bode, or Nichols plot of a given configuration from the variation of $(\Delta A/\Delta \phi)$ and $(\Delta \phi)$ with frequency. Specifically for the correlation studies that are presented in the next subsection, the data presented on Figure 27 will be used in an investigation of the effects of ω_{REF} and $\Delta\phi$ which tend to separate configurations into the Levels required for compliance with MIL-F-83300.

3.2.1.3 Correlation of "Open-Loop" Parameters for Hover and Low Speed Flight

The intent of the following discussion is to perform a preliminary correlation of pilot ratings obtained for hover and low-speed flight with the parameters $\Delta\phi$ and ω_{REF}. The responses of height, pitch (roll) attitude and heading will be examined as primarily single-loop tasks, with only low levels of secondary task or turbulence effects included for the data selected for the correlation studies. The purpose of this correlation is to illustrate that reasonable values of the parameters can be selected which would blend into the revision suggested for pitch dynamics in Reference 15 and could constitute a basis for a more generalized form for the dynamic requirements of both MIL-F-83300 and MIL-F-8785B(ASG). This could allow the dynamic requirements to include higher-order systems (i.e., specific augmentation systems), and remove the need to state dynamic response requirements in terms of particular modes of response. In addition, this would eventually allow the inclusion of time delays, first and higher-order system lags, etc., directly into the dynamic response requirements.

3.2.1.3.1 Correlation With Height Control Characteristics

For small pitch and roll attitude changes, the equation for height control in hovering and low speed flight can be written as follows (including

first-order lag in the control):

$$\frac{h(s)}{\delta(s)} = \frac{-Z_{\delta_c}}{s(s - Z_w)(\tau_h s + 1)} = \frac{K_c}{s(s + \lambda_w)(\tau_h s + 1)}$$

The data obtained for the height control investigations described in References 18 and 7, for $\tau_h = 0$, is presented in Figure 28 for various levels of available thrust-to-weight ratio (T/W). Based on the height control requirements MIL-F-8330, the data for $(T/W) < 1.05$ is separated from the other T/W ratios. Included on Figure 28 are the values of $-Z_w$ which would be associated with Level 1 and 2 values of $\Delta \not\zeta$ for $\omega_{REF} = 1.0$ rad/sec. It should be noted that the pilot rating data from Reference 18 is based on the Cooper rating scale, while the data in Reference 7 is based on the Cooper-Harper pilot rating scale. Reference 2 presents a discussion which indicates the transformation of pilot ratings obtained from these cited pilot rating scales and the level philosophy for compliance with MIL-F-83300. From Figure 28 it appears that when $\tau_h = 0$ and $T/W \geq 1.05$, Level 1 pilot ratings for height control are associated with $\omega_{REF} = 1.0$ and $\Delta \not\zeta = -70°$, while Level 2 is associated with $\omega_{REF} = 1.0$ and $\Delta \not\zeta = -100°$. That is, Level 1 indicates $|-Z_w| \geq .76$ while Level 2 indicates $|-Z_w| > .13$. It should be noted that $|-Z_w| > .13$ is also a reasonable Level 2 boundary for $(T/W) = 1.02$.

Figure 29 presents the data in Reference 18, including the influence of a first-order lag. It should be noted that when the lag is included the amount of data that can be plotted is essentially doubled, that is, the pilot rating associated with the following transfer function

a) $$\frac{K}{s(s + \lambda_w)(\tau_h s + 1)}$$

---

18 Vinje, Edward W. and Miller, David P.: "Analytical and Flight Simulator Studies to Develop Design Criteria for VTOL Aircraft Control Systems." AFFDL-TR-68-165, April 1969.

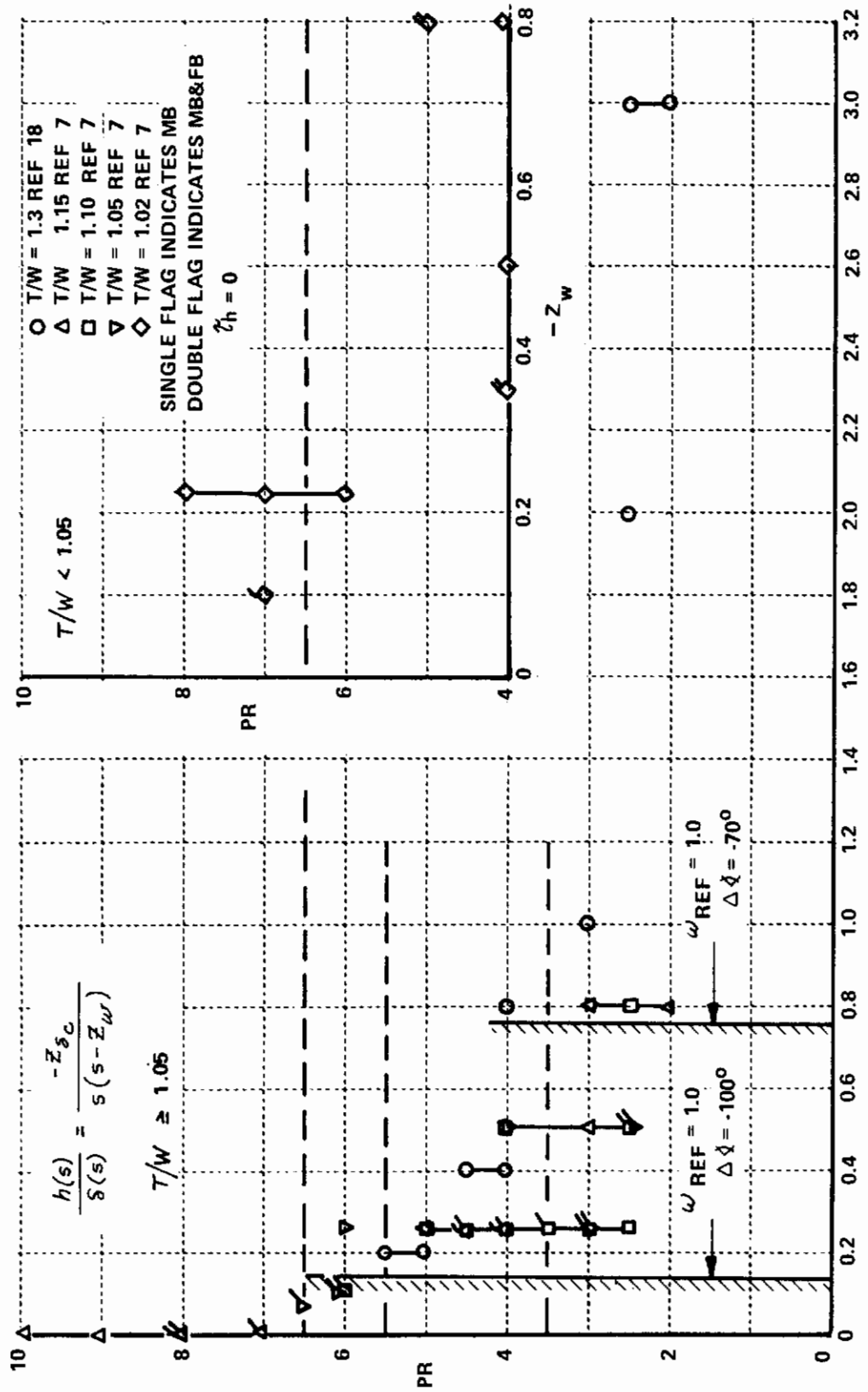

Figure 28 PILOT RATING AS A FUNCTION OF VERTICAL DAMPING AND T/W RATIO

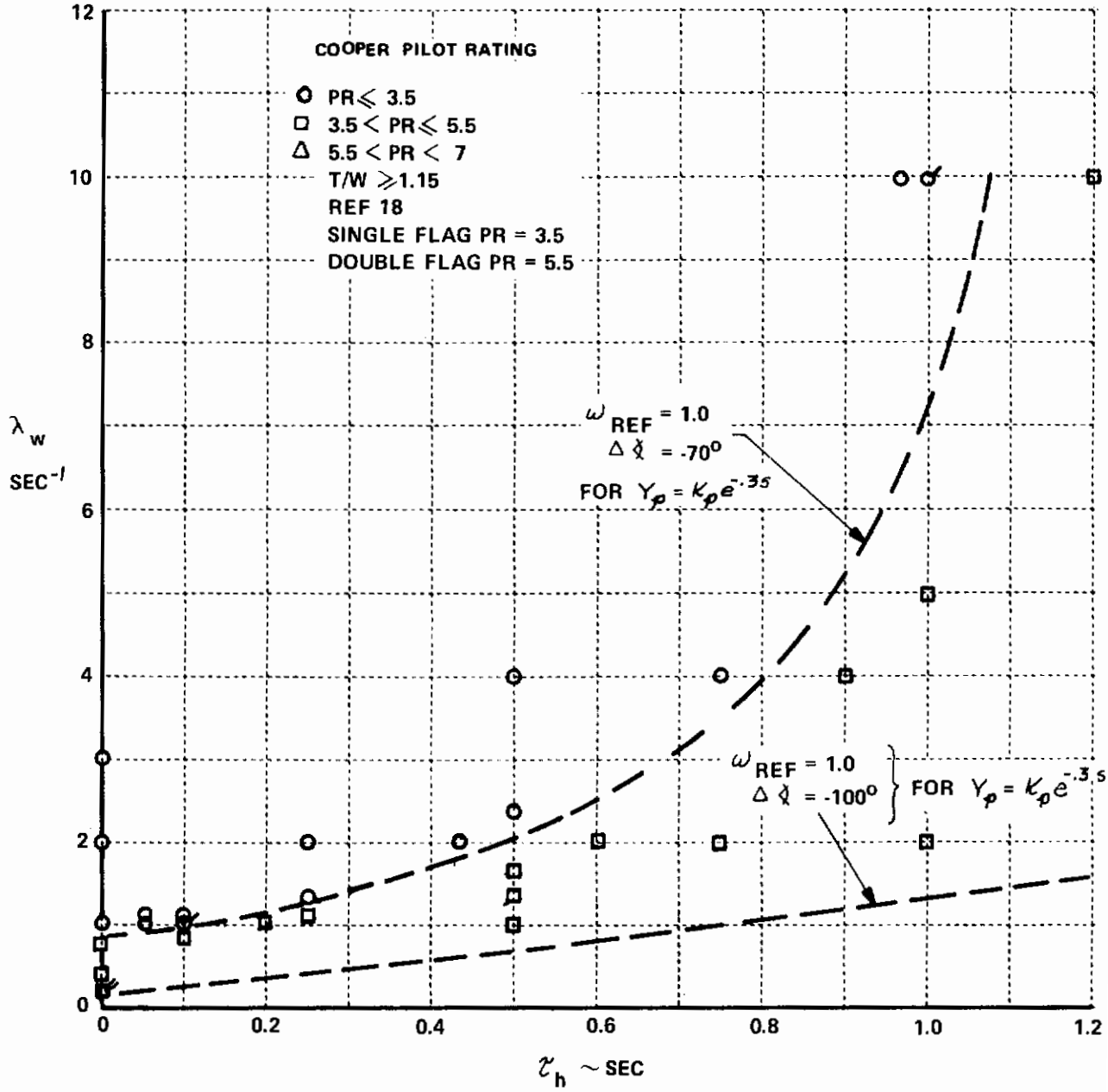

$$Y_c = \frac{K}{S\,(S + \lambda_w)(\tau_h S + 1)}$$

Figure 29 CORRELATION OF PILOT RATING WITH VERTICAL DAMPING INCLUDING A FIRST-ORDER CONTROL SYSTEM LAG, T/W ≥ 1.15

can be associated with

b) $\dfrac{K'}{s\left(\frac{1}{\lambda_w}s+1\right)\left(s+\frac{1}{\tau_h}\right)}$ where $\left[\lambda_w = -Z_w\right]$.

The curves associated with ω_{REF} and $\Delta\not{\zeta}$ were obtained by holding the values of ω_{REF} and $\Delta\not{\zeta}$ fixed and from the previously presented equation for $\Delta\not{\zeta}$ obtain the relationships between λ and τ_h illustrated on Figure 29, the time delay associated with the inclusion of the pilot is fixed at τ = .3 seconds. For the data presented, for $T/W > 1.05$ reasonable correlation of the Levels 1 and 2 boundaries is obtained using ω_{REF} = 1.0 and $\Delta\not{\zeta}$ = -70° for Level 1 and -100° for Level 2. The data presented on Figure 28 indicates that Level 3 would be associated with $-Z_w = 0$, that is, for controlled element transfer functions which are approximately K/s^2, however, insufficient data is available to determine the values of ω_{REF} and $\Delta\not{\zeta}$ which could be associated with Level 3 for either K/s^2 or slightly unstable configurations for the height control task.

The pilot rating data obtained in Reference 7 when first-order lags were included is presented in Figure 30. Illustrated on Figure 30 are the boundaries associated with ω_{REF} = 1.0 and $\Delta\not{\zeta}$ = -70°, and -100° that appear to correlate with the data in Reference 18. It may be significant to note that the data was obtained in Reference 18 with $(T/W) \geq 1.15$ while the data presented in Figure 30 has $T/W \leq 1.05$. This it is quite possible that the values of ω_{REF} and $\Delta\not{\zeta}$ associated with pilot ratings might be dependent upon the thrust-to-weight ratio. This relationship is also implied by the background discussion presented in Reference 2 for the existing height control requirements of MIL-F-83300 and may be related to steady state climb performance. Additional data and correlation investigations would be required to determine the relationship between ω_{REF} and $\Delta\not{\zeta}$ as a function of thrust-to-weight ratio (height control power), and this is beyond the scope of the present correlation investigations.

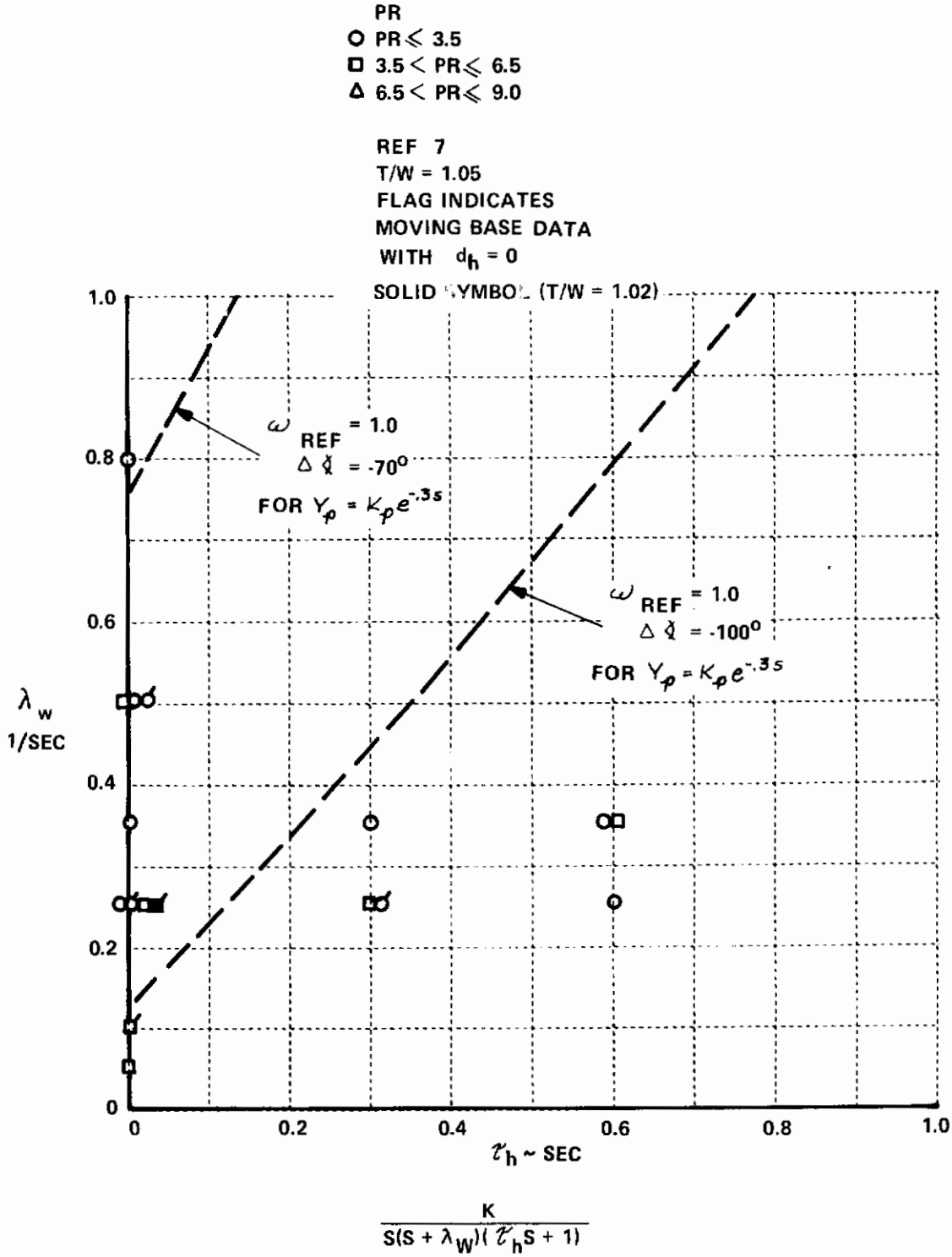

Figure 30 CORRELATION OF PILOT RATING WITH VERTICAL DAMPING INCLUDING A FIRST-ORDER CONTROL SYSTEM LAG, T/W ≤ 1.05

3.2.1.3.2 Correlation With Pitch (Roll) Attitude Control

For hover and low-speed flight the transfer function of pitch (roll) attitude to control inputs can be written as follows (including first-order lag τ_θ or τ_ϕ in the control) (i.e., Reference 18):

$$\frac{\theta}{\delta_e}(s) = \frac{M_{\delta_e}(s - X_u)}{(\tau_\theta s + 1)(s^3 - (X_u + M_q)s^2 + (M_q X_u - M_\theta)s + M_u g + X_u M_\theta)}$$

and

$$\frac{\phi}{\delta_a}(s) = \frac{L_{\delta_a}(s - Y_v)}{(\tau_\phi s + 1)(s^3 - (Y_v + L_p)s^2 + (L_p Y_v - L_\phi)s + Y_v L_\phi - L_v g)}$$

while for horizontal gust disturbances the following transfer functions apply:

$$\frac{\theta}{w_g}(s) = \frac{M_u s}{(\tau_\theta s + 1)(s^3 - (X_u + M_q)s^2 + (M_q X_u - M_\theta)s + M_u g + X_u M_\theta}$$

$$\frac{\phi}{v_g}(s) = \frac{L_v s}{(\tau_\phi s + 1)(s^3 - (Y_v + L_p)s^2 + (L_p Y_v - L_\phi)s + Y_v L_\phi - L_v g}$$

Since L_ϕ and M_θ imply attitude stabilization, these terms will be set to zero and only data with no attitude stabilization will be used for the correlation investigation of attitude control. In addition, if the ratios $|M_u g/M_q|$ and $|L_v g/L_p|$ are small, then not only are pilot complaints regarding turbulence effects on the configuration flying qualities minimized, but the attitude transfer functions can then be reasonably approximated by the following:

$$\frac{\theta}{\delta_e}(s) \simeq \frac{K_c}{s(\tau_\theta s + 1)(s - M_q')} = \frac{K_c}{s(\tau_\theta s + 1)(s + \lambda_\theta)}$$

and

$$\frac{\phi}{\delta_a}(s) \simeq \frac{K_c}{s(\tau_\phi s + 1)(s - L_p')} = \frac{K_c}{s(\tau_\phi s + 1)(s + \lambda_\phi)}$$

Thus prior to the correlation of attitude control in hover and low-speed flight with ω_{REF} and $\Delta\not\zeta$, the data of Reference 18 is first examined to remove configurations where gust effects may dominate pilot rating and mask the trends of pilot rating with the real root. The data of Reference 18 for roll attitude control is presented on Figure 31 as a function of λ_ϕ and $\left|\frac{L_v g}{L_p}\right|$ while Figure 32 presents the pitch attitude control data as a function of λ_θ and $|M_u g/M_q|$ with $\tau_\theta = \tau_\phi = 0$. Since the transfer functions of pitch and roll attitude are in a form identical for the flight conditions under examination, the value of $|M_u g/M_q| = |L_v g/L_p| = .25$ appears to reasonably filter out configurations where the pilot rating may be significantly influenced by turbulence effects, rather than M_q and L_p variations.

The data presented in Reference 18 with zero attitude stabilization for roll and pitch attitude control, with gust effects minimized, is presented on Figures 33 and 34, respectively. Also presented on these figures is the boundary that is associated with $\omega_{REF} = 1.45$, and $\Delta\not\zeta = -80^\circ$, which results in a real root limit at $\lambda \simeq 1.01$. These values appear to correlate with Level 1 (Pilot Rating ≤ 3.5) for pitch (roll) attitude control for hover and low speed flight for $\tau_\theta = \tau_\phi = 0$ and $\tau = .3$ seconds (under the turbulence effects constraint imposed).

Reference 18 also presents data which includes first-order lags in the pitch attitude transfer function. This data is presented on Figure 35 with the constraint that $|M_u g/M_q| < .25$. The technique previously described for plotting the pilot rating data as a function of λ and τ was also used for this figure. The Level 1 parameters ($\omega_{REF} = 1.45$, $\Delta\not\zeta = -80^\circ$) also appear to correlate quite satisfactorily when first-order control lags are introduced. The relationships that exist between λ_θ and τ_θ when $\omega_{REF} = 1.2$ for $\Delta\not\zeta = -80^\circ$ and -100° are also presented on Figure 35. These lines indicate values of "open-loop" parameters which might be associated with Level 2 and Level 3 pilot rating boundaries. Correlation to examine the influence of the actual magnitude of $(\Delta A/\Delta\not\zeta)_\omega$ for these systems was not performed. The magnitude of $(\Delta A/\Delta\not\zeta)$ obtained for these configurations is above the value indicated

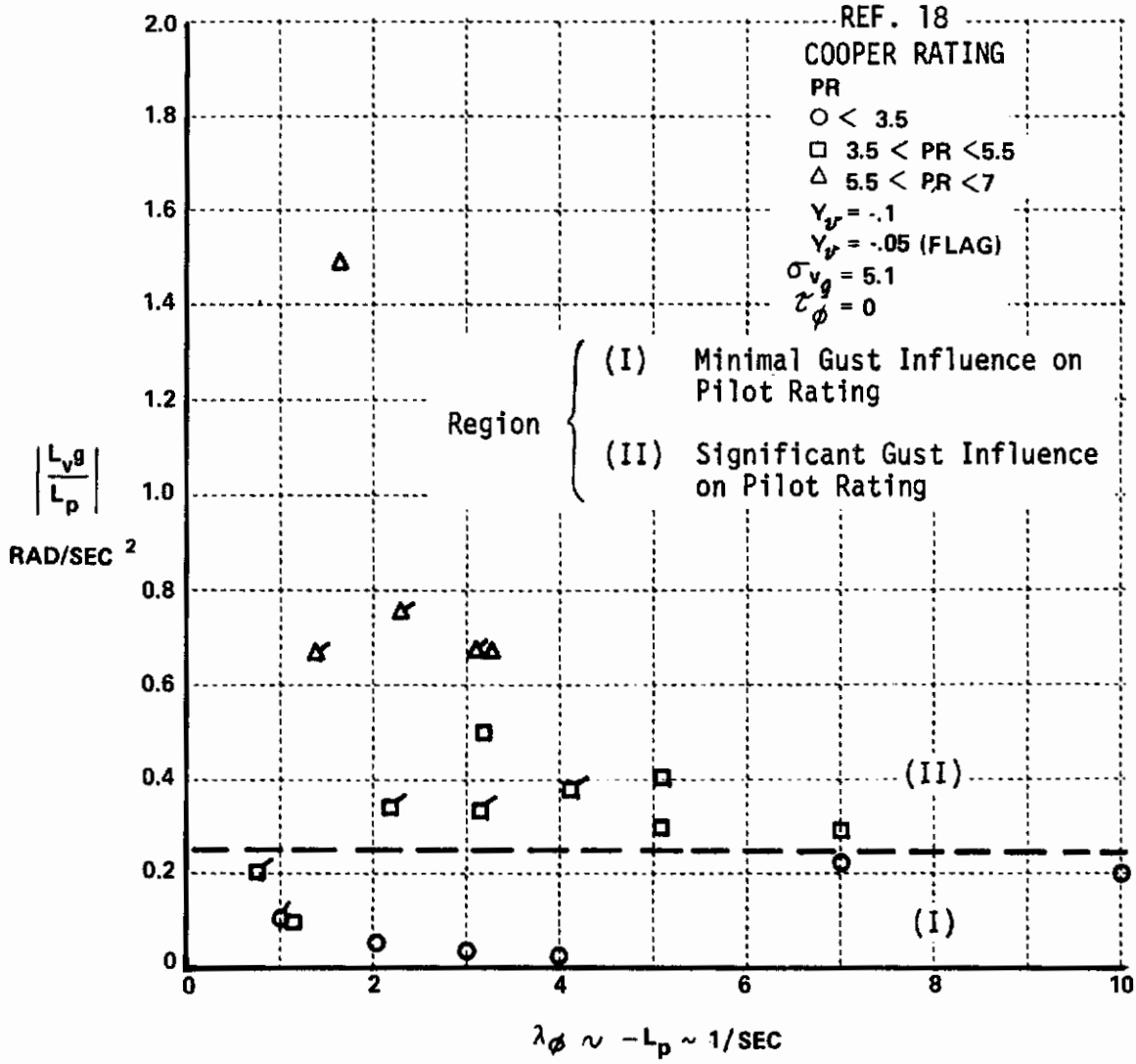

Figure 31 INFLUENCE OF GUST SENSITIVITY ON PILOT RATING (ROLL CONTROL)

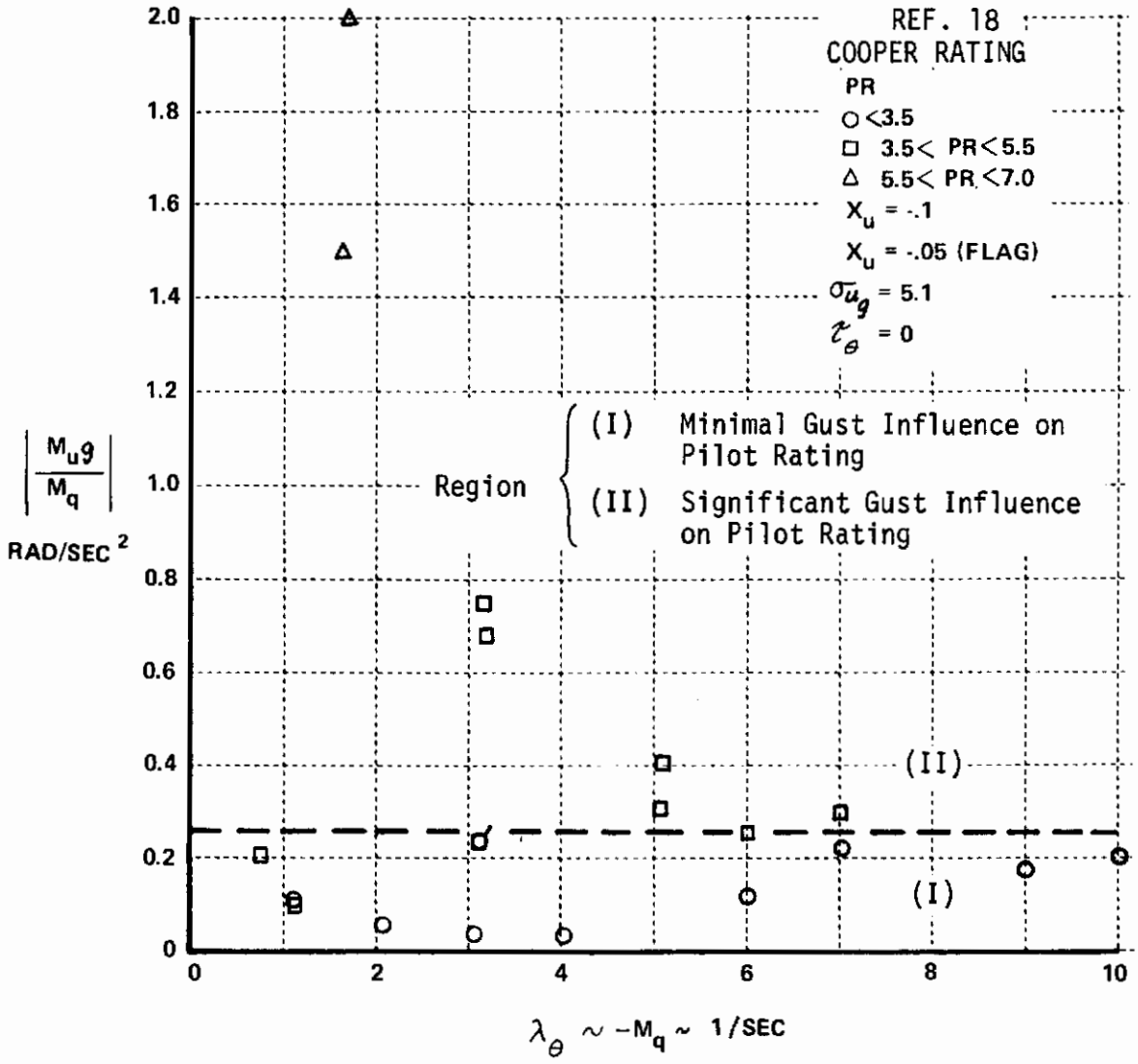

Figure 32 INFLUENCE OF GUST SENSITIVITY ON PILOT RATING (PITCH ATTITUDE CONTROL)

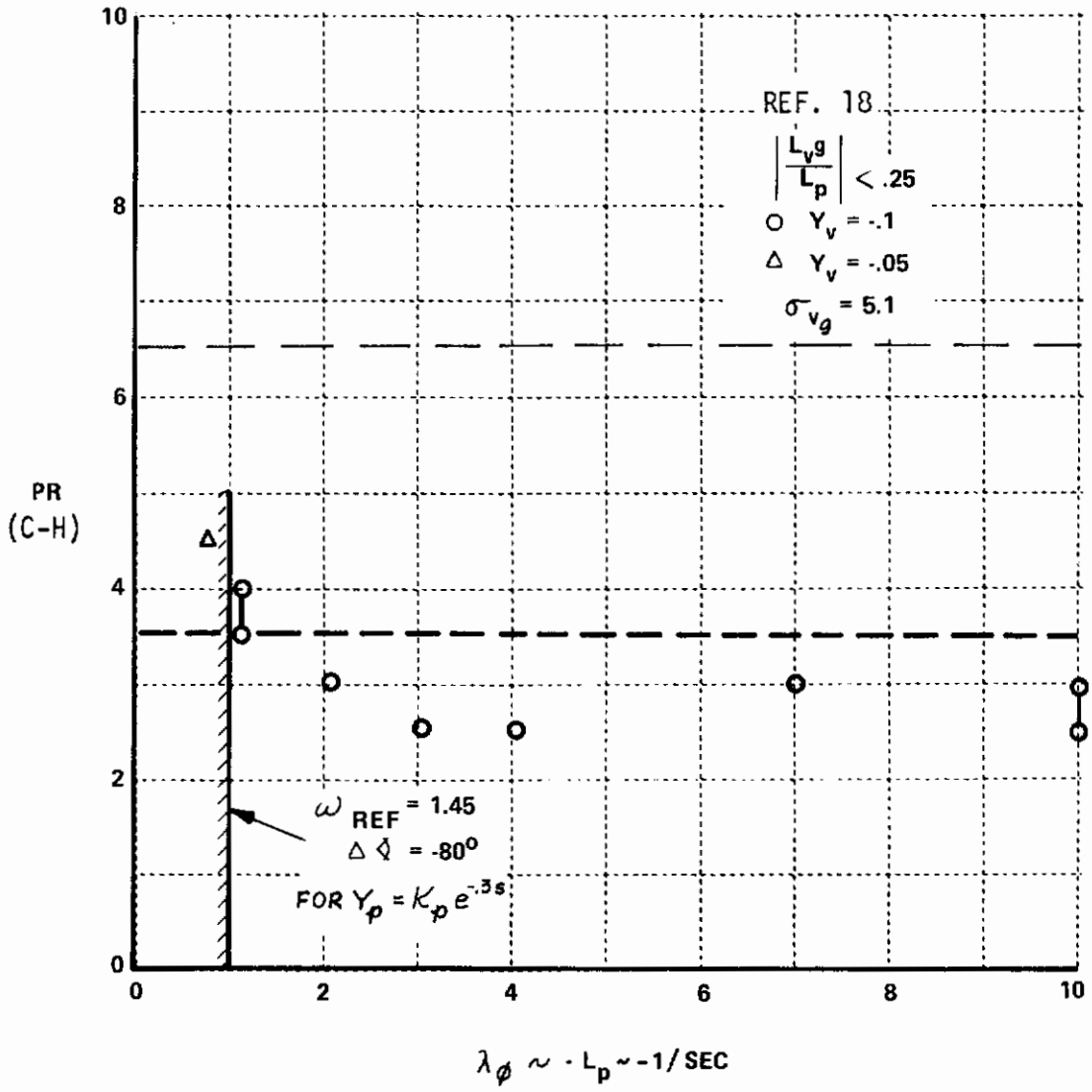

Figure 33 CORRELATION OF PILOT RATING WITH λ_r

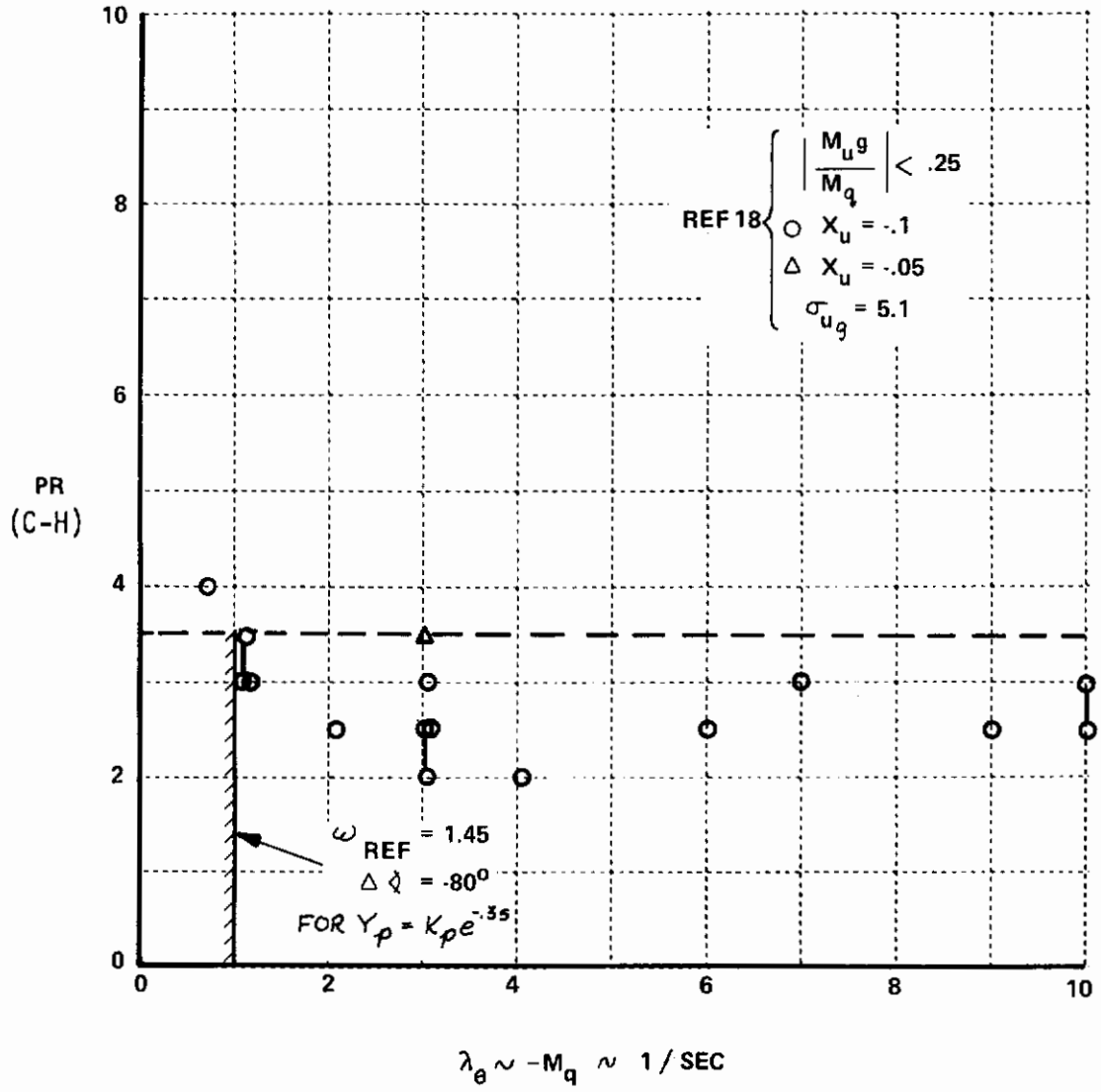

Figure 34 CORRELATION OF PILOT RATING WITH λ_θ

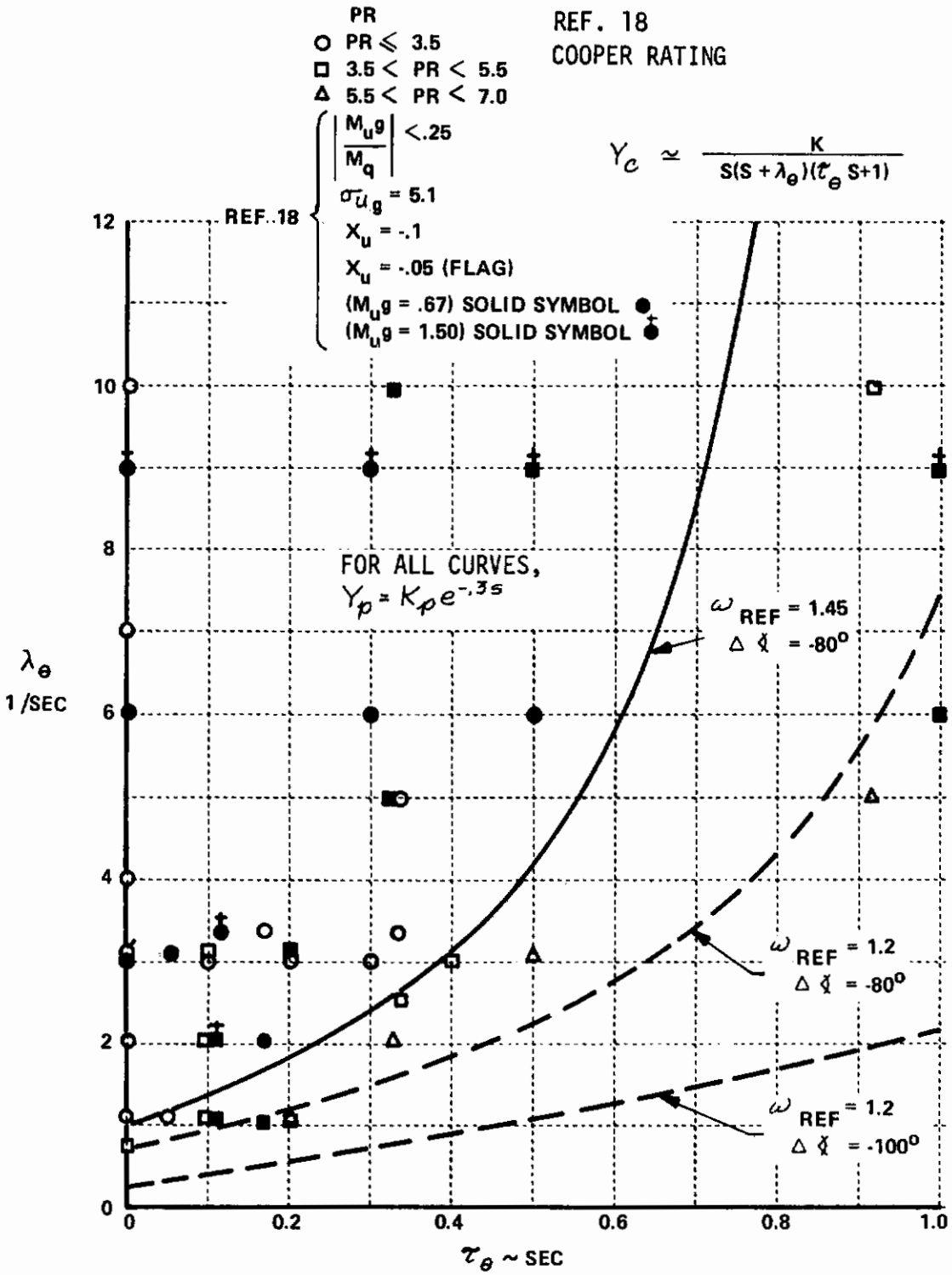

Figure 35 CORRELATION OF PILOT RATING WITH PITCH DAMPING INCLUDING A FIRST-ORDER CONTROL SYSTEM LAG

in Reference 15 for which the suggested boundaries of that reference became dependent upon $(\Delta A/\Delta \phi)_\omega$ rather than just ω_{REF} and $\Delta \phi$.

In addition, Reference 18 compares pilot ratings for both fixed and moving-base ground simulation of pitch (roll) attitude control for selected configurations. The data presented on Figure 36, obtained from Reference 18, again indicates that $|M_{ug}/M_q| = |L_{vg}/L_p| < .25$ tends to separate out configurations wherein the pilot rating is primarily determined from the influence of M_q (L_p) variations rather than turbulence effects.

Reference 16 presents pilot ratings for an in-flight investigation of longitudinal characteristics on low-speed instrument operation. The data presented on Figure 37 from Reference 16 is selected such that the pitch attitude transfer function is identically equal to $K/s(s-M_q)$, while the data presented from Reference 18 is only that data which minimizes turbulence effects. Several conclusions are suggested from this figure:

- (1) Motion cues for the program reported in Reference 18 improve pilot rating for the pitch (roll) control task investigated.

- (2) In-flight evaluation under instrument conditions for the task used in Reference 16 is generally consistent with the fixed-base ground simulation data trends previously presented on Figures 33 and 34.

- (3) Fixed-base data obtained in Reference 18 appears to be conservative in the influence of the real root (M_q, L_p) on pilot rating.

In addition, the effect of ω_{REF} = 1.20 and $\Delta \phi$ = -80°, and -100° is presented on Figure 37. These values of the "open-loop" parameters appear to be associated with the Level 2 flying qualities boundary (pilot rating

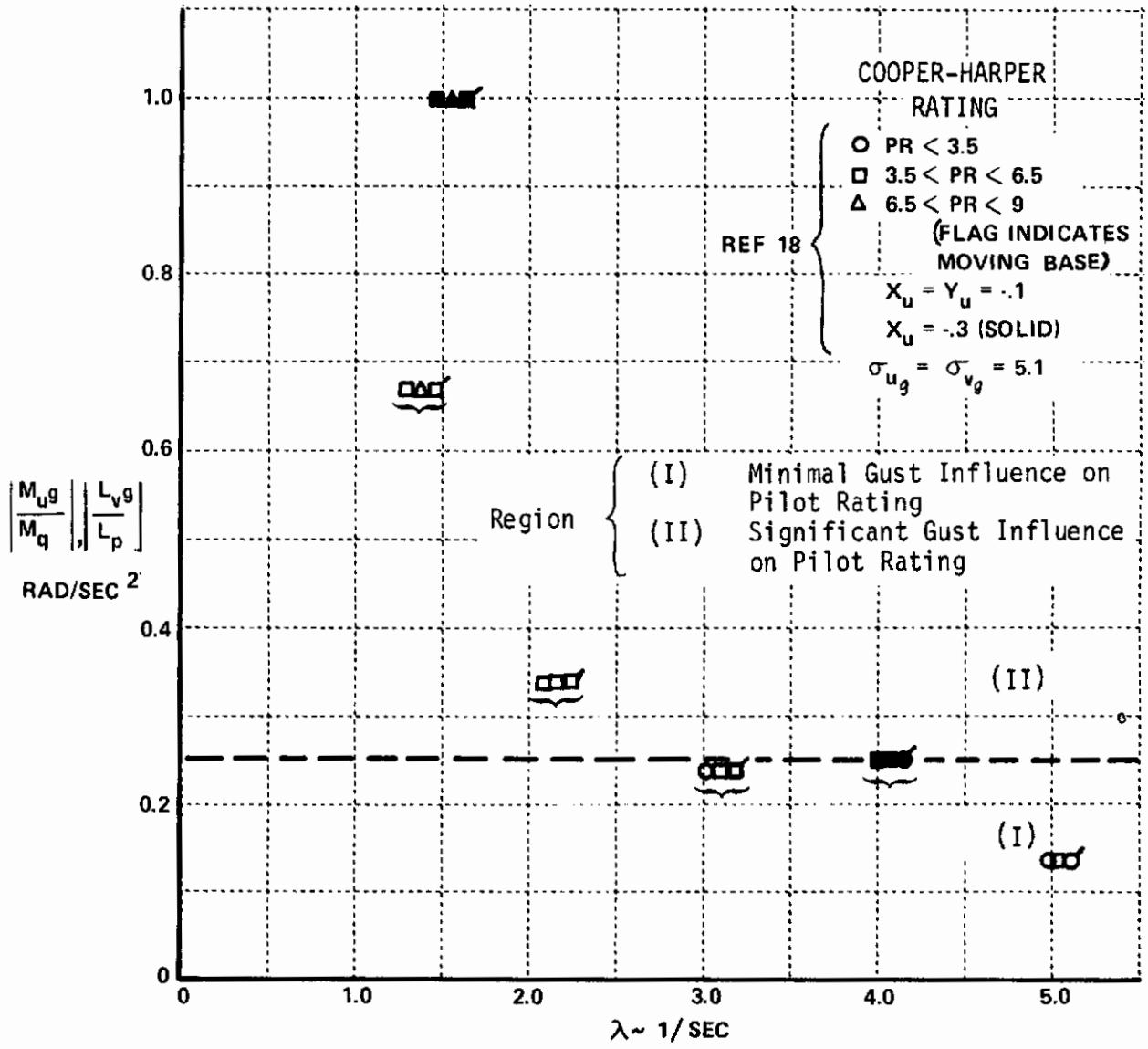

Figure 36 INFLUENCE OF GUST SENSITIVITY ON PILOT RATING

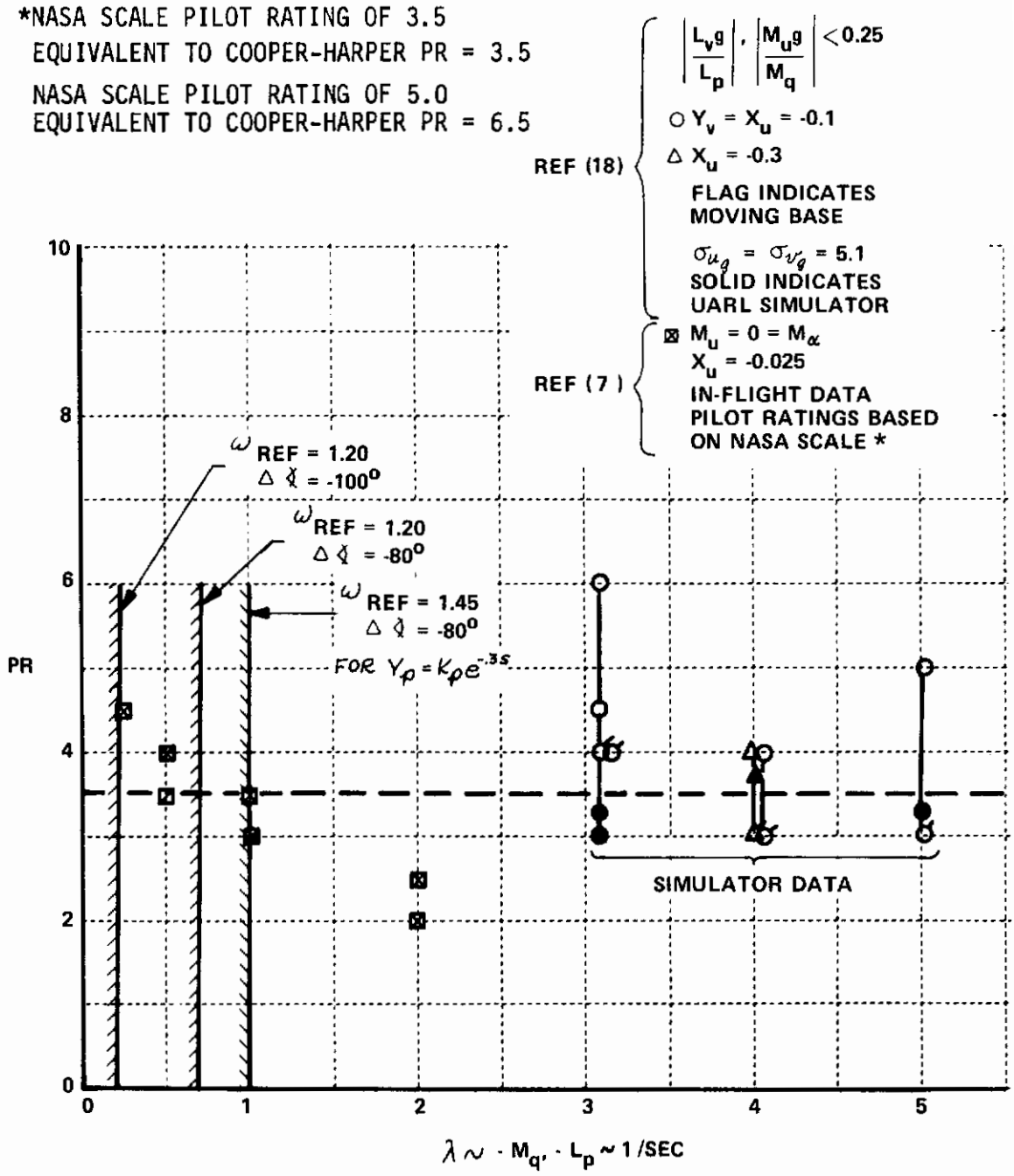

Figure 37 CORRELATION OF PILOT RATING (ATTITUDE CONTROL)

$\leq$ 6.5 on Cooper-Harper Pilot Rating Scale, Reference 2). "Open-loop" parameters of ω_{REF} = 1.20 and $\Delta\not{\phi}$ = -90° essentially correspond to the minimum requirements of AGARD 408, Reference 19 ($M_q \approx -.5$). This brief correlation examination of $\Delta\not{\phi}$ and ω_{REF} for pitch (roll) attitude control indicates that "open-loop parameters ω_{REF} and $\Delta\not{\phi}$ can be found that indicate satisfactory levels of pilot ratings. In addition, motion effects, turbulence effects, displays and piloting task can affect the "open-loop" parameters which correlate with a particular level of flying qualities. The data prescribed herein is a first attempt at correlation of pilot rating with ω_{REF} and $\Delta\not{\phi}$ for the type of aircraft transfer functions associated with pitch (roll) attitude control for hover and low-speed flight. The results of this analysis are quite encouraging.

3.2.1.3.3 Correlation With Directional (Heading) Control

For hover and low-speed flight the heading equation of motion can be presented by the following transfer function (including a first-order control lag, τ_ψ):

$$\frac{\psi}{\delta_r}(s) = \frac{N_{\delta_r}}{s(\tau_\psi s+1)(s - N_r)} = \frac{K}{s(\tau_\psi s+1)(s+\lambda_\psi)}$$

which again is of the form previously described in this section. Directional gust sensitivity is influenced by the magnitude of N_v ; thus to examine the influence of N_r and τ_ψ on pilot rating, only those configurations with $N_v \leq$ .005 were selected for correlation. The data presented in References 18 and 7 for τ_ψ = 0 is presented on Figure 38. Indicated are the boundaries that would be obtained for $-N_r$ when ω_{REF} is selected at 1.2 radians/second and $\Delta\not{\phi}$ is varied from -80° to -100°. The figure indicates that for directional control in hover and low-speed flight, when τ_ψ = 0 correlation of the Level 1 boundary and $-N_r$ = .71 (ω_{REF} = 1.2, $\Delta\not{\phi}$ = -80) is quite good; while the

---

[19] Anon.: "Recommendations for V/STOL Handling Qualities." AGARD Report No. 408A, 1962.

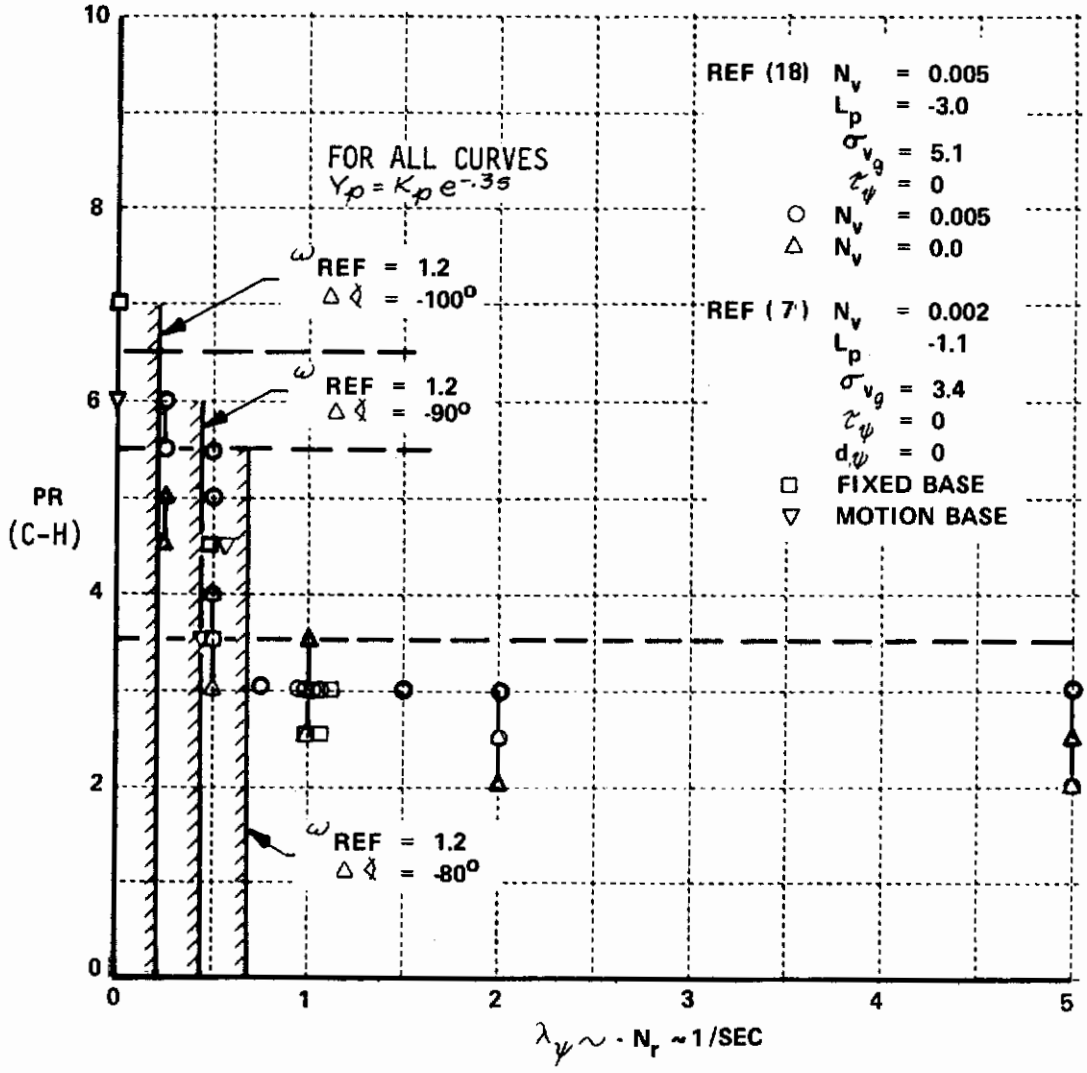

Figure 38 CORRELATION OF PILOT RATING WITH λ_ψ

Level 2 boundary appears to be generally correlated with ω_{REF} = 1.20 radians/seconds and $\Delta\phi$ = -100°. Reference 18 and 7 also present data as τ_ψ is changed for various values of N_r and N_v with σ_{v_g} = 5.1 and 3.4 ft/second. This data is presented in Figure 39, where again use is made of the relationship previously discussed in 3.2.1.3.1 to increase the pilot rating data associated with $-N_r$ and τ_ψ. The boundaries associated with various "open-loop" parameters (ω_{REF}, $\Delta\phi$) are presented on Figure 39. These boundaries reasonably correlate with the data, and in addition indicate that even for $N_v \leq .005$, "open-loop" parameters could be associated with turbulence levels. The general correlation is quite satisfactory.

3.2.1.4 Summary of "Open-Loop" Correlation Parameters

The preceding attempts at defining "open-loop" parameters (ω_{REF} and $\Delta\phi$) which correlate with pilot ratings for tasks and transfer functions associated with hover and low speed flight was quite satisfactory for the data considered. From the parameters examined, further correlation studies are definitely warranted to examine in greater depth the influence of control power, task, displays and turbulence effects on the "open-loop" parameters associated with the transfer functions appropriate to this flight regime. In addition, systematic examination using the techniques presented in this section should be performed on more complicated transfer functions which are representative of VTOL, STOL and V/STOL aircraft including augmentation and control system, etc.

In general the "open-loop" parameters associated with the hover and low-speed flight regime appear to be within the following values:

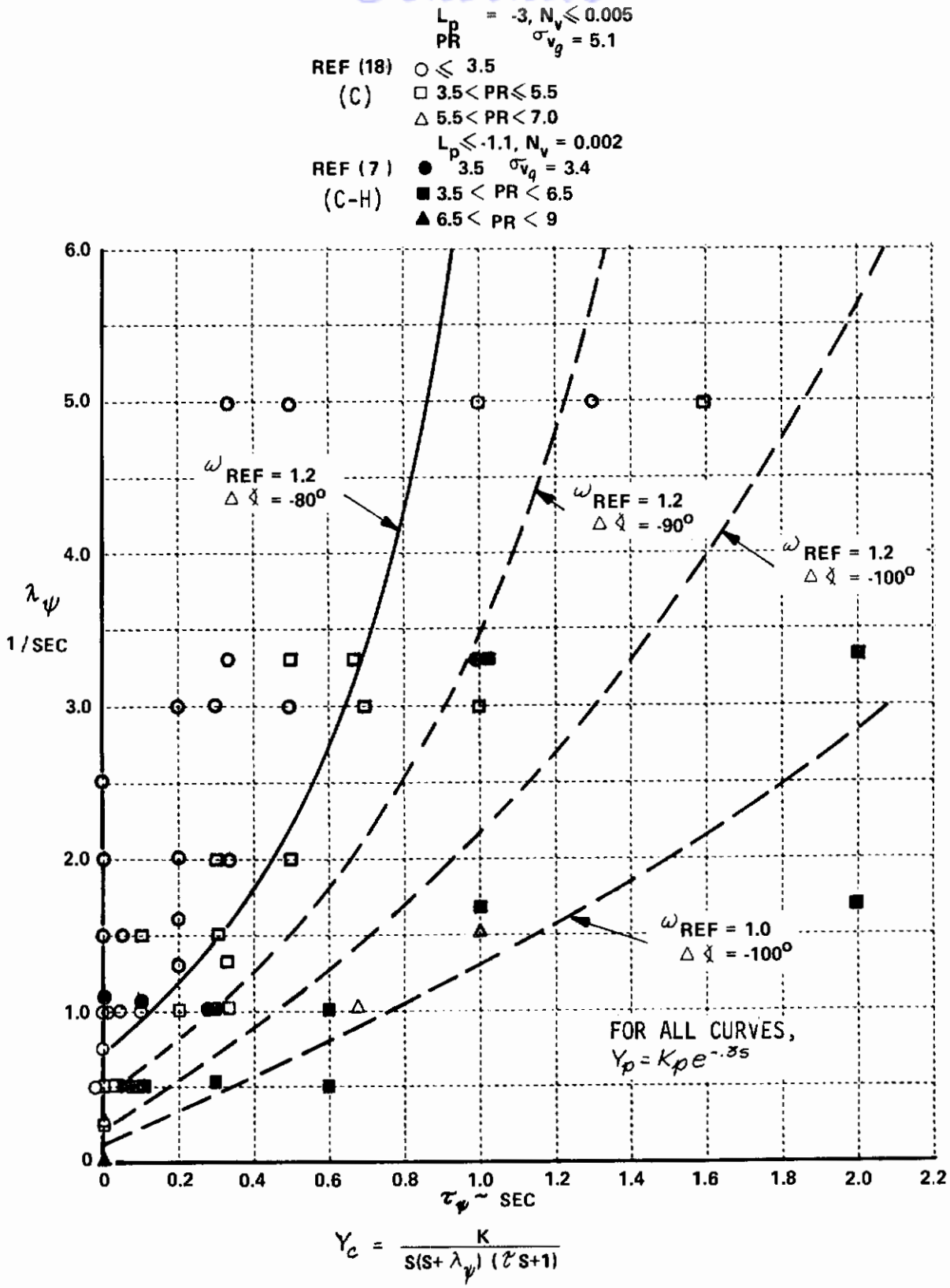

$$Y_c = \frac{K}{S(S+\lambda_\psi)(\tau S+1)}$$

Figure 39 CORRELATION OF PILOT RATING FOR DIRECTIONAL CONTROL INCLUDING A FIRST-ORDER CONTROL SYSTEM LAG

(a) $1.0 \leq \omega_{REF} \leq 1.45$

(b) $\Delta \not\propto = -70^{o}$ to -100^{o}

for the data examined in this analysis. In comparison to the proposed revision to the pitch dynamic requirements of Reference 15, the range of $\Delta \not\propto$ is quite compatible; however, ω_{REF} is different than those suggested in the cited reference. This difference is probably related to the piloting requirements associated with the flight regime and flight phase under investigation. It is therefore possible that boundaries on $\Delta \not\propto$ and ω_{REF} might be determinable as a function of flight phase and associated task for both MIL-F-8785B(ASG).

Open-loop parameters that are associated with pilot ratings are by no means unique. That is, it might be possible to establish a valid correlation with such parameters as gain margin, phase margin and crossover frequency (frequency at which $|Y_p Y_c|$ = 0 dB). For example, using ω_{REF} = 1.45 radians/second and $\Delta \not\propto$ = -80° (indicated by the Level 1 pilot ratings associated with pitch (roll) attitude control previously presented in subsection 3.2.1.3.2) indicate that when $\tau_\theta = \tau_\phi = 0$, the value of the real root associated with the selected "open-loop" parameters is equal to 1.0. Thus controlled elements of the form $K_c/s(s+1)$ would pass the boundary, while $\lambda < 1.00$ would not, for $Y_p = K_p e^{-.3s}$. Figure 40 presents the amplitude-ratio-phase angle plot (Nichols Chart) for the pilot-aircraft system open-loop transfer function $Y_p Y_c = 1.251 e^{-.3s}/s(s+1)$. The value of gain was selected such that at ω = 1.0 rad/sec the closed-loop system will have -90° phase. From Figure 40, the following parameters are obtained for the selected pilot-aircraft system:

(a) Phase Margin $\cong 32^{o}$

(b) Gain Crossover Frequency $\cong$ .92 radians/sec

(c) Gain Margin $\cong$ 9 dB

(d) Phase Crossover Frequency $\cong$ 1.74 radians/sec.

From this figure, the system resonant peak and bandwidth as discussed by Neal and Smith in Reference 14 for the condition of zero pilot lead generation (T_L = 0), are:

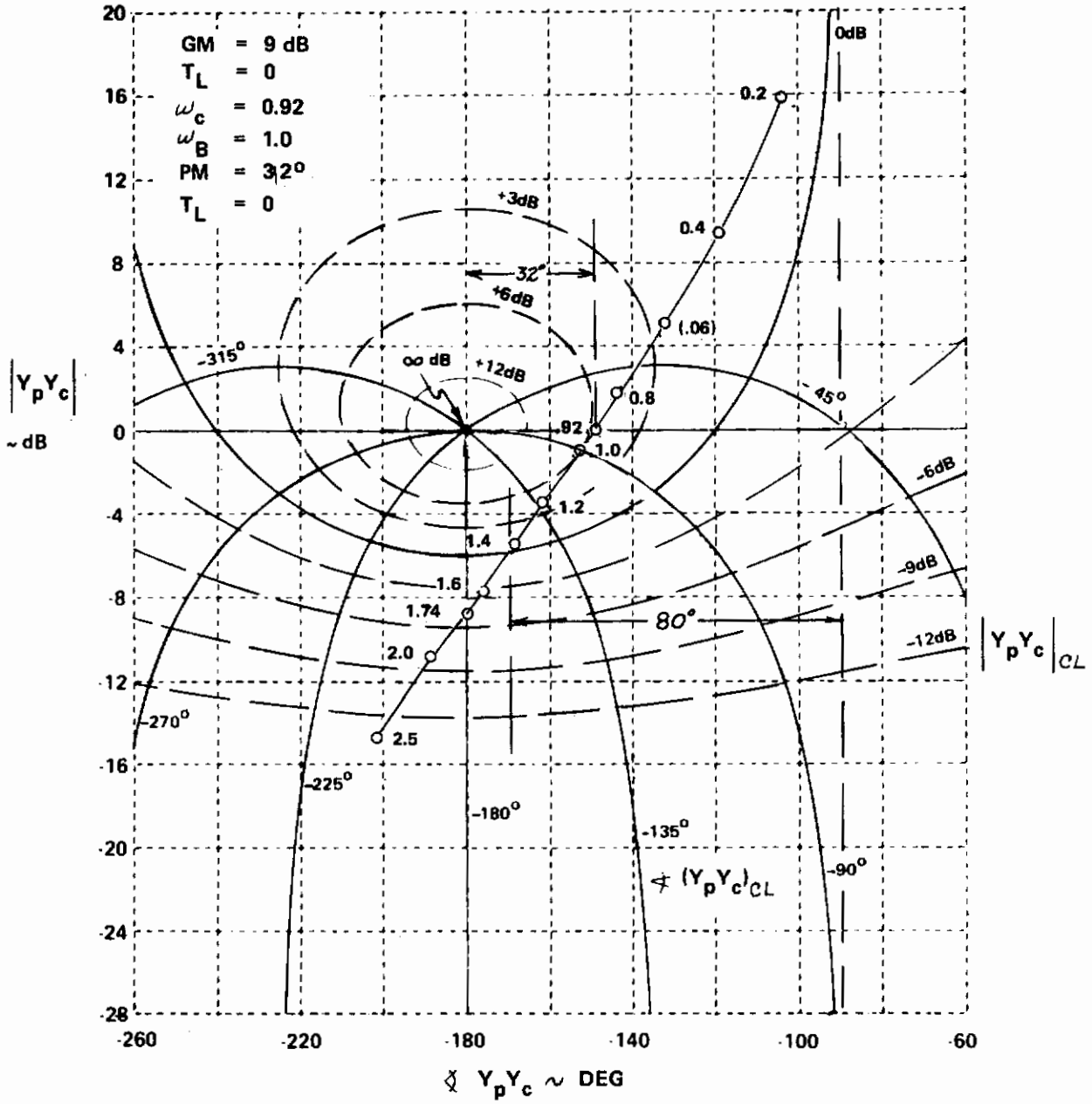

Figure 40 NICHOLS CHART FOR $Y_pY_c = \dfrac{1.25\,e^{-.3s}}{s(s+1)}$

(a) $M_p \cong$ 6 dB

(b) ω_{BW} = 1.0 rad/sec

(c) ϕ_{pc} = $\tan^{-1}(T_L \omega_B) \equiv 0$

The above brief discussion indicates that PM $> 30^{\circ}$ could possibly be associated with Level 1 flying qualities for attitude control in hover and low-speed flight for the prescribed low-order transfer functions and pilot time delay (τ = .3 seconds). In terms of closed-loop parameters, the resonant peak and pilot lead requirements have been shown in several references to be indicative of pilot ratings and system performance. These ideas will be further examined in the remainder of this section.

3.3 CLOSED-LOOP CONSIDERATIONS

The previous discussion examined correlation of pilot ratings, in hover and low-speed flight, with "open-loop" parameters (ω_{REF}, $\Delta\phi$) for various low-order transfer functions. These "open-loop" parameters originally evolved from relationships between closed-loop parameters and pilot ratings (Reference 14). The closed-loop parameters used by Neal and Smith in Reference 14 were $|\Theta/\Theta_c|_{max}$ (which is actually the closed-loop resonance peak, M_p) and the pilot compensation angle ϕ_{pc} (a measure of pilot lead/lag generation). The pilot compensation used in Reference 14 was based on specifying certain performance standards in terms of minimum bandwidth (determined by the frequency at which the closed-loop phase angle is equal to -90°) and a maximum low-frequency droop of -3 dB in the closed loop for frequencies below the prescribed minimum bandwidth. The details of the pilot-in-the-loop analysis performed in Reference 14 will not be repeated here since they are explained in sufficient detail in the referenced reports. The closed-loop criterion, however, is shown on Figure 41, to introduce the closed-loop resonance and pilot compensation parameters. It whould be noted that the task used in Reference 14 required a pitch attitude closure with dynamics representative of fighter aircraft with higher-order flight control system

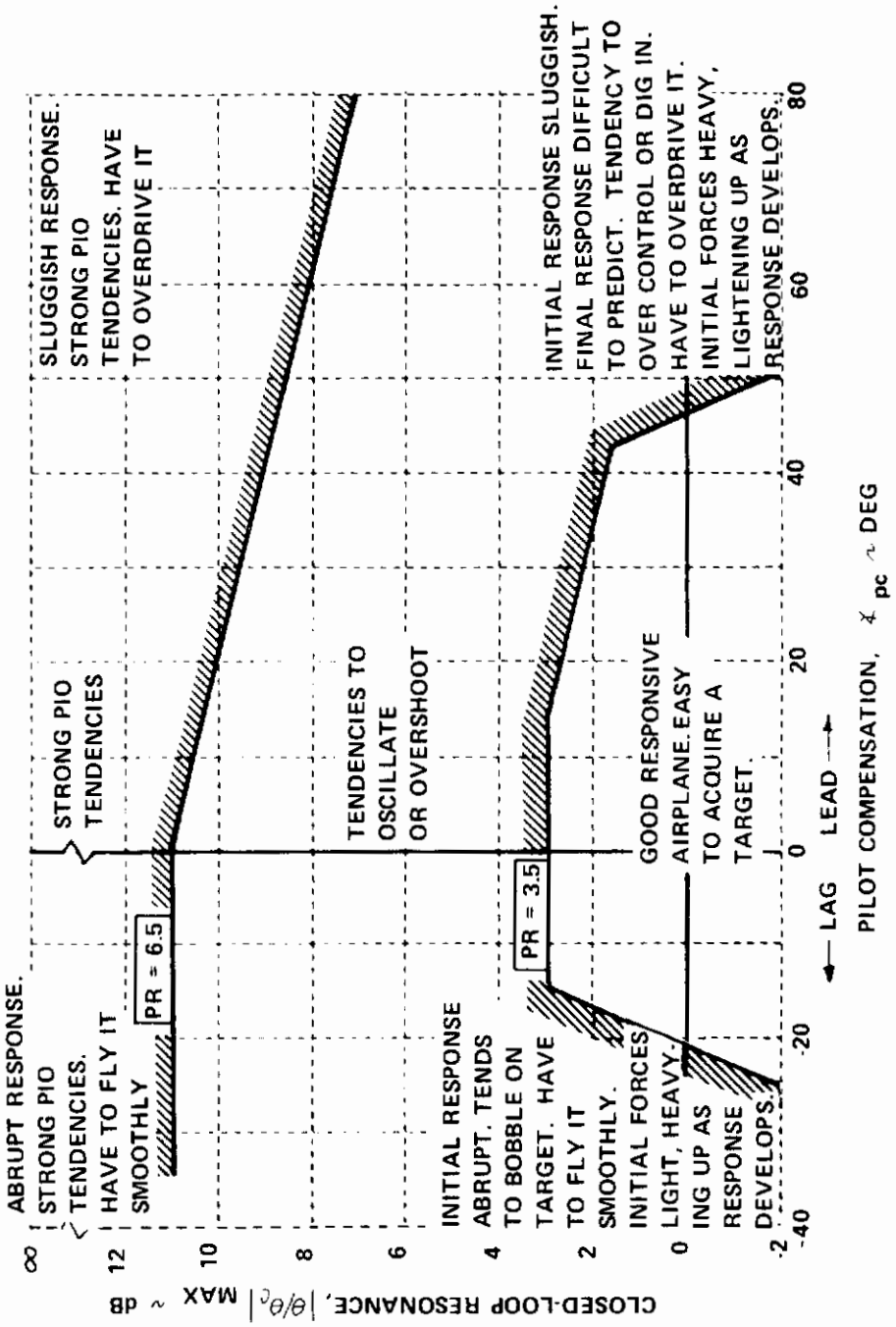

Figure 41 PROPOSED CLOSED-LOOP CRITERION FOR FIGHTER MANEUVERING DYNAMICS (REFERENCE 14)

effects. Reference 14 also initially developed the basis of the "open-loop" parameters which led to the proposed revision to pitch dynamics, etc. of Reference 15, and of course was the basis of the analytical treatment previously presented in this section.

The remainder of this subsection will examine the relationship between several "open-loop" and "closed-loop" parameters which are indicative of pilot workload and potential system performance in a task. This will be accomplished by examination of controlled elements of the form K/s and $K/s(s+\lambda)$. The effects of lead generation and system gain will be investigated and potential pilot strategy will be examined briefly.

3.3.1 Examination of K/s Systems

Several references (e.g., Reference 13) discuss pilot equalization adjustment "rules" for the controlled-element transfer functions which are of specific interest to hover and low-speed flight. Fundamental to the "rules" proposed for pilot equalization are the lead/lag adjustments by the pilot in his attempt to obtain a -20 dB/decade slope of the open-loop pilot aircraft system ($Y_p Y_c$) in the region of the gain crossover frequency. Thus a limiting situation under the proposed adjustment rules that would only require pilot gain compensation is a controlled element which can be approximated by K/s in the region of gain crossover frequency. Then, still accounting for a pilot time delay, the pilot-aircraft system can be approximated by the transfer function $(K/s)e^{-\tau s}$. The remainder of this subsection will examine relationships between "open-loop" parameters for this type of pilot-aircraft system.

Thus if $Y_p Y_c = (K/s)e^{-\tau s}$, then the following relationships can be derived. Since the gain crossover frequency is based on the condition $|Y_p Y_c| = 0$ dB, then $K = \omega_c$ and $G(\omega) = \omega_c/\omega$, while $\phi(\omega) = -90^\circ - \tau_e \omega$, where $\tau_e = (180/\pi)\tau$. The phase margin (PM) for the system is simply the expression $PM = 180^\circ + \phi(\omega_c) = 90^\circ - \tau_e \omega_c$. However, from the previous section recall that $\Delta\phi$ for this type of system can be expressed as $\Delta\phi = -\tau_e \omega_{REF}$. Therefore at any reference frequency, $PM(\omega_{REF}) - 90^\circ = \Delta\phi$. Thus if the reference frequency is selected as the desired gain crossover frequency, then $\Delta\phi$ is directly related to the phase margin. The frequency at which the phase margin equals zero (phase crossover frequency) therefore occurs when $\Delta\phi = -90^\circ$, and for the purposes of this discussion will be identified as ω^*. The relationship between ω^* and ω_c is derived from the angle relationship for this system as: $\omega^*/\omega_c = 90/(90 - PM)$. The gain margin (GM) of the system is equal to $-|Y_p Y_c|$ evaluated at ω^*. Thus $GM = -20 \log_{10}(\omega_c/\omega^*) = -20 \log_{10}\left(\frac{90 - PM}{90}\right)$. This expression can be approximated for phase margin $\leq 60^\circ$ by the following expansion: $GM = 8.686\left(\frac{2PM}{180 - PM}\right)$, which is derivable from a series expansion of the previously cited expression for gain margin. This discussion completes the relationships desired for "open-loop" parameters.

The rest of this subsection will examine "closed-loop" parameters for the K/s system. The closed-loop transfer function can be expressed as follows:

$$H(s) = \frac{\omega_c e^{-\tau s}}{s + \omega_c e^{-\tau s}}$$

First, the closed-loop resonance peak and the frequency at which this occurs is developed. From the equation for $H(s)$ the following expression can be derived for the closed-loop amplitude ratio.

$$H(\omega) = \frac{\omega_c \cos \tau\omega - i\omega_c \sin \tau\omega}{\omega_c \cos \tau\omega - i(\omega_c \sin \tau\omega - \omega)}$$

The amplitude of $H(\omega)$ can be found from

$$H^2(\omega) = H(\omega)H(-\omega) = \frac{\omega_c^2}{\omega_c^2 - 2\omega\omega_c \sin \tau\omega + \omega^2} = \frac{1}{1 + \left(\frac{\omega}{\omega_c}\right)^2 - 2\left(\frac{\omega}{\omega_c}\right)\sin \tau\omega}$$

If $|H(\omega)| = 1$ for all frequencies this requires that $\left(\frac{\omega}{\omega_c}\right)\left[\left(\frac{\omega}{\omega_c}\right) - 2\sin\tau\omega\right] = 0$. Setting the bracket to zero gives $\sin\tau\omega = 1/2(\omega/\omega_c)$ which is valid for $\omega < 2\omega_c$. At the gain crossover frequency this equation results in $\sin\tau\omega_c = 1/2$ and therefore $\tau\omega_c = 30^\circ$, or a Phase Margin of 60°. Thus it is of little value to examine this system for phase margin greater than 60°. In addition, since $H^2(\omega) = 1$ for this condition, this implies that the system is a perfect tracking system in terms of rms error for input disturbances with frequency $\omega_i < 2\omega_c$. That is $\sigma^2_{out} = \sigma^2_{in} \Rightarrow \sigma^2_{out}/\sigma^2_{in} \equiv 1$. However due to the time delay there exists phase shift in actual tracking performance.

Based on the expression derived for $H^2(\omega)$, the resonance condition occurs when the denominator for $H^2(\omega) = 0$. This is examined next. (Let $K(\omega) = 1 + (\omega/\omega_c)^2 - 2(\omega/\omega_c)\sin\tau\omega$.)

Thus

$$\frac{\partial K(\omega)}{\partial \omega} = \frac{2}{\omega_c}\left[\frac{\omega}{\omega_c} - \omega\tau\cos\tau\omega - \sin\tau\omega\right]$$

Therefore resonance occurs when $\partial K(\omega)/\partial\omega$ is set equal to zero, therefore

$$\frac{\omega_p}{\omega_c} = \omega_p\tau\cos\tau\omega_p + \sin\tau\omega_p$$

The magnitude of the resonance peak is determined by substitution of the expression for ω_p/ω_c into the expression for $H^2(\omega)$. Thus

$$|H(\omega_p)|_{max} = M_p = \frac{1}{(1+(\omega_p\tau)^2)^{1/2}\cos\tau\omega_p}$$

Thus, from the definition of Phase Margin, expressions can be derived which relate ω_p/ω_c and M_p to phase margin, regardless of the value of τ. These results will not be expressed analytically, however they will be graphically presented later in this section (Figure 42). From the previously derived expressions, it can be shown that for $|H(\omega)| = 1$ for all $\omega \leq \omega_c$ the phase margin must be PM $\geq 61.4^\circ$. Next the relationship between phase margin,

$$Y_p Y_c = \frac{K}{s} e^{-.3S}$$

$$\omega_c = K$$

$$PM = 90^o - \frac{180}{\pi} \tau \omega_c$$

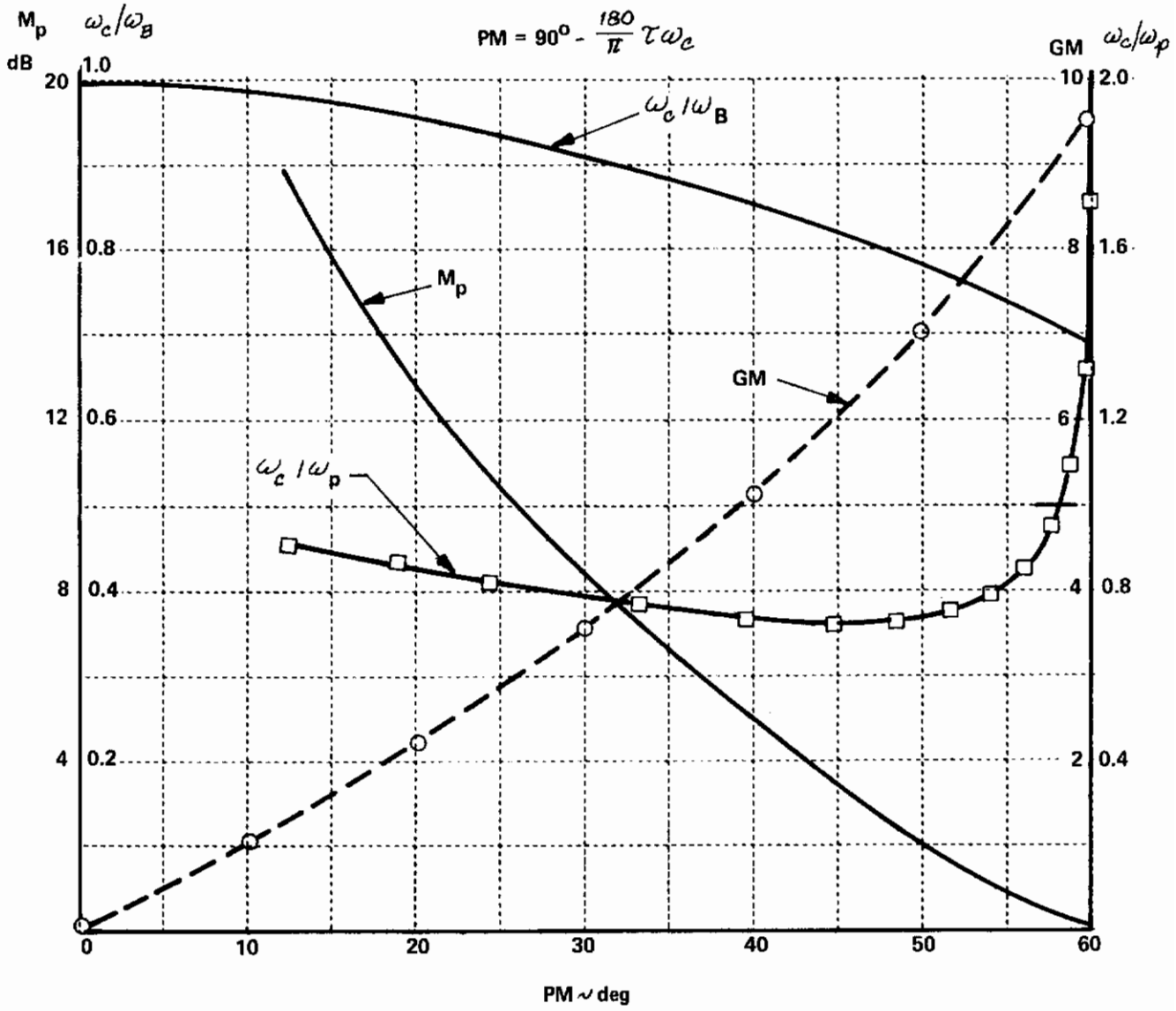

Figure 42 SYSTEM PARAMETERS FOR $Y_p Y_c = \frac{K}{s} e^{-\tau s}$

crossover frequency and the bandwidth frequency (the frequency at which closed loop phase angle = -90°) is derived. These relationships are based on the equations used to derive the Nichols Chart (Reference 20), which relate open-loop amplitude ratio and phase to closed-loop amplitude ratio and phase. The expression for $H(\omega)$ can be written as $H(i\omega) = |H(i\omega)|e^{i\alpha(\omega)} = |H|\,e^{i\alpha(\omega)}$ while the open loop can be expressed as

$$G(i\omega) = |G(i\omega)|\,e^{i\phi(\omega)} = |G|e^{i\phi(\omega)}$$

From the use of unity feedback the following relationships can be derived (Reference 20)

$$|H| = \left[\sqrt{\left(1 + \frac{\cos\phi}{|G|}\right)^2 + \left(\frac{\sin\phi}{|G|}\right)^2}\right]^{-1} \text{ and}$$

$$\alpha = \tan^{-1}\frac{\sin\phi(\omega)}{|G| + \cos\phi(\omega)}$$

If $G(i\omega) = (K/s)e^{-\tau s}$, then as previously shown $|G| = \omega_c/\omega$ and $\phi(\omega) = -90^{\circ} - \tau_e\omega$. Setting α to -90°, $(= \tan\alpha = \infty)$ implies that $|G| + \cos\phi(\omega) = 0$. Thus

$$\frac{\omega_c}{\omega_B} = \sin\tau\omega_B$$

Note: when

$$\frac{\omega_c}{\omega_B} = 1, \quad \sin\tau\omega_c = 1 \text{ and } \tau\omega_c = 90^{\circ} \text{ then } PM = 0$$

Thus,

$$PM = 90\left(1 - \frac{2\tau\omega_c}{\pi}\right) = 90\left(1 - \frac{2}{\pi}\tau\omega_B\sin\tau\omega_B\right)$$

Therefore a relationship can be directly derived between phase margin and ω_c/ω_B. The relationships derived in this section are presented in Figure 42. This figure indicates that the pilot-aircraft open-loop Phase Margin is a dominant factor in describing the closed-loop behavior (system performance) of $Y_pY_c = \frac{K}{s}e^{-\tau s}$ and that the other significant parameter is described either

---

[20] Chen, Chih-Fan and I. John Haas: "Elements of Control Systems Analysis: Classical and Modern Approaches." Prentice-Hall Publishing Company, Inc., 1968.

by system gain (K) or by its equivalent, the open-loop crossover frequency (ω_c) for K/s systems. In addition the relationship between ω_β and ω_c is uniquely determined by the open-loop system phase margin. The influence of these parameters for $K/s(s+\lambda)$ controlled elements is discussed in the next subsection of this report.

3.3.2 Examination of $K/s(s+\lambda)$ Systems

The preceding discussions developed relationships between the open and closed loop parameters for a K/s controlled element when the pilot describing transfer function was $K_p e^{-\tau s}$. This subsection will examine similar relationships when the controlled element has the form $K_c/s(s+\lambda)$.

3.3.2.1 Some Considerations in Regards to Gain Crossover Frequency (ω_c) Selection

The following development will examine relationships that exist between the breakpoint frequency (λ) of the $K_c/s(s+\lambda)$ controlled element and the selection of crossover frequency. To simplify the development it will initially be assumed that the introduction of the pilot in the loop does not introduce any time delay; later this restriction will be removed. In addition it will be assumed that the pilot describing function can be adequately represented by just gain and lead adjustments, that is $Y_p = K_p(T_L s+1)$. First consider the situation when the pilot develops sufficient lead to obtain pole-zero cancellation ($T_L = 1/\lambda$). For this situation the closed-loop pilot-aircraft system can be represented (at least in the region of gain crossover) as

$$(Y_p Y_c)_{CL} = \frac{\omega_c}{s+\omega_c} \quad \text{where} \quad \omega_c = K_c K_p T_L$$

or

$$H(s) = \frac{1}{Ts+1} \quad \text{where} \quad T = \frac{1}{\omega_c}$$

Thus ω_c is indicative of the promptness of system response, that is the time to achieve steady state following a step commanded change in the input. That

is is when θ_c = unit step, the closed-loop response is:

$$\frac{\theta}{\theta_c} = 1 - e^{-\frac{t}{\tau}} = 1 - e^{-\omega_c t}$$

thus ω_c could be selected dependent upon the desired time to achieve steady state (θ_{ss} occurs when $\omega_c t \sim 3.0$). This is illustrated on the following chart:

t_{ss} sec	ω_c rad/sec	τ sec
1	3	.333
2	1.5	.667
3	1.0	1.00
4	.75	1.333

However in terms of tracking, the pilot-aircraft transfer function

$$|H(s)||H(-s)| = \frac{1}{1+(T\omega)^2} \quad \text{, thus} \quad |H(s)|^2 = \frac{1}{1+\left(\frac{\omega}{\omega_c}\right)^2}$$

The relationship between output and input rms for the tracking task results in

$$\frac{\sigma_{out}^2}{\sigma_{in}^2} = \frac{1}{1+\left(\frac{\omega}{\omega_c}\right)^2}$$

indicating that system performance in the tracking task is strongly dependent upon the value of ω_c . Good tracking performance necessitates high crossover frequency (with respect to the input bandwidth frequency); however, for the discrete task, high crossover frequency could result in a system that is overly responsive initially. To track errors to within 10%, the crossover frequency should be on the order of three times the task input bandwidth.

Next consider the situation when the pilot does not generate lead ($\tau_L = 0$). For the simplified case under consideration the closed-loop and open-loop pilot-aircraft system can be represented by the following transfer functions:

$$(Y_p Y_c)_{CL} = \frac{K_p K_c}{s(s+\lambda) + K_p K_c} = H(s)$$

$$(Y_p Y_c) = \frac{K_p K_c}{s(s+\lambda)} = G(s)$$

For this situation the relationship between $K_p K_c$ and ω_c we can be written as follows by equating the magnitude of $|Y_p Y_c| = 1$

$$K_p K_c = \omega_c (\omega_c^2 + \lambda^2)^{\frac{1}{2}} = \omega_c^2 \left(1 + \left(\frac{\lambda}{\omega_c}\right)^2\right)^{\frac{1}{2}}$$

The closed-loop system is just a simple second-order system with $\omega_n^2 = K_p K_c$ and $2\zeta\omega_n = \lambda$. The relationship between ζ and (λ/ω_c) can be written as follows:

$$\zeta = \frac{\frac{1}{2}\left(\frac{\lambda}{\omega_c}\right)}{\left[1 + \left(\frac{\lambda}{\omega_c}\right)^2\right]^{\frac{1}{4}}}$$

Using the relationships that exist for second-order systems, (Reference 21) the following table presents Phase Margin and resonant peak magnitude vs. (λ/ω_c) for the pilot-aircraft system under discussion.

λ/ω_c	PM deg	M_p ~dB
.1	5.73	20.0
.5	26.5	6.8
1.0	45.0	2.3
1.5	56.5	.60
2.0	64.5	.05

21 Melsa, James L. and Donald G. Schultz: "Linear Control Systems." McGraw-Hill Book Company, 1969.

Based on the definition of bandwidth used in this analysis, for the simple second-order system $\omega_n = \omega_B$. Figure 43 presents data for the simple second-order system for comparison with the results previously presented on Figure 42 for K/s systems with time delay included. Thus if the introduction of the pilot into the loop did not introduce time delays or lags then without lead generation, acceptable system performance could be achieved for

$$\frac{\lambda}{\omega_c} \geq .790 \; (\zeta_{cL} \simeq .35, \quad PM = 38.3^\circ).$$

For this situation, if we assume that to obtain good tracking performance the pilot desires the closed-loop bandwidth to be on the order of three times the input bandwidth, then the crossover frequency is related to input bandwidth by $\omega_c/\omega_i = 3\,\omega_c/\omega_B$. From the data presented on Figure 43 (with the assumption that $\omega_B/\omega_i = 3$) the following data results:

$\frac{\lambda}{\omega_c}$	PM deg	M_p dB	$\frac{\omega_c}{\omega_i}$	$\frac{\lambda}{\omega_i}$
.1	5.73	20.0	2.97	.297
.5	26.5	6.8	2.84	1.422
.79	38.3	3.67	2.66	2.10
1.0	45.0	2.3	2.52	2.52
1.5	56.5	.60	2.25	3.38
2.0	64.5	.05	2.01	4.02

Thus for the simplified example under consideration, the analysis indicates that for a satisfactory system the gain crossover frequency (ω_c) should be selected to be approximately 2.5 times the input bandwidth associated with the task. In addition the break frequency of the system (λ) should be at least twice the input bandwidth, and then $\omega_c/\lambda < 1.27$.

For example, if $\lambda = 1.0$, the above analysis indicates that ω_c would be selected at 1.27 radians/sec or less if the input bandwidth was less than .48 radians/sec. That is, if the pilot did not introduce time delay into the

$$Y_p Y_c = \frac{K_p K_c}{S(S+\lambda)} = \frac{\omega^2_B}{S(S+2\zeta\omega_B)}$$

$$\left(\frac{\omega_c}{\omega_B}\right) = \left[\sqrt{4\zeta^4+1} - 2\zeta^2\right]^{1/2}, \quad \frac{\omega_p}{\omega_B} = \sqrt{1-2\zeta^2}\left(\frac{\omega_c}{\omega_B}\right)$$

$$PM = \cos^{-1}\left(\left(\frac{\omega_c}{\omega_B}\right)^2\right)$$

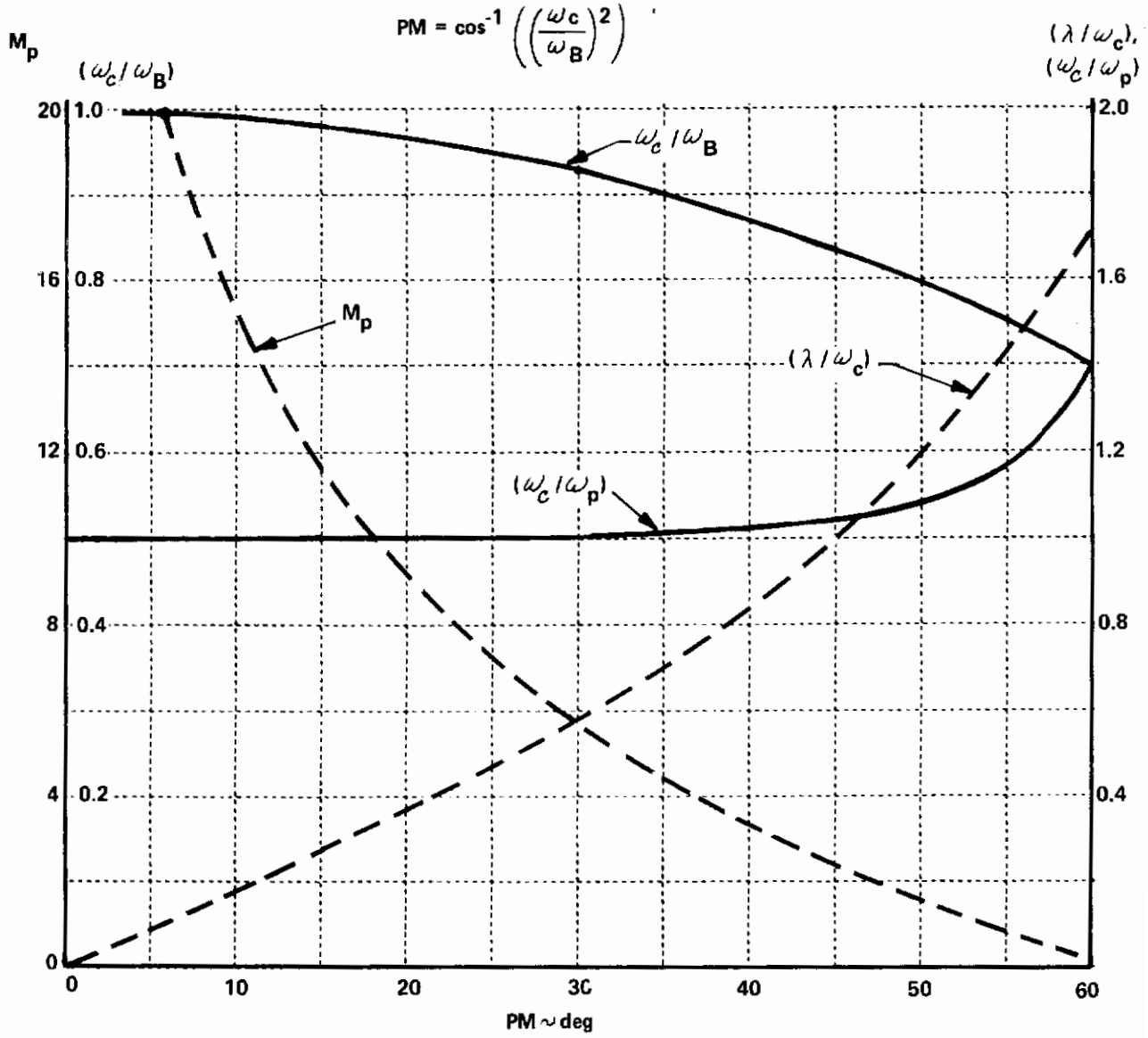

Figure 43 SYSTEM PARAMETERS FOR $Y_p Y_c = \frac{K}{s(s+\lambda)}$

system, pilot lead requirements would be held to zero ($T_L = 0$), and acceptable performance could be achieved.

With the previous discussion as background information, the following development will examine the effect of introducing time delay into the system. For the following discussion, the controlled-element transfer function is still $K_c/s(s+\lambda)$, however, now the pilot-describing function is $Y_p = K_p (T_L s + 1)e^{-\tau s}$. First consider the case of pole-zero cancellation, for this situation

$$Y_p Y_c = \frac{\omega_c}{s} e^{-\tau s}$$

and the analysis previously presented in 3.3.1 is directly applicable. From the data presented on Figure 42, the following information can be obtained (again assuming $\omega_B/\omega_i = 3.0$):

			$\tau = .3$ sec	
PM deg	M_p dB	$\frac{\omega_c}{\omega_i}$	ω_c rad/sec	ω_i rad/sec
26.5	9.7	2.79	3.69	1.32
38.3	5.5	2.60	3.00	1.15
45.0	3.4	2.45	2.62	1.07
56.5	.60	2.18	1.95	.89
64.5	0	1.92	1.48	.77

These results again indicate that for this situation the pilot would tend to adjust his gain and lead equalization to attempt to achieve gain crossover at approximately 2.5 times the input task bandwidth in the tracking task. The last two columns indicate the gain crossover frequency (ω_c) and input bandwidth that would enable the pilot to achieve the closed-loop performance associated with either M_p or phase margin if the time delay was equal to .3 seconds. The pilot equalization adjustment "rules" presented in Reference 13 indicate that when $\lambda = 1/\tau$, the pilot might not introduce low-frequency lead ($T_L = 0$). For $\tau = .3$, this implies that $T_L = 0$ for $\lambda > 3.3$ rad/sec. The above data indicates that lead generation will tend to increase the

resonance peak at a prescribed phase margin, thereby degrading closed-loop performance. However, this effect is minimal for phase margins in excess of 50°. Next examine the situation when the pilot does not introduce lead equalization to either compensate for the phase shift introduced by pilot-in-the-loop time delays or to achieve pole-zero cancellation.

For this situation the appropriate open-loop and closed-loop transfer functions can be expressed as follows:

$$G(s) = \frac{K_p K_c e^{-\tau s}}{s(s+\lambda)} = |G(\omega)| e^{i\phi(\omega)}$$

$$H(s) = \frac{K_p K_c e^{-\tau s}}{s(s+\lambda) + K_p K_c e^{-\tau s}}$$

where

$$|G(\omega)| = \frac{K_p \cdot c}{\omega(\omega^2 + \lambda^2)^{1/2}}$$

$$\phi(\omega) = -90^{\circ} - \tan^{-1}\left(\frac{\omega}{\lambda}\right) - \tau_e \omega, \quad \text{where } \tau_e = \frac{180}{\pi}\tau$$

At the crossover frequency

$$|G(\omega)| = 1 = \frac{K_p K_c}{\omega_c^2 \left(1 + \left(\frac{\lambda}{\omega_c}\right)^2\right)^{\frac{1}{2}}}$$

$$\therefore K_p K_c = \omega_c^2 \left(1 + \left(\frac{\lambda}{\omega_c}\right)^2\right)^{\frac{1}{2}}$$

Therefore in general

$$|G(\omega)| = \frac{\omega_c}{\omega}\left[\frac{\omega_c^2 + \lambda^2}{\omega^2 + \lambda^2}\right]^{\frac{1}{2}}$$

and the phase margin can be expressed as

$$PM = 90^\circ - \tan^{-1}\left(\frac{\omega_c}{\lambda}\right) - \tau_e \omega_c$$

Since it becomes rather unwieldy to determine the closed-loop gain and phase for this system, even applying the equations presented in 3.3.1, this will not be done. Rather the phase margin relationship will be examined analytically. The equation for the phase margin can be written as follows:

$$\frac{\omega_c}{\lambda} = \tan(90^\circ - PM - \tau_e \omega_c)$$

This equation illustrates that the phase margin achieved with $T_L = 0$ will asymptotically approach the phase margin that results from perfect pole-zero cancellation as the ratio $\frac{\omega_c}{\lambda} \rightarrow 0$, or $\frac{\lambda}{\omega_c} \rightarrow \infty$. The other limiting situation ($\tau = 0$) has been previously discussed. The above equation is presented on Figure 44 for various phase margins. The figure indicates the gain crossove frequency associated with the real root location for the $K/s(s+\lambda)$ when the pilot does not use lead equalization. If the combination of phase margin, crossover frequency and pilot gain is satisfactory for the given task for the value of λ that characterizes the controlled element transfer function in the region of crossover, then it is reasonable to assume that the pilot would not have to provide lead equalization. However if the crossover frequency is insufficient to provide satisfactory system performance the pilot would probably choose to initiate gain and lead adjustments. It is assumed in this discussion that the pilot is more efficient at these adjustments than attempting to significantly modify time delay.

From the equations previously presented the following relationship can be derived that relates the pilot gain when he does not use lead equalization, to the situation when the pilot provides the lead equalization necessary to achieve pole-zero cancellation:

$$\frac{K_p\,(T_L = 0)}{K_p\,(\lambda T_L = 1)} = \left[1 + \left(\frac{\omega_c}{\lambda}\right)^2\right]^{\frac{1}{2}} \equiv K'$$

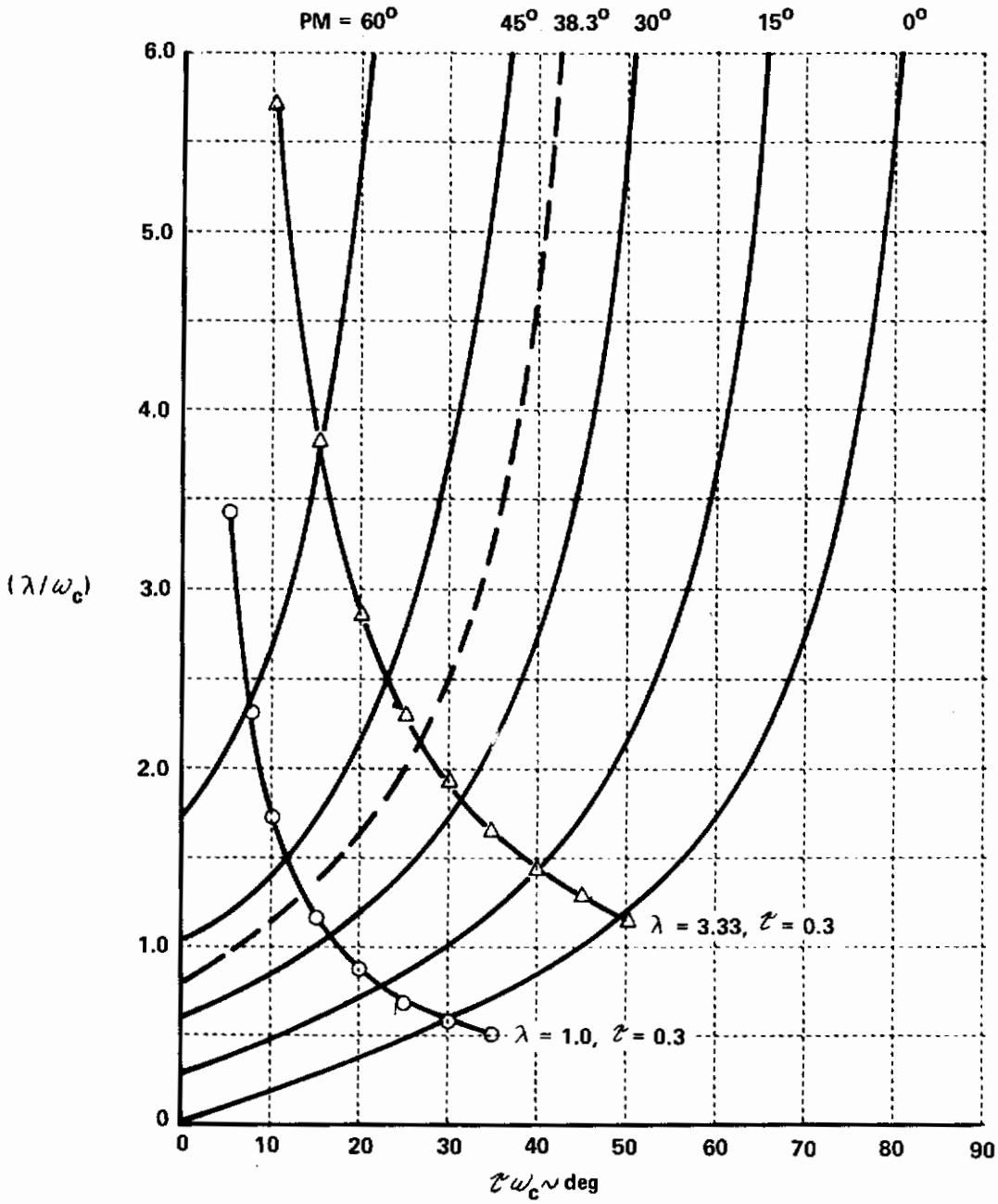

Figure 44 RELATIONSHIP BETWEEN λ/ω_c AND PM FOR $Y_p Y_c = \frac{K}{s(s+\lambda)} e^{-\tau s}$

This equation illustrates that the pilot gain requirement reduces when he generates lead for a given λ and ω_c. However it should be noted that if $(\omega_c/\lambda)<1$, the effects of pilot gain adjustments may be rather insignificant. As a final point in this discussion, let us examine the relationship that exists between λ and ω_c at a given phase margin. From previous discussions it was assumed the PM $\sim 38.3^{o}$ would yield a reasonable system performance without lead adjustments by the pilot. Selecting this as the phase margin of interest the preceding equation and Figure 44 may be used to explicitly define the relationship between ω_c and λ for T_L = 0 and τ = .3 seconds. This relationship is presented on Figure 45. From the data on this figure, the following observations are made:

(1) If $\omega_c \simeq 1.55$ rad/sec is satisfactory for the task, then the pilot should not have to use lead equalization when $\lambda > 3.33$ rad/sec.

(2) Pole-zero cancellation for a phase margin of 38.7^{o} results in a gain crossover frequency of 3.0 rad/sec. If this crossover frequency is not sufficient for the task then higher crossover frequency will result in reduced phase margin, and increased closed-loop resonance. Thereby the closed-loop tracking performance will deteriorate.

(3) Reduction of the required gain crossover frequency for the task would either:
   (a) eliminate the need for pilot lead equalization as the controlled element pole approached the origin, or
   (b) increase system performance increasing the phase margin and reducing closed-loop resonance as the pilot introduced lead equalization.

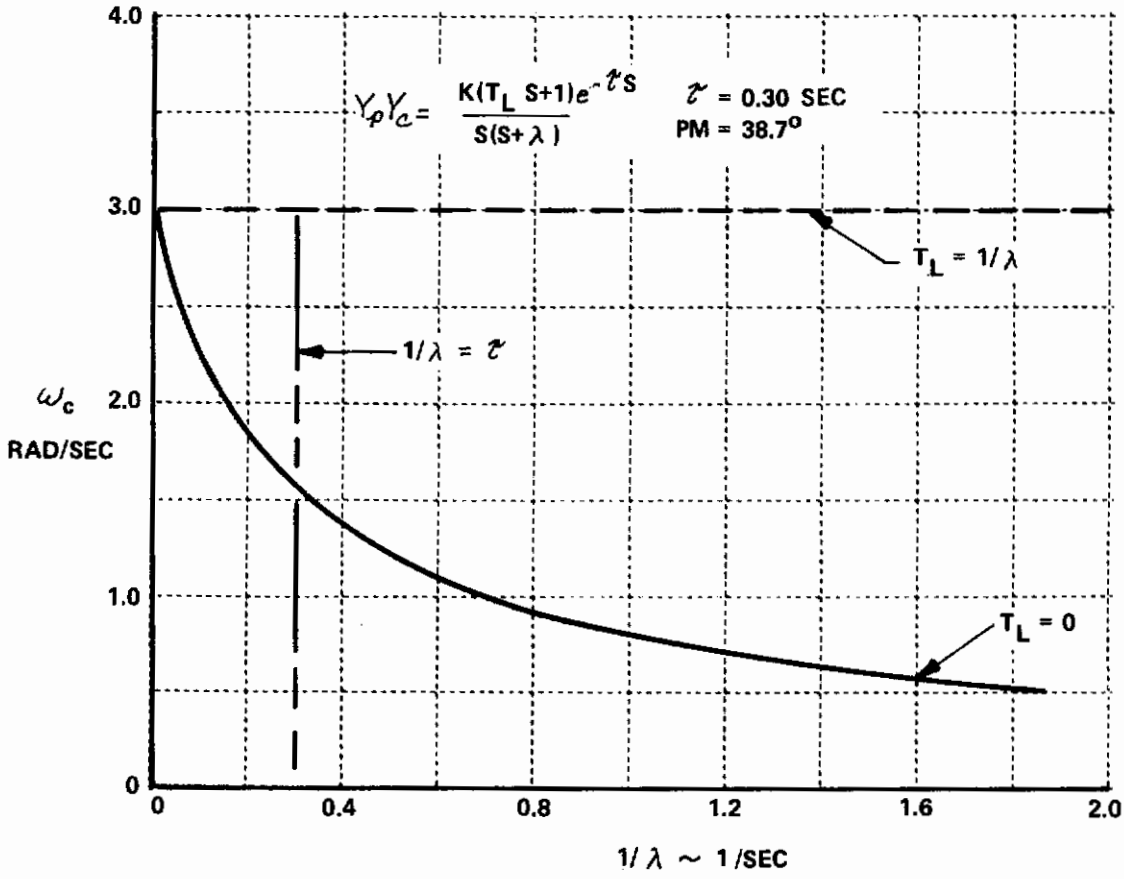

Figure 45 RELATIONSHIP BETWEEN ω_c AND λ WHEN $T_L = 0$ AND PM = 38.7°

3.3.3 Effects of Pilot Lead Equalization on Closed-Loop Performance

Based on the preceding discussion, it was decided to examine two configurations in the "closed-loop" parameter plane suggested by Neal & Smith in Reference 14. For the data to be presented in this subsection the time delay introduced by the pilot in the loop was held fixed at .3 seconds. The data was obtained by assuming the pilot describing function to be of the form $K_p(T_L s+1)e^{-.3s}$, and the controlled element to be either $K_c/s(s+1)$ or $K_c/s(s+4)$. Thus the open-loop pilot-aircraft system can be represented by the following transfer function:

$$Y_p Y_c = \frac{K(T_L s+1)e^{-.3s}}{s(s+\lambda)}, \quad with \quad \lambda = 1, 4$$

The figures to be presented in this discussion were obtained by selecting either ω_c and PM or T_L and ω_B ($\phi_{CL} = -90^\circ$). Digital programs were used to obtain the remaining parameters of interest. For example when certain data was specified, the following data was obtained for a selected configuration in the order noted:

(a) Specify $(PM, \omega_c, \lambda) \Rightarrow (K, T_L) \Rightarrow (\omega_B, M_p, GM)$

(b) Specify $(T_L, \omega_B, \lambda) \Rightarrow (K) \Rightarrow (PM, \omega_c, M_p, GM)$

3.3.3.1 Controlled Element: $\left[K_c/s(s+1)\right]$

The data obtained from the examination of the effects of lead and gain adjustment are presented on Figures 46, 47, 48. The first figure illustrates the relationships that exist between ω_c, ω_B, PM and T_L for the selected system. System gain as a function of T_L, ω_B and PM is presented on the second figure, and the data is presented in terms of resonance peak and pilot lead angle adjustment $\left[\tan^{-1}(T_L \omega_B)\right]$ on the third figure. The following observations are made concerning the data presented on these figures:

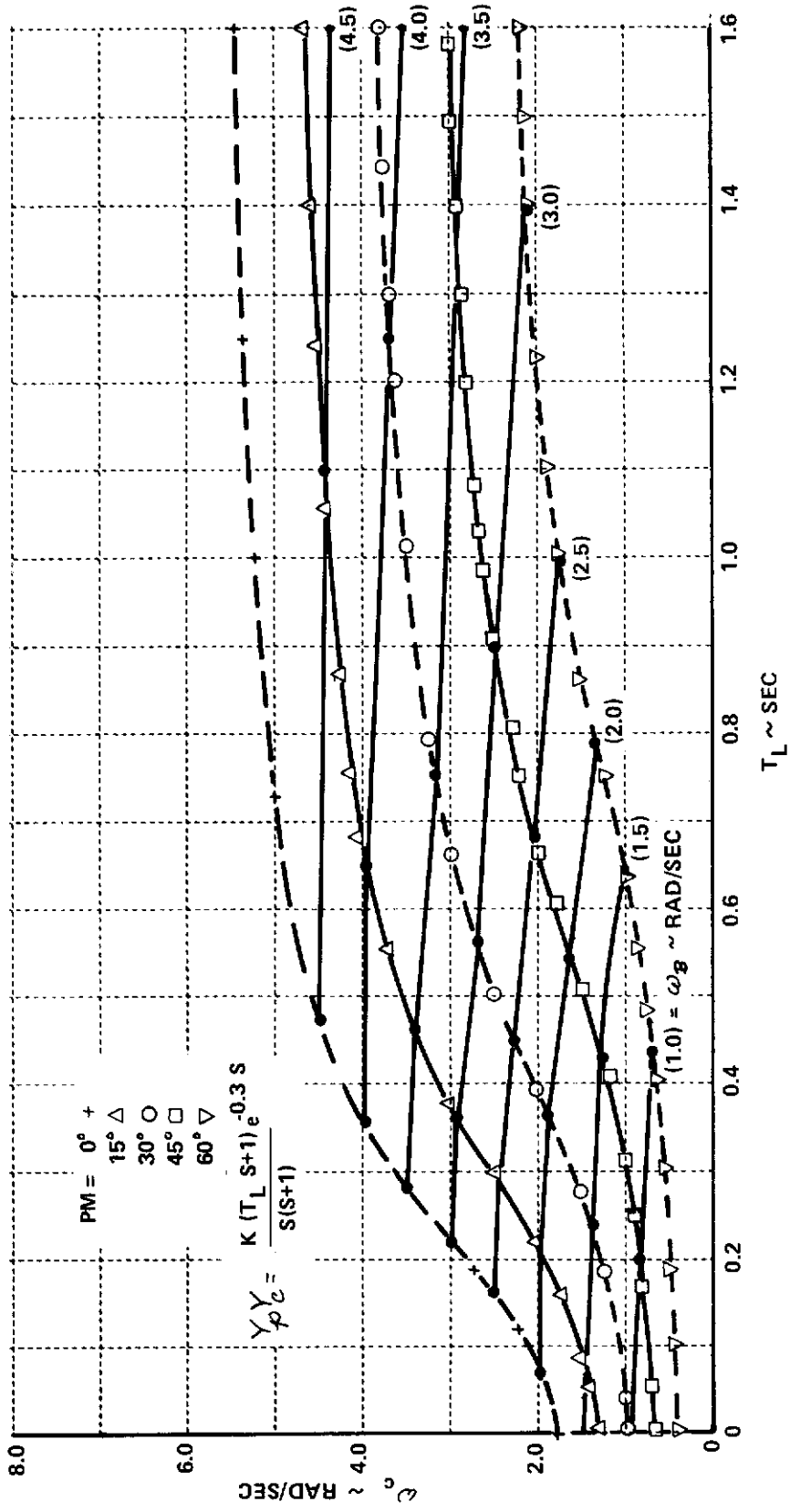

Figure 46 INFLUENCE OF LEAD EQUALIZATION, AT CONSTANT PHASE MARGIN, ON CROSSOVER FREQUENCY, $\left(Y_c = \frac{K_c}{s(s+1)}\right)$

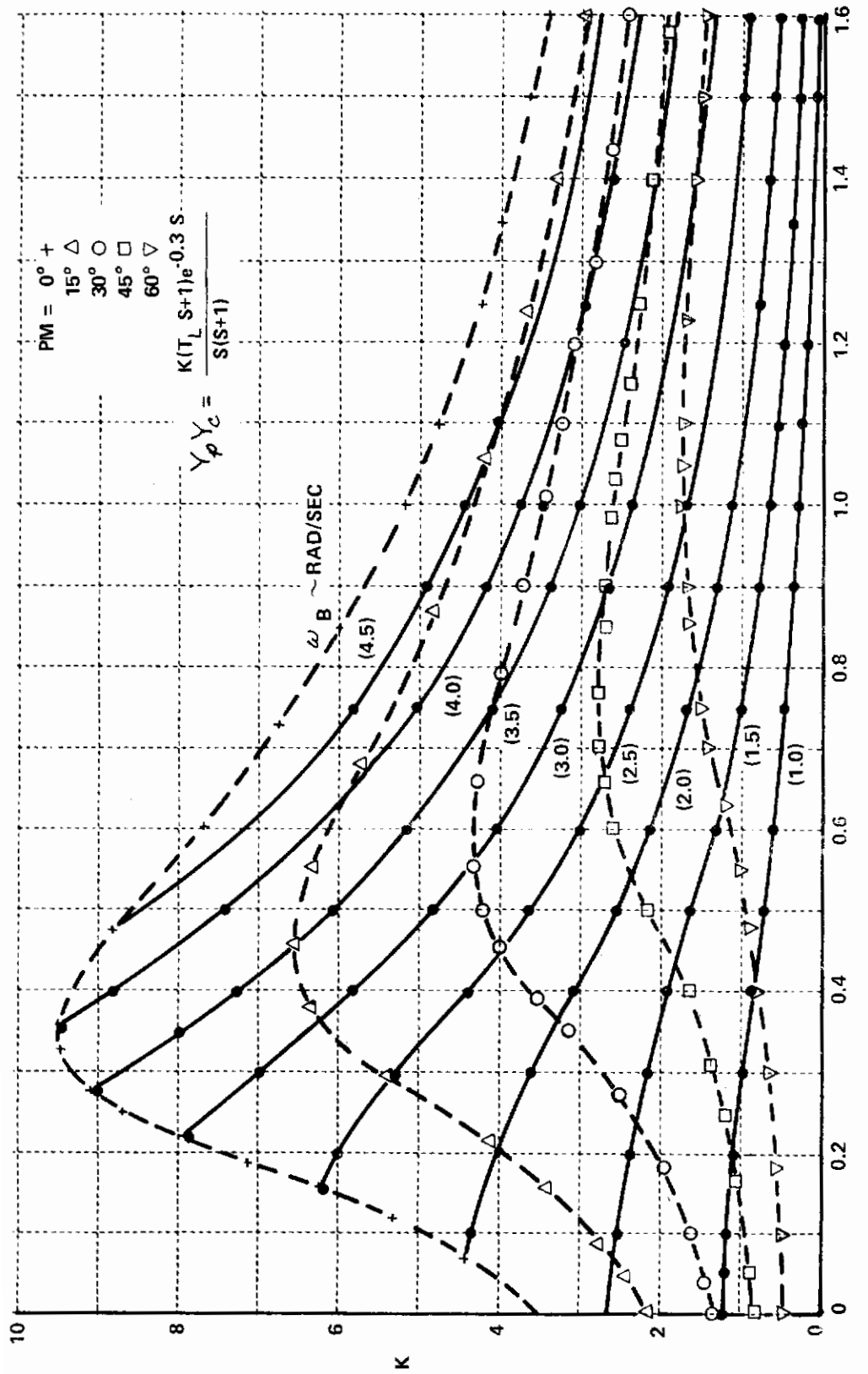

Figure 47 SYSTEM GAIN RELATIONSHIP WITH LEAD EQUALIZATION AT CONSTANT PHASE MARGIN OR BANDWIDTH $\left(Y_c = \frac{K_c}{S(S+1)}\right)$

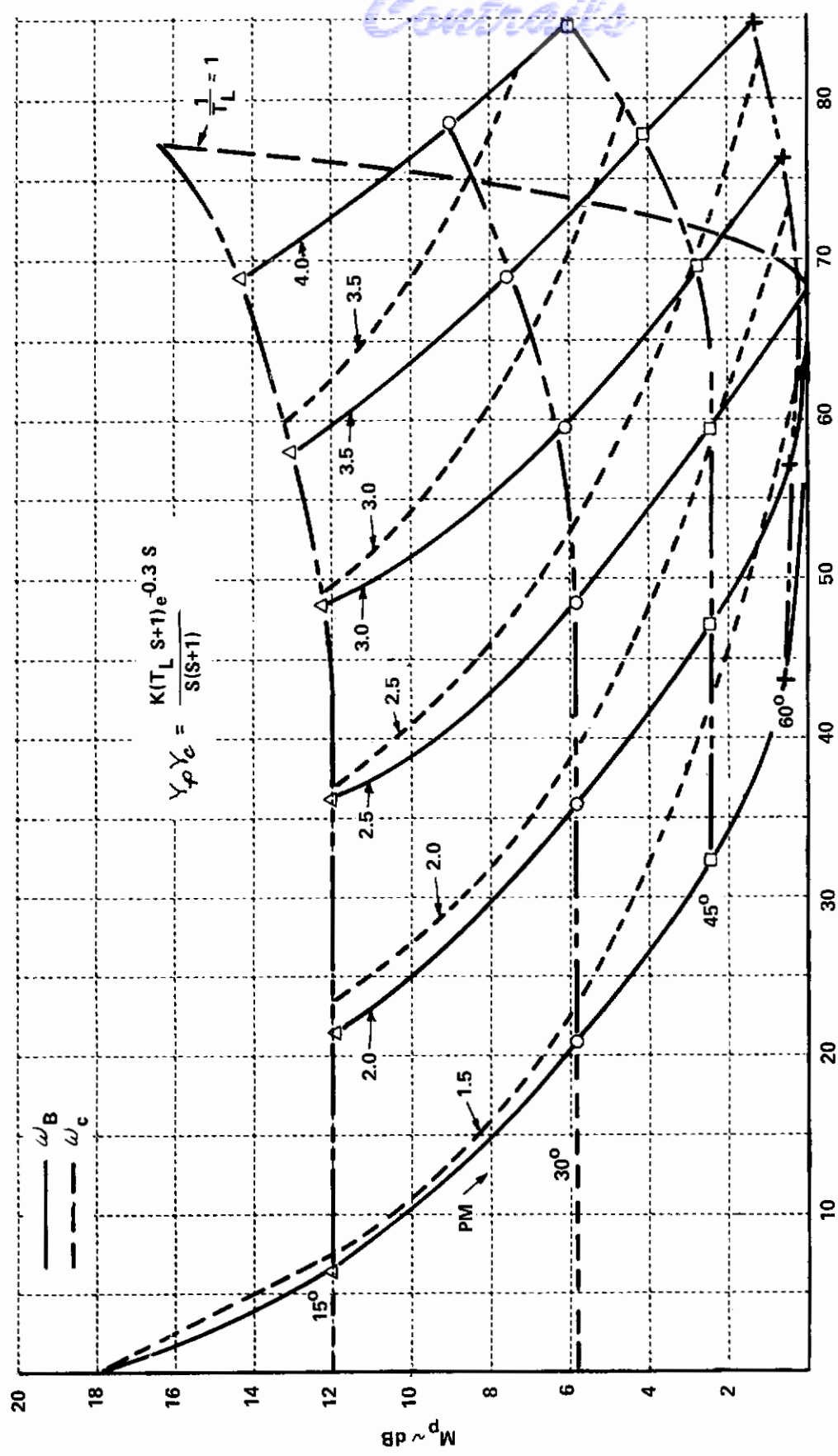

Figure 48 CLOSED-LOOP PARAMETER PLANE, $Y_c = \frac{K_c}{s(s+1)}$

(1) Pole-zero cancellation for this system may only be warranted when crossover frequency is greater than 3 rad/sec or bandwidth is greater than 3.5 rad/sec.

(2) Lead generation will not significantly influence closed-loop resonance or open-loop phase margin if proper pilot gain adjustment is provided.

(3) Large bandwidths or crossover frequencies require lead generation just to stabilize the pilot-aircraft system, and required additional lead generation to obtain "reasonable" closed-loop performance ($M_p < 6$ dB).

(4) Generation of T_L in excess of that required to produce pole-zero cancellation will make the system performance more sensitive to pilot gain than for $T_L \leq 1/\lambda$.

(5) Crossover frequency or bandwidth less than 1.0 rad/sec does not require lead equalization for "reasonable" closed-loop performance.

(6) Open-loop phase margin is indicative of closed-loop resonance peak amplitude regardless of the values of T_L for $\omega_B \leq 3.0$ rad.

(7) There are regions where system gain can be held essentially constant at the value associated with a desired phase margin while T_L is varied to increase bandwidth. For example:

PM	K	T_L	ω_B
30^o	~4	.45 → .80	2.5 → 3.6
45^o	~2.8	.66 → .90	2.5 → 3.0
60^o	~1.7	.80 → 1.4	2.0 → 3.0

Thus if the pilot prefers to use lead equalization rather than gain adjustments to achieve a desired bandwidth the data indicates that the pilot might select $.45 < T_L < .80$ with phase margin in the vicinity of 30^o ($M_p < 6$ dB), rather than pole-zero cancellation. To further illustrate this point, $Y_c = K_c/s(s+1)$ is presented in Figure 49, where K is fixed at 1.25 and T_L varied from 0 to 1. This system with $T_L = 0$ was previously discussed in the analysis of open-loop parameters. Figure 49 indicates that there is little need to provide $T_L > .64$ for this system. The slight increases in phase margin, crossover frequency and bandwidth that result from increasing lead to achieve pole-zero cancellation may be offset by the reduction in gain margin.

The effect of lead equalization for this system on gain margin is presented on Figure 50. This figure again illustrates that pole-zero cancellation is not necessarily warranted to achieve a "reasonable" system ($GM \geq 6$dB). In fact, to maintain a desired phase margin, increasing T_L will reduce gain margin. On the other hand, if a bandwidth of 3.0 rad/sec is required for the task, Figure 50 indicates that $GM \sim 6$ dB can be achieved with phase margins between 30 and 45 degrees with T_L between .56 and .90. In addition the figure indicates that for $T_L > .70$ further increases in lead equalization to obtain pole-zero cancellation do not significantly influence open-loop pilot-aircraft gain margin. Furthermore, the data shown on Figure 47 indicates that the sensitivity of phase margin or closed-loop resonance peak is minimal for $.2 < T_L < .7$. That is, at values of lead $< .70$ and > 0.2, the pilot could make greater changes in gain without degrading closed-loop performance than when $T_L > .70$. This can be illustrated simply by examination of the ratio in system gain at 30^o phase margin to system gain at 60^o phase for various values of T_L :

T_L	$K30°/K60°$
.2	3.62
.3	4.18
.4	4.56
.5	4.44

T_L	$K30°/K60°$
.6	3.84
.7	2.96
.8	2.53
1.0	2.0

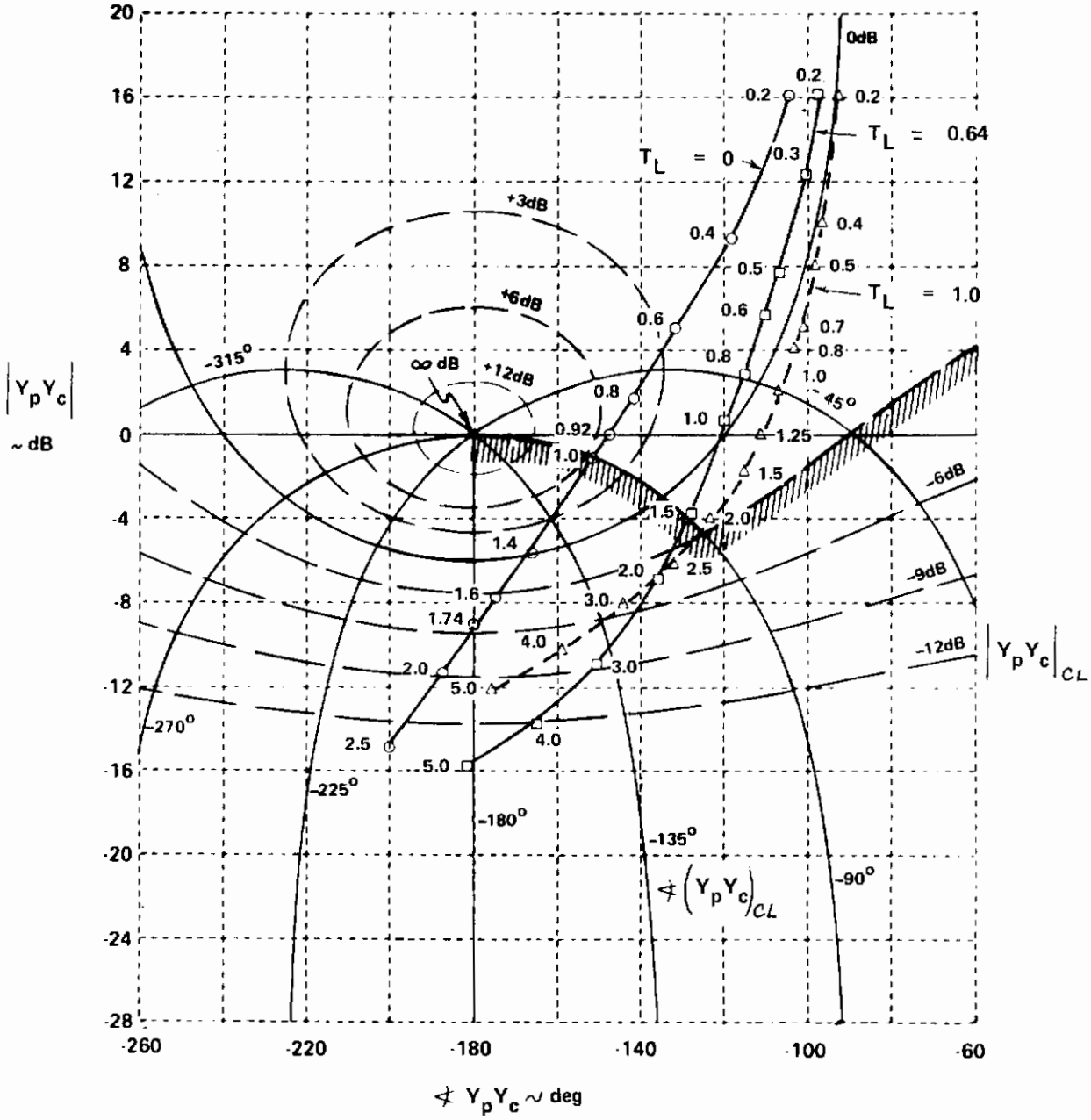

Figure 49 NICHOLS CHART FOR $Y_pY_c = \frac{1.25(\tau_L s+1)e^{-.3s}}{s(s+1)}$ AS LEAD EQUALIZATION IS VARIED FROM 0 TO 1.0

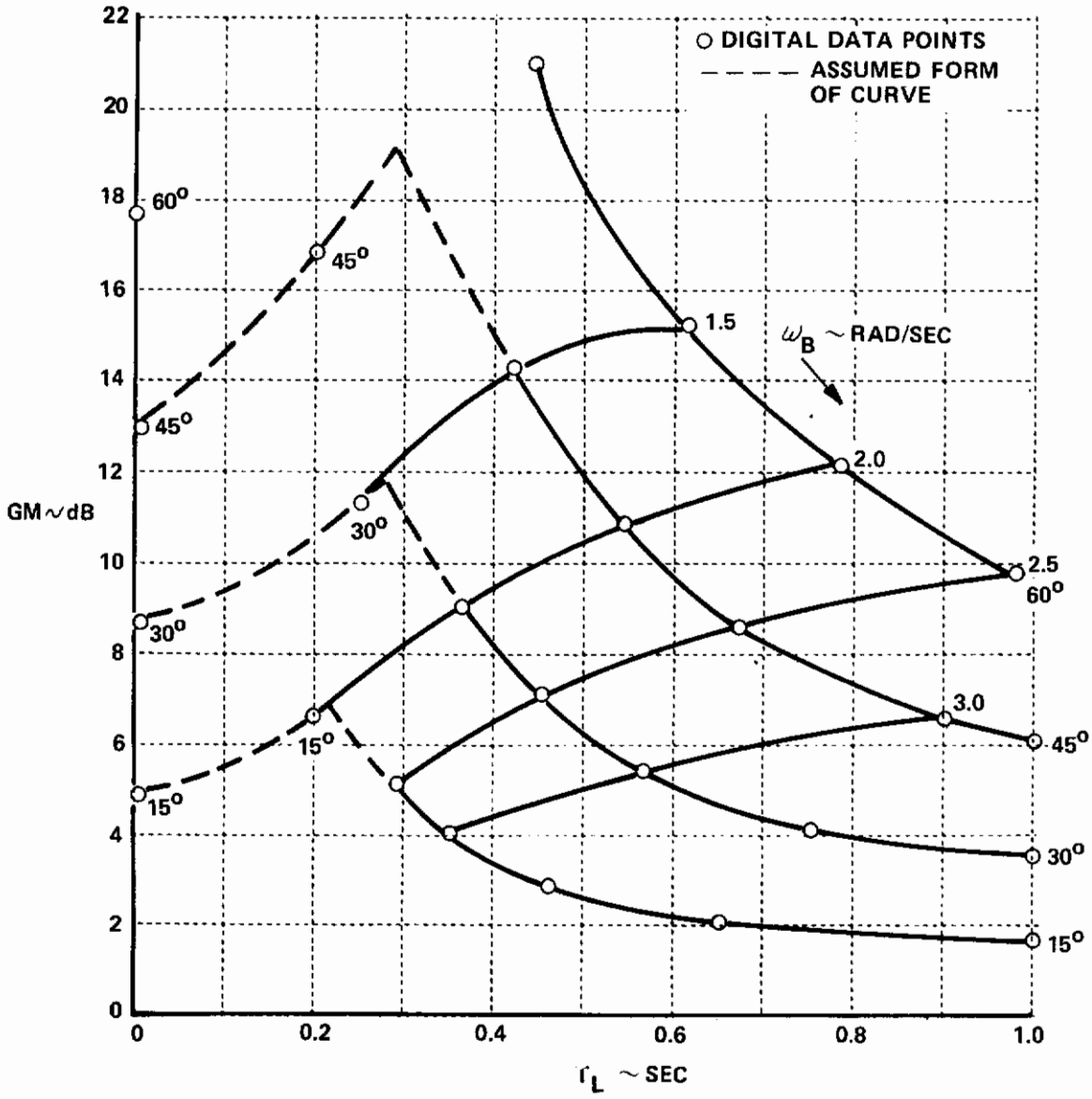

Figure 50 GAIN MARGIN FOR $Y_p Y_c = \frac{K(T_L s + 1)e^{-.3s}}{s(s+1)}$

The examination of the $K/s(s+1)$ system does not indicate significant benefits that can be achieved from pilot lead equalization to obtain pole cancellation. Rather the analysis indicates that perhaps a more reasonable strategy for the pilot to adopt is to generate lead less than that required to obtain a "perfect" K/s system in terms of amplitude ratio in the vicinity of crossover. For this situation, a possible lower limit on T_L is that just required to negate the influence of time-delay on phase margin ($T_L \cong .3$) or that required to initially provide at least 15^o of phase margin at a desired bandwidth (e.g., $\omega_B = 3 \Rightarrow T_L = .36$ for PM = 15^o) . Once this situation has been achieved, and as the pilot becomes more familiar with the characteristics of the system and the performance he requires for the task, or within his capability to adjust his parameters to influence closed-loop performance, additional lead equalization could be introduced. The analysis presented for the $K/s(s+1)$ system in this report indicates the pilot reaches a point of diminishing returns (i.e., improved performance) for $T_L > .70$. In addition if lead generation can be considered an index of pilot workload, then it is quite possible that the pilot will generate as little lead equalization as required to obtain "reasonable" performance.

3.3.3.2 Controlled Elements: $\left[K_c/s(s+4)\right]$

The preceding analysis examined the system $K_c/s(s+1)$ with $Y_p = K_p(T_L s+1)e^{-.3s}$. Based on the equalization "rule" presented in Reference 13, that system would be a candidate for pilot low frequency lead equalization since $T > \tau$. Before proceeding to the next subsection which involves "measured" pilot equalization for the types of controlled elements examined in this section, it is of value to compare the previous results with those obtained for a system which under the cited adjustment 'rules' is not a candidate for low-frequency lead equalization. To achieve this purpose, the controlled element transfer function $K_c/s(s+4)$ will be examined next, with $\tau = .3$ (therefore $T < \tau$). This configuration is also pertinent to the discussion of a comparison of the analysis performed in this section with the data presented in Reference 11.

The data obtained from the examination of lead and gain adjustment are presented on Figures 51, 52, and 53. Figure 51 presents the relationships that exist between ω_c, ω_B, PM and T_L for the selected system. System gain as a function of T_L, ω_B and phase margin is presented on Figure 52, while Figure 53 presents the data in terms of the "closed-loop" parameters suggested by Reference 14. The following observations are made concerning the data presented on these figures:

(1) Lead equalization may not be necessary to achieve reasonable performance provided the bandwidth frequency or the gain crossover frequency is less than 2.0 rad/sec.

(2) For constant crossover frequency, increased lead generation will not appreciably reduce reasonance peak from the value obtained for pole-zero cancellation.

(3) If system bandwidth is more important to task performance than crossover frequency, then for constant bandwidth the resonance peak can be significantly reduced by generating lead in excess of the amount required for pole-zero cancellation.

(4) For large bandwidth requirements ($\omega_B \geq 3.5$) the lead required to create a system with normal stability is approximately equal to that required to provide pole cancellation.

(5) Increasing T_L above that required to cancel the aircraft pole, at constant phase margin, can deteriorate closed-loop performance (e.g. M_p increases).

(6) Open-loop phase margin is directly indicative of closed-loop resonance for $\omega_B \leq 3.5$ rad/sec.

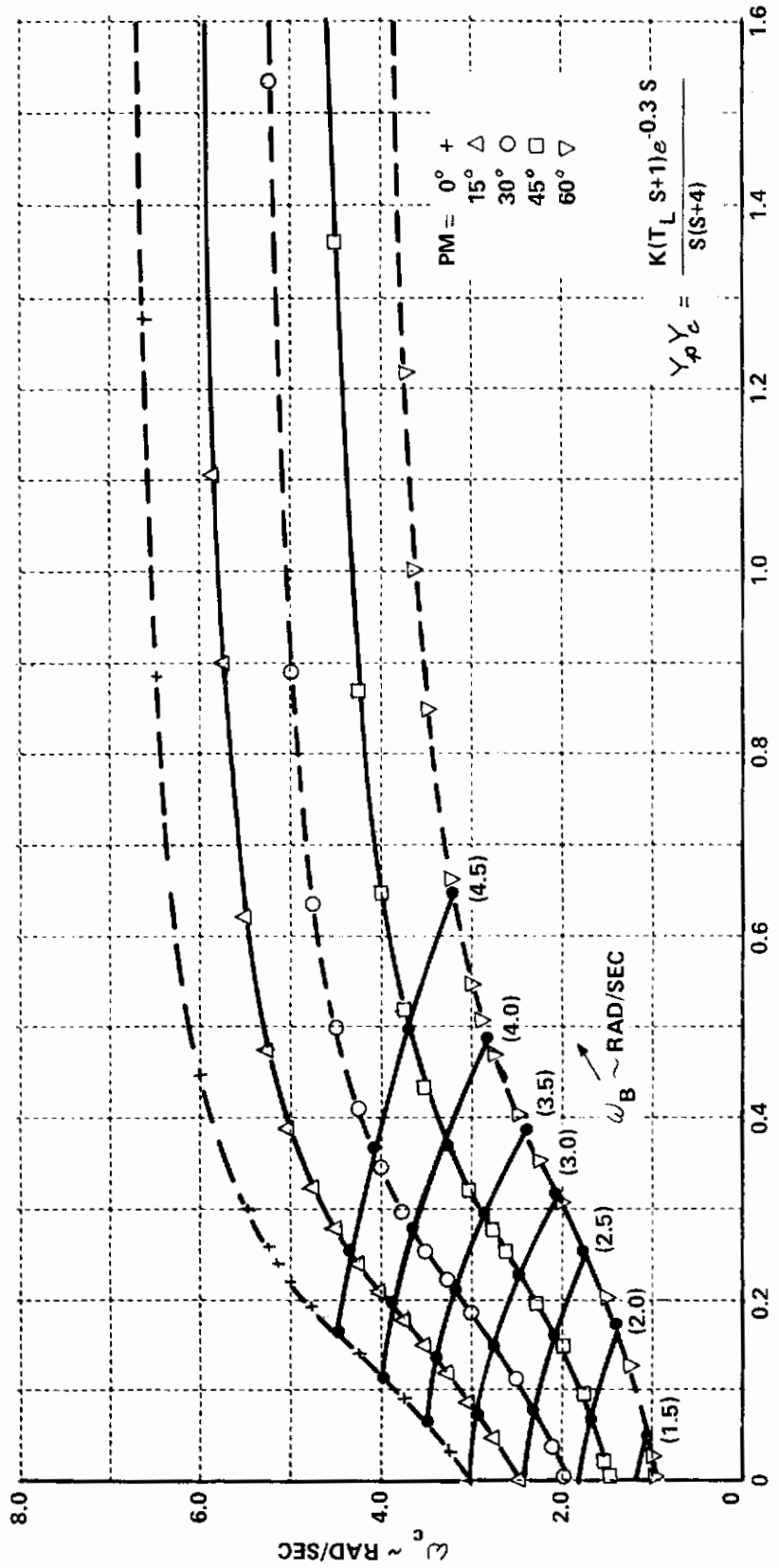

Figure 51 INFLUENCE OF LEAD EQUALIZATION, AT CONSTANT PHASE MARGIN, ON CROSSOVER FREQUENCY $\left(Y_c = \frac{K_c}{S(S+4)}\right)$

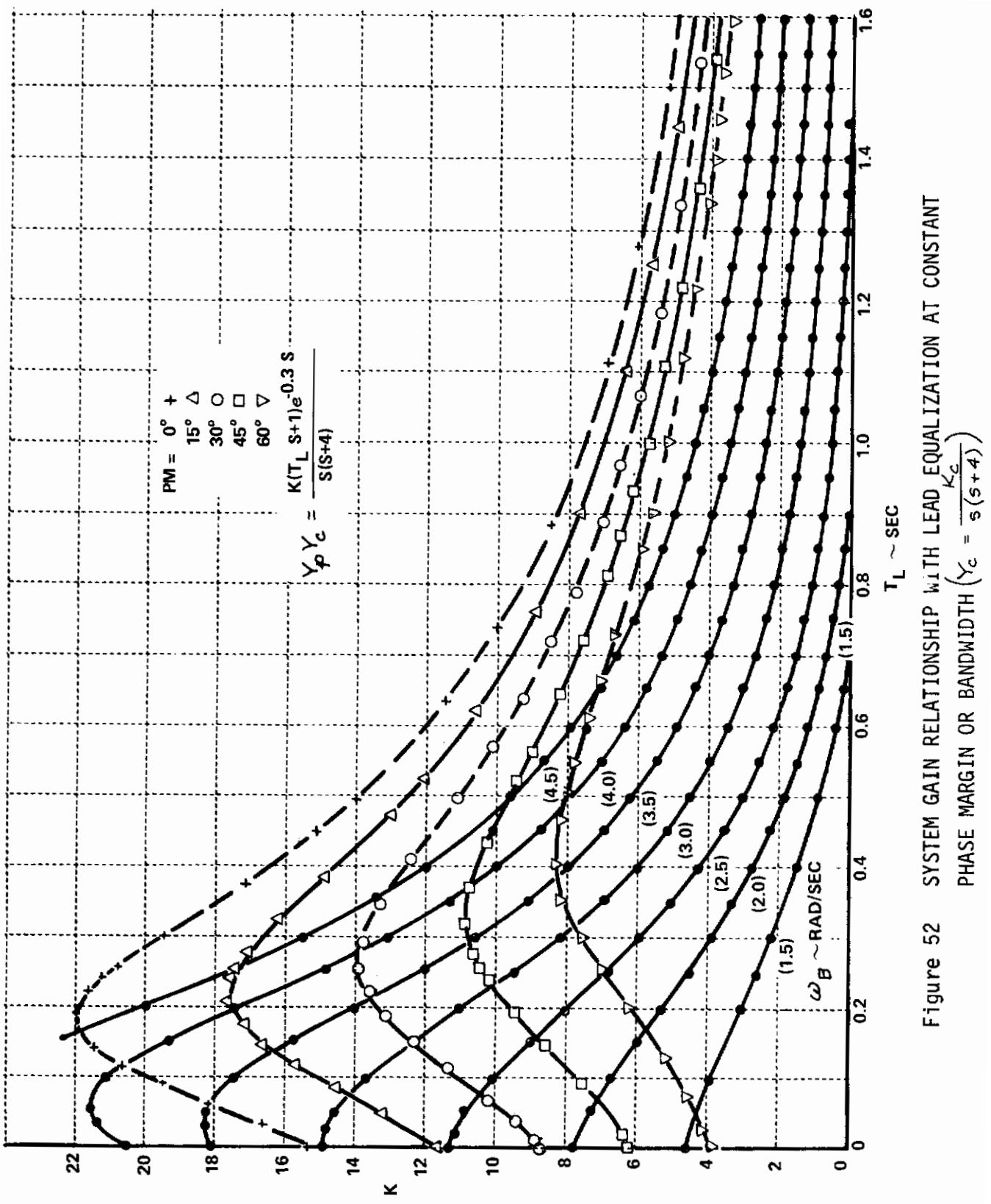

Figure 52 SYSTEM GAIN RELATIONSHIP WITH LEAD EQUALIZATION AT CONSTANT PHASE MARGIN OR BANDWIDTH $\left(Y_c = \frac{K_c}{s(s+4)}\right)$

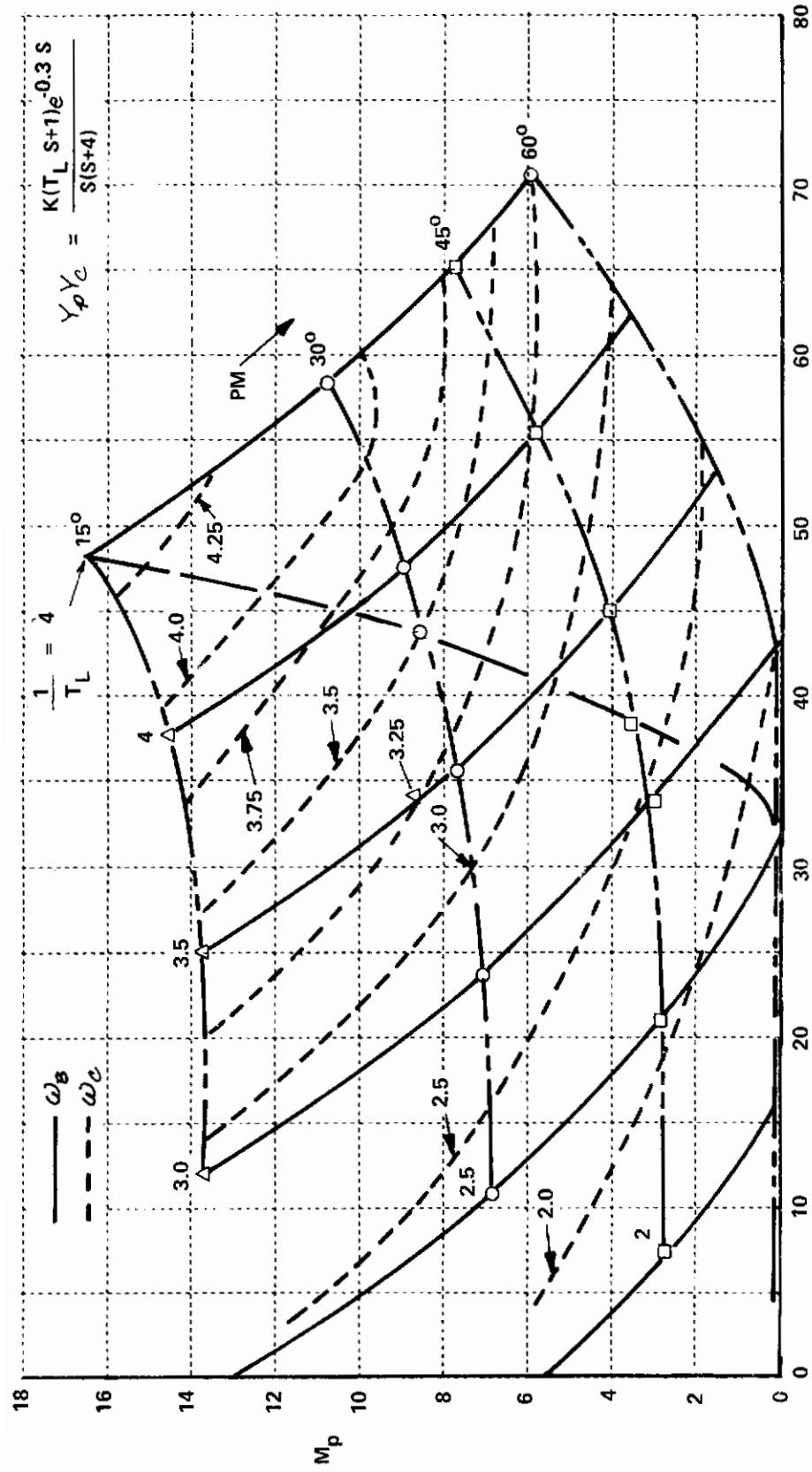

Figure 53 GAIN MARGIN FOR $Y_c = \frac{K_c}{s(s+4)}$

(7) Crossover frequency greater than 3.0 rad/sec requires lead generation to provide a stable system.

(8) This system is more sensitive to pilot gain variations than $K_c/s(s+1)$; however, as previously discussed, pilot gain requirements reduce at constant bandwidth with increased lead generation. For lead generation in the vicinity of that required for pole cancellation, the product of $K_p T_L$ remains essentially constant at constant bandwidth. The magnitude of $K_p T_L$ is directly proportional to the desired bandwidth.

The following chart illustrates the sensitivity of the system to pilot gain changes at fixed values of T_L , by ratioing the system gain at 30° phase margin to the system gain at 60° phase margin.

T_L	$K_{30^\circ}/K_{60^\circ}$
0	2.20
.1	2.29
.2	2.19
.3	2.09
.4	1.48
.5	1.36

This data indicates that this measure of the system sensitivity remains essentially constant as lead varies from T_L = 0 to T_L = .3.

The effects of lead equalization at essentially constant system gain are illustrated on Figure 54 for the $K_c/s(s+4)$controlled element transfer function with τ = .3 seconds. For this configuration, the pilot can create a system which could, from a linear viewpoint, perfectly track the rms input signal by either selecting $T_L \geq .25$ or by providing gain adjustment. However, for the system with pole-zero cancellation this can only be accomplished for $\omega_B < 2.6$ radians ($\omega_c < 1.8$). If the lead is set to .313 as shown on Figure 54, the bandwidth can be increased to 3.0 rad/sec and the crossover frequency

$$Y_p Y_c = \frac{K(T_L S+1)e^{-\tau S}}{S(S+4)}$$

○	△	□
K = 7.82	K = 7.82	K = 7.77
ω_c = 1.785	T_L = 0.25	T_L = 0.313
ω_B = 2.0	τ = 0.3	τ = 0.3
PM = 35°	PM = 56°	PM = 60°
T_L = 0	ω_c = 1.955	ω_c = 2.06
τ = 0.3	ω_B = 2.68	ω_B = 3.0

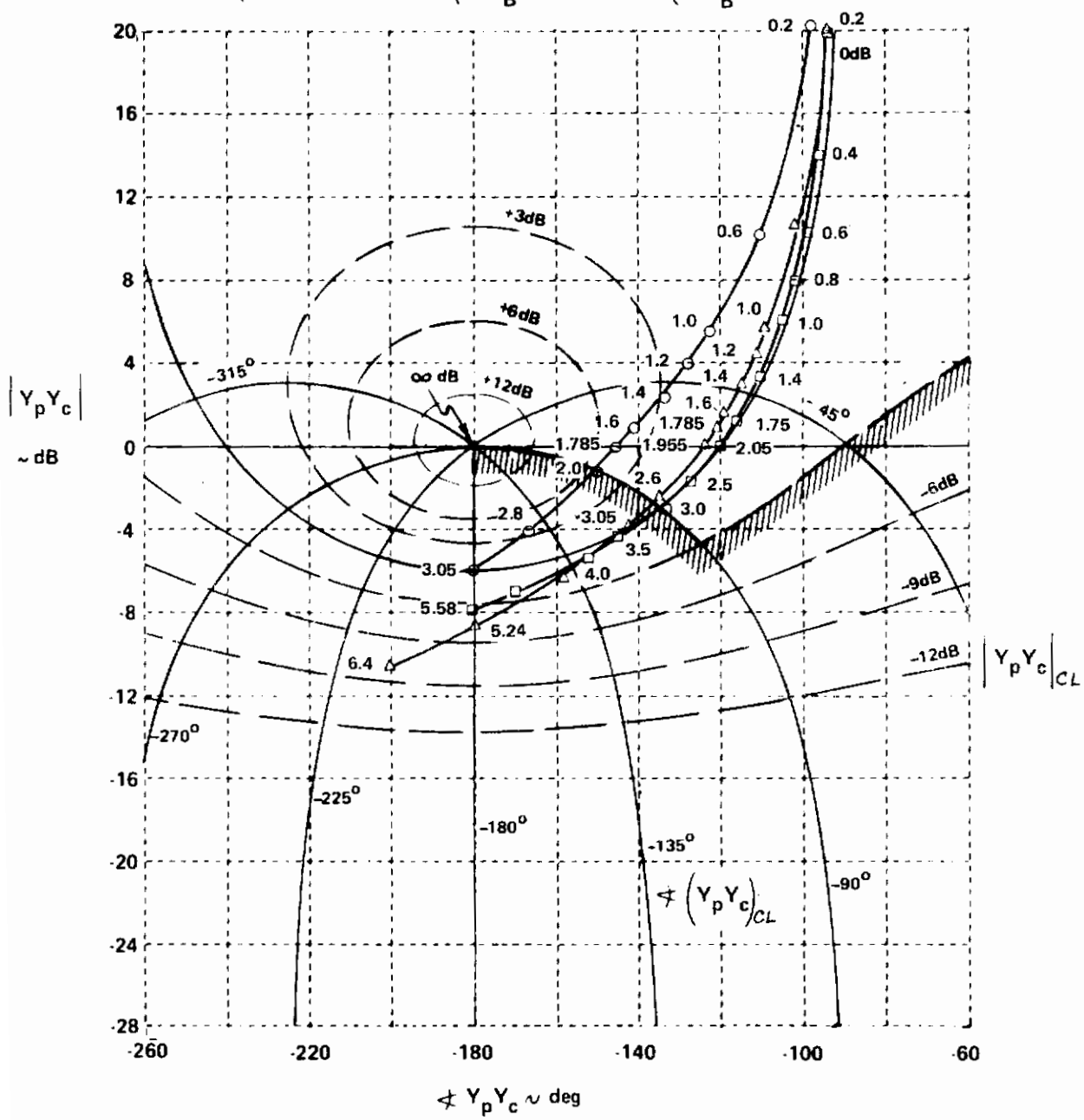

Figure 54 EFFECT OF LEAD EQUALIZATION AT ESSENTIALLY CONSTANT SYSTEM GAIN

to 2.05 rad/sec.

Figure 55 presents the relationships that exist between open-loop phase margin and gain margin for various bandwidths as a function of the pilot lead equalization when the controlled element transfer function is $K/s(s+4)$ and pilot-in-the-loop time delay is fixed at .3 seconds. Thus to achieve a gain margin > 6 dB, the pilot could adjust lead between .2 (ω_B = 3.0) and .36 (ω_B = 3.5) and also achieve satisfactory closed-loop performance (in terms of phase margin or resonance peak). Increasing the bandwidth requirements would either result in using excessive lead to maintain phase margin, with an accompanying reduction in gain margin, or maintaining T_L fixed and reducing phase margin and gain margin simultaneously.

3.3.4 Summary of Closed-Loop Parameters

This portion of the report has developed the relationships between various "open-loop" and "closed-loop" parameters which are indicative of system performance and pilot workload. From the data presented, observations have been made concerning the effects of lead equalization by the pilot on the system. The data indicates the various alternatives faced by the pilot, and the potential benefit of selecting certain parameters, and their influence on pilot workload and performance. To this point, the comments presented are nothing more than observations in regard to what the "pilot" could achieve with gain and lead adjustment for controlled-element transfer functions that are representative of hover and low-speed flight operation for VTOL, STOL and V/STOL aircraft. Reference 11 presents data obtained in a ground simulator investigation of similar controlled-element transfer functions. This reference presents "measured" pilot data for this system. The data presented is examined in the next subsection of this report.

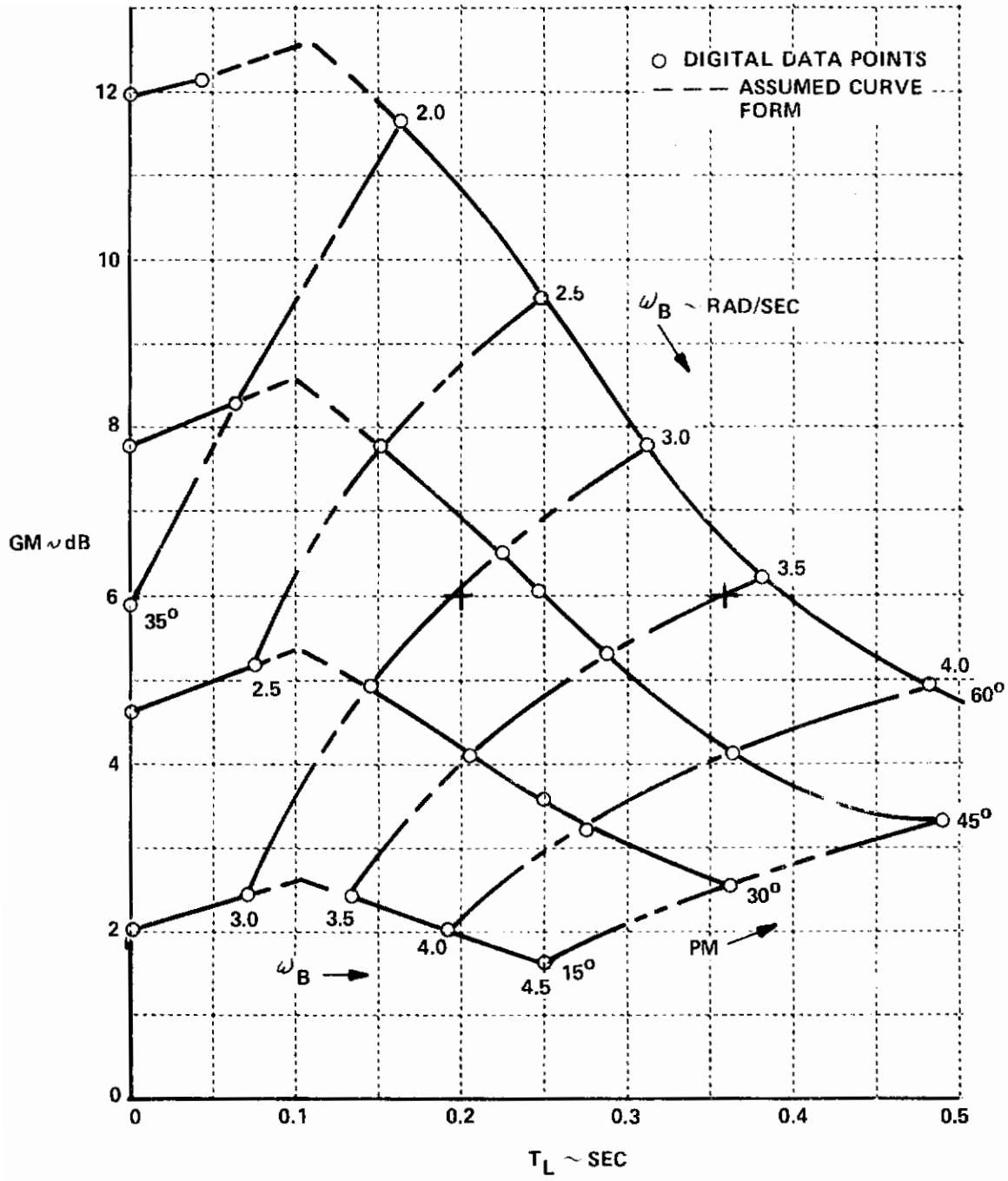

Figure 55 GAIN MARGIN FOR $Y_p Y_c = \dfrac{K(T_L s+1)e^{-.3s}}{s(s+4)}$

3.4 EXAMINATION OF "MEASURED" PILOT EQUALIZATION FOR LOW-ORDER SYSTEM TRANSFER FUNCTIONS

The intent of the following discussion is to examine the pilot adjustment data and the ratings obtained for the data presented by McDonnell in Reference 11, with respect to the parameters developed in the preceding discussions. The task used in this reference was compensatory tracking, primarily in a single-loop situation, for a fixed base simulation. The controlled-element transfer functions investigated correspond to those previously discussed (e.g., $K_c s$, $K_c/s(s+\lambda)$, K_c/s^2 , etc.), and the gain of the controlled element was discretely varied around a "best" value (K_B) selected by one of the test subjects. Secondary task effects were introduced as described in Reference 11. In the following discussion, the data will be examined to attempt to correlate with the open-loop and closed-loop parameters discussed in this section. In addition a comparison will be made for several selected configurations evaluated to independently determine the pilot lead and gain adjustment. This data will then be examined in light of the data presented in Reference 11 that correlates T_L with pilot rating. Specifically the configurations to be examined are K_c/s, $K_c/s(s+\lambda)$ and K_c/s^2 . Although data is presented in Reference 11 for unstable systems and second-order systems, this data will not be investigated in this report. In addition, since the primary subject used in the cited reference was designated as JDM, and since only his equalization parameters and experimental measures are presented, only his data will be examined. Furthermore the data represented by run numbers in Reference 11 will be presented in this report with a slightly different notation. That is in Table C-I of Reference 11, the run numbers are indicated, for example, as 671005-11. For the following presentation the identification run number will be shortened to 5-11. In attempting to correlate the data presented on Table C-I with certain figures in Reference 11, inconsistencies were uncovered. For example on Figure 20(a) of the cited reference for the K/s system with K/K_B = .1 and the task designated as $B6^{11}$ - 1.88-1, a pilot rating (Cooper Scale) of 3.5 is presented. However for run number 29-9 in Table C-I, presumably the same condition, the Cooper rating shown is 7. For the purpose

of examining the data in Reference 11, it will always be assumed that the tabulated data on Table C-I is correct.

In order to relieve the reader of the burden to constantly cross-reference to the data in Reference 11, certain data pertinent to the correlation analysis to be presented in this discussion is presented on the following table as a matter of convenience (where ω and σ refer to the input bandwidth and rms amplitude):

CONFIGURATION & TASK			Y_p			$Y_p Y_c$		PILOT RATING	
Run No.	Y_c/K_B	i ω,σ	τ (sec.)	T_L (sec.)	T_I (sec.)	ω_c (rad/sec)	ϕ_M (deg)	C*	CH**
29-9	.1/s	1,2	.270	0	0	3.1	44	7	U7
5-21	↓	1,3	.450	--	--	2.75	54	8	U8
11-3	.5/s	1,2	.133	0	0	3.6	48	3	A3
5-15	↓	1,3	.217	0	0	3.0	38	3	A3
11-11	1/s	1,1	.193	0	0	3.4	48	2	A2
11-5	↓	1,2	.200	0	0	4.0	40	2.5	A2.5
5-11	↓	1,3	.192	0	0	4.0	28	4.5	A5
11-13	↓	1,3	.200	0	0	3.6	48	4	A4
11-15	↓	2,1	.189	0	0	4.3	40	2	A1.5
11-7	↓	2,2	.192	0	0	4.2	40	3	A3
11-17	↓	2,3	.182	0	0	5.0	36	5	A5
11-9	↓	3,2	.147	0	0	4.5	50	5	A5
6-29	5/s	1,2	.208	0	0	4.3	30	4	A4
6-13	10/s	1,1	.192	0	0	4.5	28	4	A5
6-15	↓	1,2	.167	0	0	4.5	28	4	A5
6-11	↓	1,3	.194	0	0	4.6	30	5.5	A5.5
5-17	.1/s(s+4)	1,2	.40	0	0	2.0	40	4	A4.5
29-3	1/s(s+4)	1,2	.250	.250	0	4.2	26	4	A4.5
9-5	10/s(s+4)	1,2	.222	2.27	0	5.0	16	7.5	U7.5
29-1	1/s(s+2)	1,2	.264	.50	0	4.2	24	4	A4.5

(table continued next page)

CONFIGURATION & TASK			Y_p			$Y_p\ Y_c$		PILOT RATING	
RUN No.	Y_c / K_B	i ω, σ	τ (sec.)	T_L (sec.)	T_I (sec.)	ω_c (rad/sec)	ϕ_M (deg)	C*	CH**
6-1	$.1/s(s+1)$	1,2	--	1.0	--	3.4	12	4.5	A5
29-7	↓	1,2	.384	1.0	0	2.8	28	5.5	A5.5
9-7	$1/s(s+1)$	1,2	.294	~ 1	0	3.4	16	5	A5.5
29-13	↓	1,2	.244	1	0	3.8	40	5.5	A5.5
11-1	$10/s(s+1)$	1,2	.172	1	0	2.8	50	8	U9
5-19	$.1/s^2$	1,1	.435	$>>1$	1/4.5	2.0	36	7	U7
29-5	↓	1,2	.333	>1	0	1.5	40	8	U8
6-3	$.5/s^2$	1,2	.357	>3.3	0	3.3	12	4.5	A4.5
11-25	$1/s^2$	1,1	.344	>1	0	3.2	16	3.4	A3.4
11-19		1,2	.333	>1	0	2.9	20	7	U7
29-11		1,2	.330	>1	0	4.0	11	6	A6
29-15		1,2	.300	>1	0	3.3	20	6	A6
5-13		1,3	.334	$>>1$	0	3.0	28	6	A6
11-27		2,1	.278	>3.3	0	4.0	20	4	A4
11-21		2,2	.286	>1	0	3.0	24	8.5	U8.5
11-29		2,3	.400	>1.5	0	3.2	8	8.0	U8.5
11-23	↓	3,2	.250	>3.3	0	2.4	40	8.5	U8.5
6-31	$5/s^2$	1,2	.295	>1	0	3.8	18	7.5	U7.5
6-19	$10/s^2$	1,1	.238	--	--	5.0	20	7	U7
6-23		1,2	.244	~ 3	0	4.8	14	8.5	U9
6-21	↓	1,3	.263	>1	0	3.3	28	9	U9.5

NOTE: ω_1 = 1.88 rad/sec σ_1 = 0.5 cm/sec
ω_2 = 2.89 rad/sec σ_2 = 1.0 cm/sec
ω_3 = 4.78 rad/sec σ_3 = 1.5 cm/sec

Therefore task with ω = 1.88 rps, σ = 1.0 cm/sec is denoted as 1,2

*Cooper Pilot Rating

**Cooper-Harper Pilot Rating

3.4.1 Examination of Controlled Elements With Transfer Function $Y_c / K_\beta = K/s$. ($K_\beta = .586$)

The data presented in Reference 11 for the open-loop gain and phase for the measured $Y_p Y_c$ was first re-examined by plotting the data on Nichols charts in order to extract the following parameters: ω_c, PM, GM, ω_β, and M_p. Rather than actually attempting to fit the data with a prescribed form for $Y_p Y_c$ the discrete points presented in Reference 11 were fitted with a smooth curve to extract the desired parameters. The following table presents the data obtained with the crossover frequency and phase margin "measured" by McDonnell and presented in Reference 11.

K	RUN No.	$Y_p Y_c$ (Ref. 11)		$Y_p Y_c$					PILOT RATINGS
		ω_c (rad/sec)	ϕ_M (deg)	ω_c (rad/sec)	ϕ_M (deg)	GM (dB)	ω_β (rad/sec)	M_p (dB)	C-H
.1	29-9	3.1	44	3.0	45	7.0	4.0	3+	U7
↓	5-21	2.75	54	3.0	45	7.0	3.5	3+	U8
.5	11-3	3.6	48	3.8	45	10.5	4.5	2.5	A3
↓	5-15	3.0	38	3.2	40	8.0	4.0	4.0	A3
1.0	11-11	3.4	48	2.9	60	7.0	4.5	1.0	A2
	11-5	4.0	40	3.8	45	7.0	4.0	3.0	A2.5
	5-11	4.0	28	3.8	28	8.0	4.0	6.0	A5
	11-13	3.6	48	3.2	52	7.0	4.6	2.0	A4
	11-15	4.3	40	4.0	45	6.0	5.0	3.0	A1.5
	11-7	4.2	40	5.0	35	6.0	5.5	5.0	A3
	11-17	5.0	36	4.7	45	5.0	5.5	5.0	A5
↓	11-9	4.5	50	4.5	55	7.0	6.0	3.0	A5
5	6-29	4.3	30	4.0	32	6.5	4.5	6.0	A4
10	6-13	4.5	28	4.0	33	7.0	4.5	5.5	A5
↓	6-15	4.5	28	3.8	35	7.5	4.1	4.5	A5
	6-11	4.6	30	3.8	36	9.0	4.3	5.0	A5.5

Thus, in general, the correlation obtained between the crossover frequency and phase margin presented in Reference 11 with the data obtained from the Nichols chart is quite satisfactory. The data presented also indicates that the pilot did essentially provide only gain equalization for these configurations; however, the magnitude of τ presented in Reference 11 appears to optimistic for the values of ω_c and ϕ_M presented. For the configurations with $K = 1$, the following comparison is presented between the data for pilot induced time delay. The value of τ_c is computed by the relationship for $\frac{K}{s} e^{-\tau s}$ systems, $\tau_c = \frac{\pi(90 - PM)}{180\,\omega_c}$.

RUN No.	τ (sec)	ω_c (rad/sec)	ϕ_M (deg)	τ_c (sec)	ω_c (rad/sec)	ϕ_M (deg)	τ_c (sec)
11-11	.193	3.4	48	.216	2.9	60	.181
11-5	.200	4.0	40	.218	3.8	45	.207
5-11	.192	4.0	28	.271	3.8	28	.285
11-13	.200	3.6	48	.204	3.2	52	.207
11-15	.189	4.3	40	.203	4.0	45	.196
11-7	.192	4.2	40	.208	5.0	35	.192
11-17	.182	5.0	36	.188	4.7	45	.167
11-9	.147	4.5	50	.155	4.5	55	.136
	Ref. 11				NICHOLS CHART		

This data indicates that the value of $\tau = .3$ previously used in the open-loop discussions may be slightly conservative. However, $\tau = .3$ for analysis/design purposes represents a reasonable upper bound for the system under investigation.

Since the parameters of interest for the K/s system obtained from "measured" pilot data have been determined, the next step is to examine the relationships between these parameters and the pilot ratings. The following table first examines the relationship between the input bandwidth and the crossover frequency (ω_c) and closed-loop bandwidth (ω_B) obtained from the Nichols chart for the $Y_c/K_B = K/s$ systems.

RUN No.	i ω, σ	ω_c/ω_i	ω_B/ω_i	ω_i	K	PILOT RATING C-H
29-9	1,2	1.6	2.1	1.88	.1	U7
5-21	1,3	1.6	1.9	1.88	↓	U8
11-3	1,2	1.3	2.4	1.88	.5	A3
5-15	1,3	1.7	2.1	1.88	↓	A3
11-11	1,1	1.5	2.4	1.88	1.0	A2
11-5	1,2	2.0	2.1	1.88		A2.5
5-11	1,3	2.0	2.1	1.88		A5
11-13	1,3	1.7	2.4	1.88		A4
11-15	2,1	1.4	1.7	2.89		A1.5
11-7	2,2	1.7	1.9	2.89		A3
11-17	2,3	1.6	1.9	2.89		A5
11-9	3,2	.9	1.3	4.78	↓	A5
6-29	1,2	2.1	2.4	1.88	5.0	A4
6-13	1,1	2.1	2.4	1.88	10.0	A5
6-15	1,2	2.0	2.2	1.88		A5
6-11	1,3	2.0	2.3	1.88	↓	A5.5

For input bandwidth ω_i = 1.88 rad/sec, the data indicates that the pilot achieved on the average a ratio of ω_B/ω_i = 2.2. This value is somewhat lower than the value anticipated in the closed-loop analysis previously presented in this report. This may be due to a saturation of the pilot for the input bandwidth used in the task. That is, to achieve a ratio of ω_B/ω_i = 3.0 for even the lowest input bandwidth would force the pilot to achieve a closed-loop bandwidth on the order of one cps. From data presented in Reference 11, it appears that the pilot cannot effectively achieve this magnitude of closed-loop bandwidth without increasing remnant (pilot nonlinear behavior). Thus, it appears that the pilot may regress to a ratio of ω_B/ω_i which still allows him to be relatively smooth (and linear) in the task. The data also indicates some regression in the ratio of ω_B/ω_i when the rms amplitude of the task was increased at constant ω_i. This may be associated with the

phenomenon that the pilot tends to question the credibility of the task, and does not chase the high-frequency or large-amplitude changes in the task but rather tends to try to smooth out the task. This type of behavior was recently observed in the terrain-following task investigated in Reference 22.

Figure 56 presents the pilot rating data using the Cooper-Harper values of Reference 11 with the open-loop pilot-system phase margin and the pilot-system closed-loop resonance peak. For those conditions where the input bandwidth was less than 2.9 rad/sec and the task amplitude rms was less than our equal to one cm/sec, the data indicates that a PM of at least 35° and a closed-loop resonance peak of 5 dB or less would yield Level 1 flying qualities when the system sensitivity is properly selected. These values correlate quite well with the values previously discussed in this section for open-loop and closed-loop parameters. The value of resonance peak obtained from this data, however, is higher than that determined by Neal and Smith in Reference 14, for systems that did not require lead compensation by the adjustment rules they used.

3.4.2 Examination of Controlled Elements with Transfer Function $Y_c/K_B = K/s(s+\lambda)$ (K_B = 2.15)

Using the method previously discussed, the following information was obtained for the controlled-element configurations of the form $Y_c = K_c/s(s+\lambda)$ examined in Reference 11. For this discussion, comparison of the values of τ_L presented in Reference 11 with values independently obtained from the open-loop pilot-system amplitude ratio and phase angle will not be presented. This is a subject that will be presented later in this report. The following table presents a comparison of the open-loop parameters (ω_c, ϕ_M) presented in the cited reference with the values obtained from the Nichols chart examination of the measured gain and phase data.

---

[22] Wasserman, Richard and Paul R. Motyka: "In-Flight Investigation of the B-1 Control System." AFFDL-TR-73-139, December 1973.

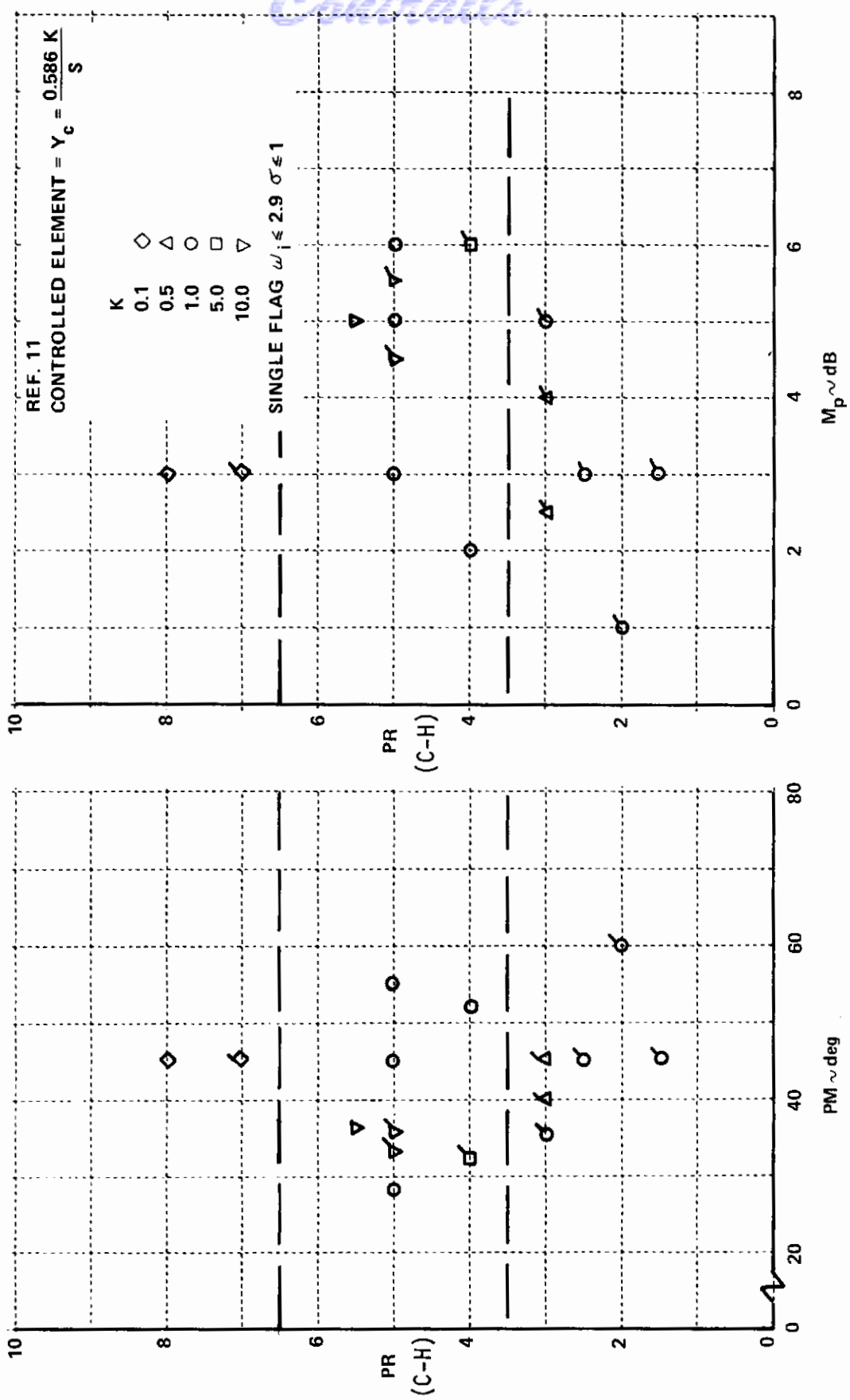

Figure 56 PILOT RATING AS A FUNCTION OF PM AND M_p FOR $Y_c = .568\ \frac{K}{S}$

K, λ	RUN No.	Y_pY_c (Ref. 11)		Y_pY_c					PILOT RATING C-H
		ω_c (rad/sec)	ϕ_M (deg)	ω_c (rad/sec)	ϕ_M (deg)	GM (dB)	ω_B (rad/sec)	M_p (dB)	
.1, 4	5-17	2.0	40	2.0	48	4.8	2.5	5	A4.5
1, 4	29-3	4.2	26	4.0	45	4.5	4.8	7	A4.5
10, 4	9-5	5.0	16	4.3	32	4.0	4.5	6	U7.5
1, 2	29-1	4.2	24	3.0	38	4.6	4.0	4.5	A4.5
.1, 1	6-1	3.4	12	3.0	18	3.0	3.1	12	A5
.1, 1	29-7	2.8	28	3.0	30	3.5	3.2	9	A5.5
1, 1	9-7	3.4	16	3.3	16	3.5	3.5	12	A5.5
1, 1	29-13	3.8	40	4.0	30	3.9	4.4	6	A5.5
10, 1	11-1	2.8	50	2.9	60	7.0	3.8	1	U9

NOTE: For all configurations the task parameters used were ω_i = 1.88 rad/sec, σ = 1.0 cm/sec, $(\omega_i, \sigma) \rightarrow (1, 2)$

The above data, in general, indicates a reasonable correlation between the values of ω_c and ϕ_M presented in Reference 11 and the data obtained from the Nichols charts used in this analysis. The primary differences appear to be related by the attempt in Reference 11 to exactly match the data for these systems with pole-zero cancellation ($\tau_L = 1/\lambda$). The following table examines the ratio of ω_c and ω_B to the input bandwidth (for the values of ω_c and ω_B determined from the Nichols charts)

RUN No.	ω_c/ω_i	ω_B/ω_i	K	λ (1/sec)	PILOT RATING C-H
5-17	1.1	1.3	.1	4	A4.5
29-3	2.1	2.6	1	4	A4.5
9-5	2.3	2.4	10	4	U7.5
29-1	1.6	2.1	1	2	A4.5
6-1	1.6	1.6	.1	1	A5
29-7	1.6	1.7	.1	↓	A5.5
9-7	1.8	1.9	1	↓	A5.5
29-13	2.1	2.3	1	↓	A5.5
11-1	1.5	2.0	10	↓	U9

For the input bandwidth, ω_i = 1.88 rps, the data indicates that on the average the pilot attempted to achieve a ratio of ω_B/ω_i = 2.0, which is just slightly lower than what was achieved, on the average, for the K/s systems. The data also indicates that for this set of configurations the pilot could not achieve a gain margin of 6 dB, except for the high-gain configuration with λ = 1 (11-1). The rating for this configuration, which appears to be satisfactory from the examination of phase margin, gain margin, etc. could possibly be attributed to the value of the controlled-element steady-state gain, or to the large amount of remnant indicated by Table C-I (ρ^2_{ac} = .0973). Thus for this configuration, the pilot behavior was almost entirely uncorrelated with a linear model; and therefore this configuration will be excluded from the remaining correlation analysis. Another comment on the gains selected is that the trend in pilot rating with gain illustrated by the data on the previous table does not indicate that setting K/K_B = 1 significantly influenced the pilot rating. In fact the trends in rating with the value of K/K_B indicate that an optimum value of this parameter might be somewhere between K/K_B =.1 and K/K_B = 1.0. This presents a partial but not necessarily unsurmountable obstacle in the analysis of the data. That is, we don't necessarily have the "best" configurations to examine the effects of the particular parameters without wondering what the result would be if the pilot had truly optimized the controlled element gain for the task.

First let us examine this data in terms of correlating the Cooper-Harper pilot rating with phase margin and resonance peak. This information is presented on Figure 57. It was noted in Section 3.4.1 that for the K/s systems, Level 1 pilot ratings appeared to be correlated with phase margins in excess of 35^o and resonance peaks less than 5 dB. It should be noted that all these K/s systems had gain margins equal to or greater than 6 dB for the task with ω_i < 2.9 rad/sec, $\sigma \leq$ 1 cm/sec. For the $K/s(s+\lambda)$ there are essentially three configurations that would pass the phase margin and/or resonance peak tests but were rated worse than Level 1 (however, for these $K/s(s+\lambda)$ configurations, the pilot was not able to achieve a 6dB gain margin).

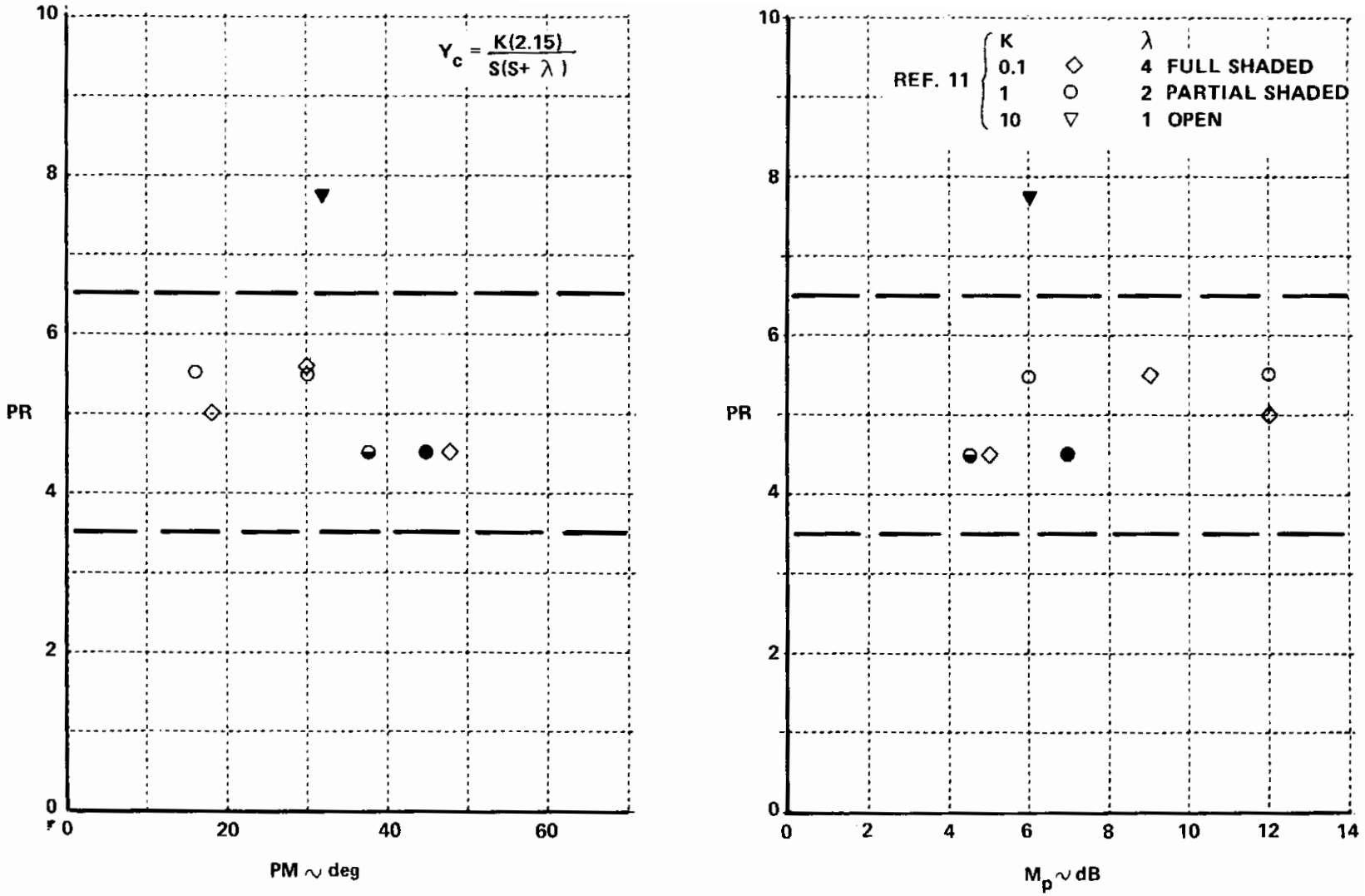

Figure 57 PILOT RATING AS A FUNCTION OF PM AND M_p FOR $Y_c = 2.15\frac{K}{s(s+\lambda)}$

Next examine these configurations in terms of the closed-loop parameters suggested by Neal and Smith in Reference 14, and previously developed in Section 3.3.3, for $K/s(s+4)$ and $K/s(s+1)$. Since we have not yet determined the value of lead equalization used by the pilot, the data will be presented as areas on these figures based on the values of ω_c , ω_B and M_p determined from the Nichols chart examination of the "measured" pilot-system data. The figures previously developed were based on τ = .3 seconds, examination of the value of τ measured by McDonnell for these configurations is on the average close to .3 seconds.

Examination of Figures 58 and 59 first indicates that the pilot did not achieve pole-zero cancellation. If he would have used lead equalization to cancel the system pole exactly, the regions should tend to fall exactly on the lines presented for $1/T_L = \lambda$. This point will be pursued in later discussions. In general, the data obtained from Reference 11 tends to indicate regions of Levels 2 and 3 pilot ratings in the closed-loop parameter plane (M_p , $\tan^{-1}(T_L \omega_B)$). Configuration 5-17 appears to be misplaced; that is, the pilot rating appears to be worse than the parameters (either closed-loop or open-loop) would indicate. There are several possible explanations for this configuration:

(a) insufficient gain margin (4.8 dB)

(b) ω_B/ω_i too low (1.3) to achieve desired performance

(c) low system sensitivity ($K = .1\, K_B$) required excessive pilot gain compensation.

Although pilot comments are not presented in Reference 11, the various rating scales used indicate that the effects of the deficiencies were moderately objectionable and this configuration was demanding of pilot attention, skill, or effort. These ratings appear to correlate with the possible explanations offered previously; however, without examination of the exact comments this is still in the realm of engineering judgment rather than fact. In general therefore, the data presented on Figures 58 and 59 seem to correlate with the discussion of closed-loop parameters previously presented in Section 3.3.3.

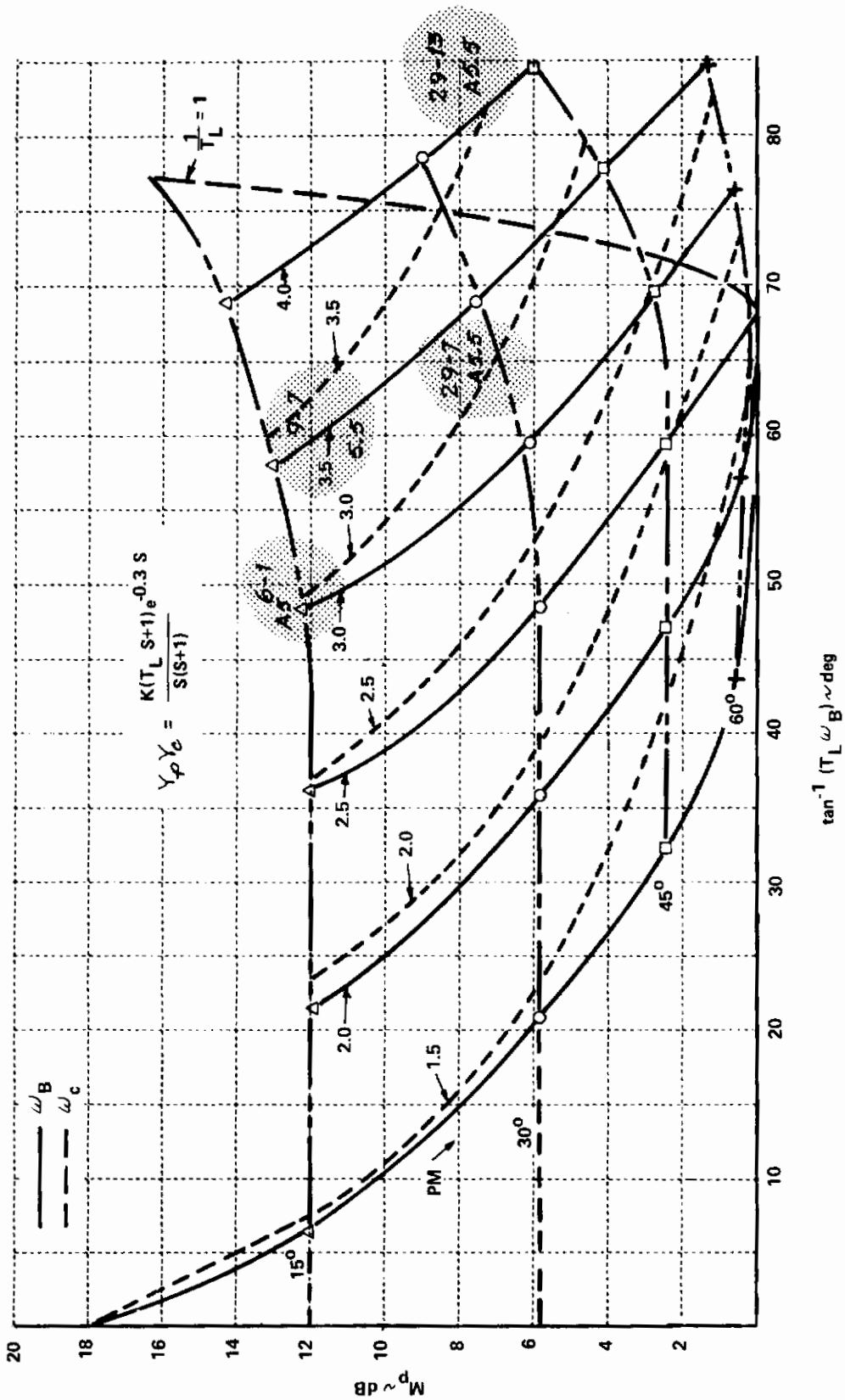

Figure 58 PILOT RATING AS A FUNCTION OF CLOSED-LOOP PARAMETERS FOR $Y_c = K/s(s+1)$

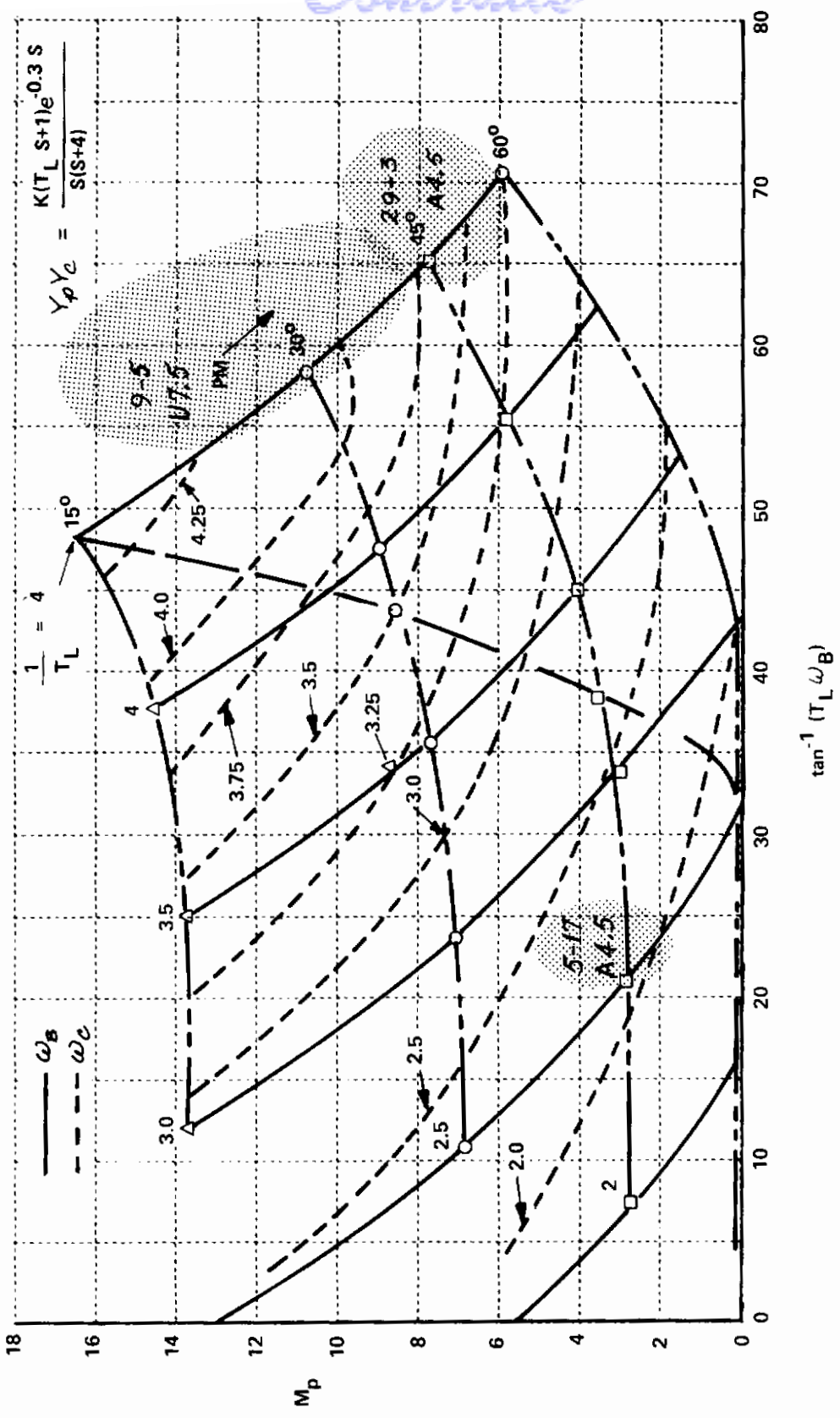

Figure 59 PILOT RATING AS A FUNCTION OF CLOSED-LOOP PARAMETERS FOR $Y_c = K/s(s+4)$

However, insufficient data is available to prescribe exact boundaries, at least in terms of a handling qualities specification. The data presented at this stage of development may be useful, however, for design purposes.

3.4.3 Examination of Controlled Elements With Transfer Function $Y_c/K_\beta = K/s^2$ (K_β = 1.17)

The following table presents a comparison of Table C-I of Reference 11 with the Nichols chart analysis of the measured pilot-system ($Y_p Y_c$) amplitude ratio and phase. For these configurations we should expect to see some deterioration of pilot rating with increased phase margin above some nominal value. Because of the nature of the configuration, large phase margins are indicative of excessive lead equalization, which in general yields poor pilot ratings.

K	RUN No.	$Y_p Y_c$ (REF. 11)		$Y_p Y_c$					PILOT RATING C-H
		ω_c (rad/sec)	ϕ_M (deg)	ω_c (rad/sec)	ϕ_M (deg)	GM (dB)	ω_β (rad/sec)	M_p (dB)	
.1	5-19	2.0	36	1.9	34	4.5	2.2	6	U7
.5	6-3	3.3	12	3.1	22	3.5	3.3	9	A4.5
1	11-25	3.2	16	2.5	30	4.0	2.9	7	A3.4
	11-19	2.9	20	3.0	20	5.5	3.3	9	U7
	29-11	4.0	11	3.8	17	3.2	4.0	10	A6
	29-15	3.3	20	3.0	24	4.0	3.4	9	A6
	5-13	3.0	28	2.9	24	4.5	3.1	9	A6
	11-27	4.0	20	3.0	34	4.0	3.8	6	A4
	11-21	3.0	24	2.9	40	5.5	3.6	3.5	U8.5
	11-29	3.2	8	2.9	20	2.5	3.2	12	U8.5
↓	11-23	2.4	40	1.8	50	7.0	2.7	2.5	U8.5
5	6-31	3.8	18	3.6	12	3.5	3.8	12+	U7.5
10	6-19	5.0	20	4.0	24	4.0	4.5	9.0	U7
↓	6-23	4.8	14	3.5	23	3.2	3.8	10.0	U9

Run numbers 29-5 and 6-21 were not examined since the data in Reference 11 indicates that the measured amplitude ratio and/or phase of $Y_p Y_c$ was considered to be unreliable, because of signal-to-noise ratio, in the vicinity of gain crossover frequency. In general, there exists reasonable correlation between the crossover frequencies and phase margins obtained from the Nichols charts and the data in Reference 11. Configurations 11-21 and 11-23 both indicate excessive lead compensation, and were rated Level 3 although the pilot achieved adequate phase margin and gain margin in the vicinity of 6 dB. In addition, due to the large phase margin, the closed-loop resonance was held to minimal values. It therefore appears these configurations indicate a possible boundary on lead generation in the closed-loop parameter plane ($M_p, \tan^{-1}(T_L \omega_B)$). The following table indicates the relationships obtained between the input bandwidth, the gain crossover frequency (ω_c) and the closed-loop bandwidth (ω_B) from the Nichols charts plots for the $Y_c / K_B = K_c / s^2$ systems investigated.

RUN No.	i ω, σ	ω_c/ω_i	ω_B/ω_i	ω_i	K	PILOT RATING C-H
5-19	1, 1	1.0	1.2	1.88	.1	U7
6-3	1, 2	1.6	1.8	1.88	.5	A4.5
11-25	1, 1	1.3	1.5	1.88	1.0	A3.4
11-19	1, 2	1.6	1.8	↓	↓	U7
29-11	1, 2	2.0	2.1	↓	↓	A6
29-15	1, 2	1.6	1.8	↓	↓	A6
5-13	1, 3	1.5	1.6	↓	↓	A6
11-27	2, 1	1.0	1.3	2.89	↓	A4
11-21	2, 2	1.0	1.2	↓	↓	U8.5
11-29	2, 3	1.0	1.1	↓	↓	U8.5
11-23	3, 2	.4	.6	4.78	↓	U8.5
6-31	1, 2	1.9	2.0	1.88	5	U7.5
6-19	1, 1	2.1	2.4	1.88	10	U7
6-23	1, 2	1.9	2.0	↓	↓	U9

For the input bandwidth ω_i = 1.88 rad/sec, the data indicates that on the average the pilot attempted to achieve a ratio of ω_B/ω_i = 1.9 which is in reasonable proximity to the value of 2.0 obtained from the $K/s(s+\lambda)$ configurations and the value of 2.2 obtained for the K/s systems. In general the data for the K/s^2 systems indicates that the higher input bandwidths tended to overpower the pilot, and he would have difficulty providing any equalization that would yield reasonable pilot-system performance.

Next examine the pilot rating data as a function of M_p and phase margin. This data is presented on Figure 60 for the K/s^2 systems. Examination of the data on Figure 60 indicates that when the pilot did not attempt to overcompensate the system (run numbers 11-25 and 11-27), phase margin on the order of 30° and $M_p \leq 7$ dB yielded pilot ratings that bracket Level 1. The gain margin for those configurations was approximately 4 dB. However it should be noted that for those configurations the rms of the amplitude in the tracking task was the lowest value examined, σ = .5 cm/sec. Thus the ratings may indicate that the system sensitivity was adequate for the task. However it is also interesting to note that for these configurations the ratings associated with response characteristics, ease and precision of control, demands on the pilot and the effects of deficiencies on performance were among the best obtained for the experiment. This appears to be entirely inconsistent with the data presented on Figure 43 of the McDonnell report (Reference 11), and raises questions as to the validity of the data for the cited run numbers, especially in light of the lead equalization the pilot provided for these configurations as indicated on the table in Section 3.4.

3.4.4 Examination of Functional Dependency of the Measured Pilot Open-Loop and Closed-Loop Parameter and Pilot Ratings

In Section 3.3 it was shown that there exists a strong relationship for these types of controlled element between phase margin and closed-loop resonance, almost independent of pilot lead equalization. This relationship will be explored next for the measured pilot equalization data from

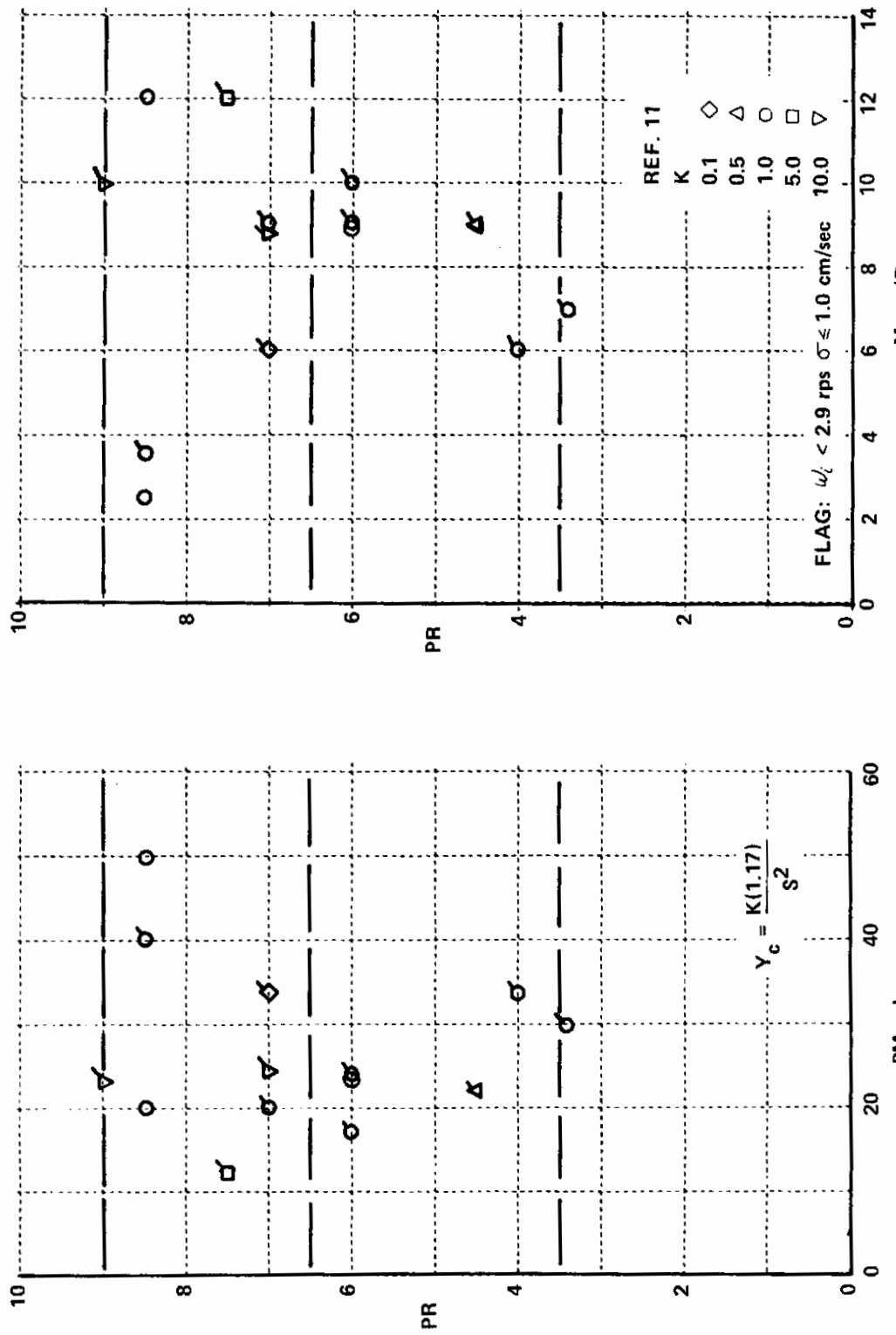

Figure 60 PILOT RATING AS A FUNCTION OF M_p AND PM FOR $Y_c = 1.17 \frac{K}{s^2}$

Reference 11, presented on Figure 61. This figure again illustrates the essentially one-to-one relationship between phase margin and closed-loop resonance for the low-order controlled elements investigated. In addition, the ratio of (ω_c/ω_B) from the "measured" pilot equalization data is approximately the same as that developed for the simplified systems examined previously in Section 3.3.

Next examine the relationship among gain margin, phase margin, ω_B/ω_c, and controlled-element gain presented on Figure 62, essentially summarizing the results thus far obtained from the "measured" pilot equalization. From these figures the following observations can be made on parameters which essentially yield Level 1 handling qualities:

(a) $\omega_B/\omega_i \geq 1.5$
(b) PM $\geq 30°$ ($M_p \leq 7$ dB)
(c) $GM \geq 4$ dB
(d) system sensitivity properly selected for the task

In addition from previous comments the task for simulation experiments must be properly selected, such that the pilot is not saturated and has no difficulty performing the task with the equalization he adapts. To some degree this is indicated by Figure 32 of Reference 11. This figure presents pilot rating for the K_B/s and K_B/s^2 controlled elements as a function of the input bandwidth and the rms amplitude of the task. The data for measured pilot equalization for both of these systems (K_B/s and K_B/s^2) is essentially independent of the input bandwidth, and generally speaking the crossover and phase margin remained relatively constant as the task parameters were changed. Since the pilot cannot "optimize" the system sensitivity for the task, the ratings may indicate unrealistic constraints imposed upon the pilot especially at the higher input bandwidths and large values of input amplitude rms. As previously shown from fixed- and moving-base ground simulator data in Section 3.2.1.3.2, Level 1 pilot ratings were achieved for $K/s(s+\lambda)$ controlled elements for the same values of λ investigated by McDonnell. This cannot be said for the ratings obtained

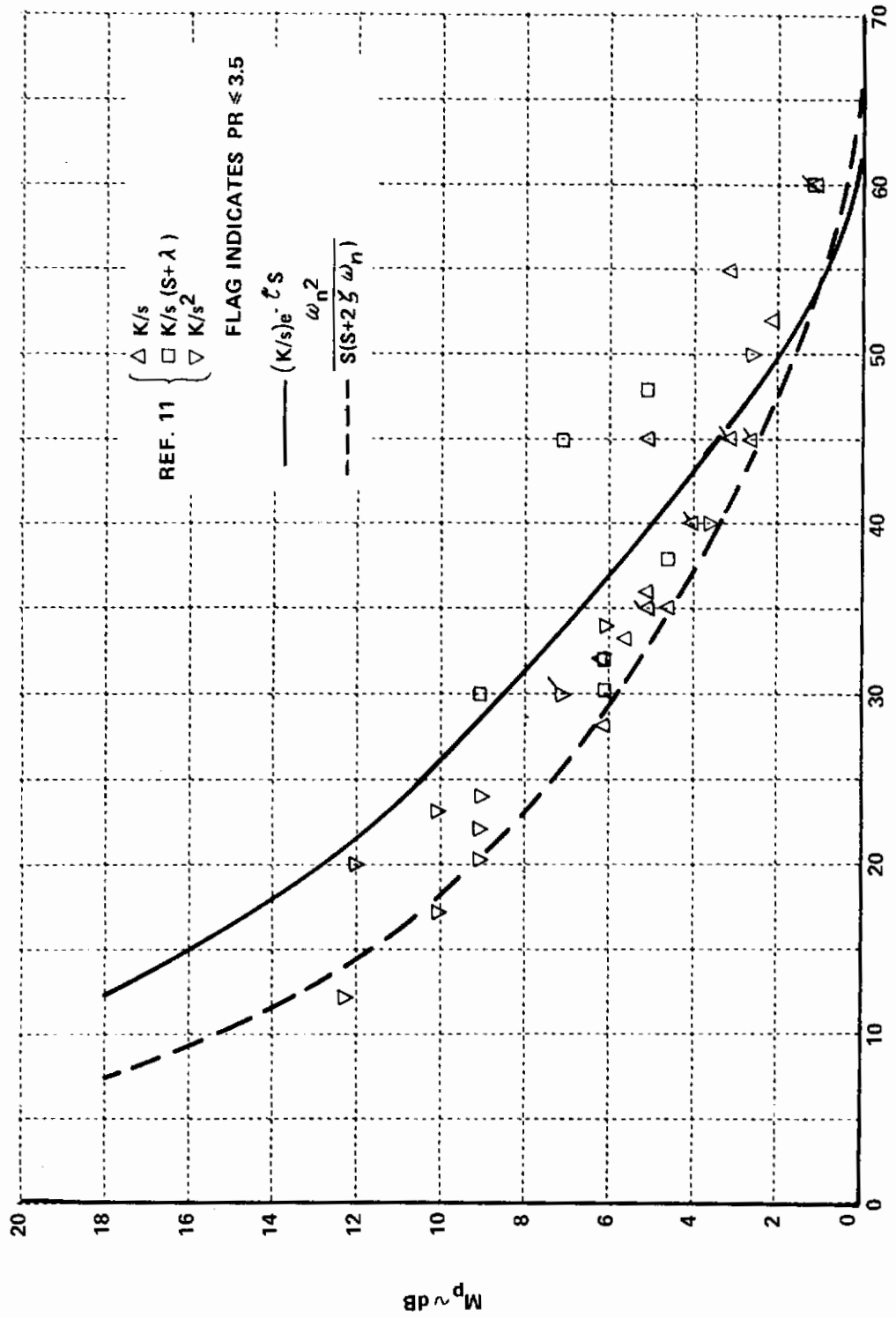

Figure 61 RELATIONSHIP BETWEEN M_p AND PM FOR LOW-ORDER CONTROLLED ELEMENTS

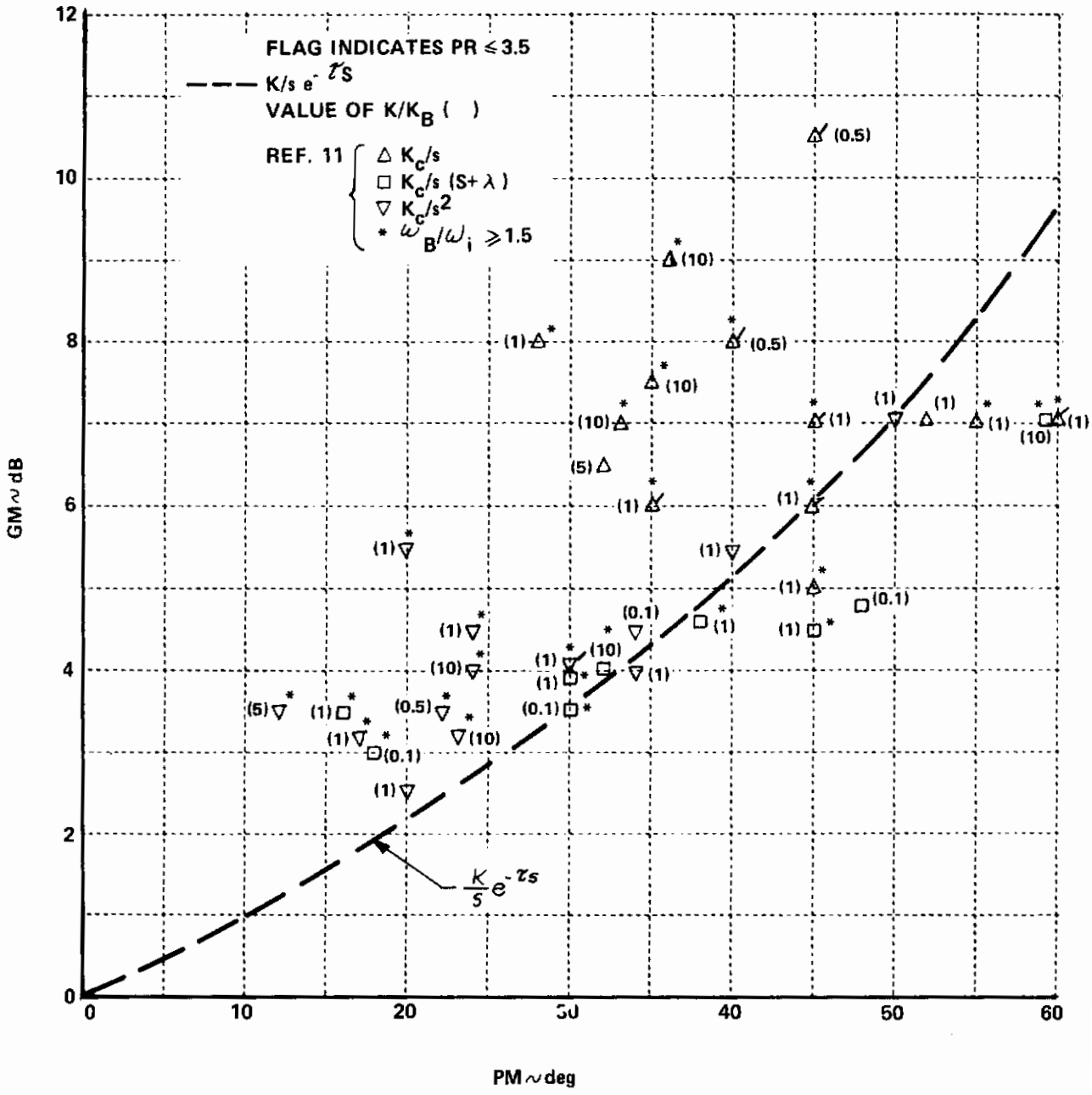

Figure 62 GAIN MARGIN AS A FUNCTION OF PHASE MARGIN FOR "MEASURED" PILOT LEAD EQUALIZATION

for these types of systems for ω_i = 1.88 rad/sec and σ_i = 1.0 cm/sec. For the crossover frequencies and/or bandwidths the pilot was forced to achieve in order to obtain reasonable tracking performance (as indicated on Figure 58 and 59), the result was Level 2 pilot ratings, even for K = 1, the "best" gain situation imposed in the referenced experiment. Therefore, in many instances the pilot rating may reflect an unrealistically imposed tracking task, rather then the effects of pilot equalization. To this point, no mention has been made directly concerning the measured lead equalization for the $K_\beta/s(s+\lambda)$ and K_β/s^2 systems evaluated. The following discussion will address this point.

3.4.5 Examination of Pilot Lead Equalization From "Measured" Pilot-in-the-Loop Data

In Reference 11 the author implies that the pilot does cancel system lag with his lead equalization, thereby resolving the problem of the uncertainty of lead placement and the connections that had been previously inferred (e.g., Reference 13) between pilot rating and lead equalization. Reference 11 then presents a figure that indicates the variation of pilot rating with pilot lead equalization for a selected input bandwidth and input rms amplitude (ω_i = 1.88 rad/sec, σ_i = 1 cm/sec). In addition, only the "best" gains situations were examined, possibly in an attempt to compare apples with apples rather than with oranges. It has been previously stated in this section that the trend in pilot rating as a function of system gain (especially for the $K/s(s+\lambda)$ controlled elements) does not ncessarily indicate that truly a best system sensitivity is a function of the system damping (λ). In Reference 11, the same value of K_β was used for λ = 1, 2 and 4; therefore, there remains some question as to whether or not the influence of the prescribed "best" gain used in this exeperimental situation truly removes sensitivity problems and allows one to correlate pilot rating with pilot lead equalization to the degree inferred by the author of Reference 11. In addition, although the task was held constant, the realism of the task for the controlled elements investigated has been also questioned. These remarks aside, let us assume that one can correlate

pilot ratings with pilot lead equalization for the data presented in Reference 11. The primary question still remains to be examined, that is, does the pilot actually achieve pole cancellation with his lead equalization? Figure 63 (from Reference 11) is presented for the convenience of the reader. In addition, the following table again presents the data as "measured" by the author of Reference 11 for the configurations pertinent to this discussion (with $i(\omega,\sigma)$ = 1, 2):

Pilot JDM

Configuration	K_B	RUN No.	τ (sec)	T_L (sec)	ω_c (rad/sec)	ϕ_M (deg)	PILOT RATING C	PILOT RATING CH
K_B/s	.586	671011-5	.200	0	4.0	40	2.5	A2.5
$K_B/s(s+4)$	2.15	671129-3	.250	.250	4.2	26	4	A4.5
$K_B/s(s+2)$	2.15	671129-1	.264	.500	4.2	24	4	A4.5
$K_B/s(s+1)$	2.15	671129-13	.244	1.0	3.8	40	5.5	A5.5
$K_B/s(s+1)$	2.15	671009-7	.294	~1	3.4	16	5.0	A5.5
K_B/s^2	1.17	671011-19	.333	> 1	2.9	20	7	U7
K_B/s^2	1.17	671129-11	.330	> 1	4.0	11	6	A6
K_B/s^2	1.17	671129-15	.300	> 1	3.3	20	6	A6

Extracted from Table C-I of Reference 11

The expression that relates phase margin to τ, ω_c and T_L for the general system $Y_p Y_c = K(T_L s+1)e^{-\tau s}/s(s+\lambda)$ is presented below:

$$\phi_M = 180 - \tau\omega_c - 90 - \tan^{-1}\left(\frac{\omega_c}{\lambda}\right) + \tan^{-1}\left(T_L\omega_c\right)$$

$$= 90 - \left[\tau\omega_c + \tan^{-1}\left(\frac{\omega_c}{\lambda}\right)\right] + \tan^{-1}\left(T_L\omega_c\right)$$

where $\tau_e = \frac{180}{\pi}\tau$

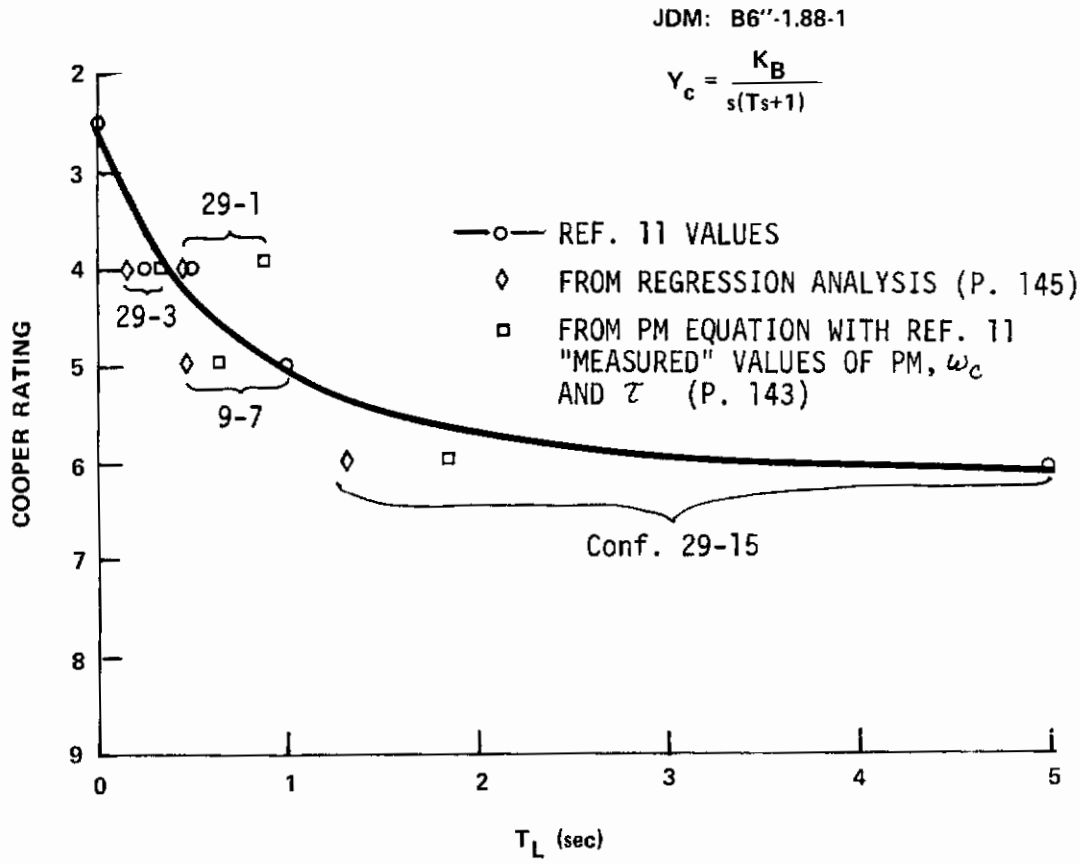

Figure 63 VARIATION OF PILOT RATING WITH PILOT LEAD

The "measured" data of Reference 11 is used and the following computations were performed. The first column presents the value of phase margin (ϕ_M) that would be computed from the equation for phase margin using the "measured" values for T_L, τ, and ω_c; ① the second column presents the value of T_L computed from the phase margin equation using the "measured" values for ϕ_M, τ, and ω_c; ② while the third column presents the value of τ that would be obtained if the "measured" values of ϕ_M, T_L and ω_c were used, to compute τ from the phase margin equation ③:

Run	Configuration	λ	ϕ_M	ϕ_M ① (deg)	T_L ② (sec)	τ ③ (sec)
11-5	K_B/s	∞	$PM = 90 - \tau_e \omega_c + \tan^{-1}(T_L \omega_c)$	44.2	.018	.218
29-3	$K_B/s(s+\lambda)$	4	$PM = 90 - \tau_e \omega_c + \tan^{-1}(T_L \omega_c) - \tan^{-1}(\omega_c/\lambda)$	29.8	.219	.266
29-1		2		26.5	.449	.274
29-13		1		36.9	1.280	.230
9-7		1		32.7*	.451	.380*
11-19	K_B/s^2	0	$PM = \tan^{-1}(T_L \omega_c) - \tau_e \omega_c$	30.7**	1.317	.398**
29-11				11.5**	4.246	.332**
29-15				29.8**	1.284	.352**

NOTE: When the 'measured' value of T_L was not directly indicated in the reference the following values were used:

(a) * (single asterisk) $\Longrightarrow T_L = 1.0$, the value required for pole-zero cancellation.

(b) ** (double asterisk) $\Longrightarrow T_L = 5.0$, the value inferred in Reference 11 for the K_B/s^2 configuration.

The results of the computations indicate that there are still some questions as to lead equalization using the phase margin relationship and the "measured" values from Reference 11. It should be noted that only a simple crossover model was used for the computations rather than an extended crossover model as suggested, for example, in Reference 13. This extended crossover model might possibly explain some of the differences in a comparison of the measured parameters and the computed values; however, there is no indication of the use of an extended crossover model to obtain the 'measured' values of the parameters of interest in Reference 11. In fact, the measured values appear to be the consequence of initially fitting the measured amplitude ratio of $Y_p Y_c$ with a slope of -20 dB decade (as would be the case if $Y_p Y_c = (K/s)e^{-\tau s}$) and extracting the "measured" parameters for τ_L and ω_c, and then evaluating ϕ_M and τ from the phase data for $Y_p Y_c$.

Since the controlled element is prescribed, and the "measured" values of $|Y_p Y_c|$ and the phase of $Y_p Y_c$ are presented, it was decided to examine the data using linear and nonlinear regression techinques. The procedure used was to remove the gain and phase of the controlled element (Y_c) from the data presented for $Y_p Y_c$. This would then yield the amplitude ratio and phase shift that could be attributed to the pilot in the loop. The amplitude ratio data was then examined, basically using a model for the pilot of $Y_p = K_p(\tau_L s + 1)$ Linear and nonlinear regression techniques were then applied to determine the appropriate values for K_p and τ_L. Once the value of τ_L was determined by this technique, regression analysis was applied to the phase angle attributed to the pilot, to remove the influence of pilot lead generation on the pilot-induced phase angle. Linear regression analysis was then used to determine a best fit value for phase angle due to the introduction of time delay. These techniques could also be used to examine more complex pilot models; however, this was not considered necessary in this instance. In addition, only those configurations and run numbers that were presented by the author of Reference 11 on Figure 22 of the cited reference (Figure 63 of this section) were examined. Since the author did not use all the run numbers for a particular case, examination of the data on the figure infers that run number 9-7 was selected

to be representative of $K_B/s(s+1)$. This is inferred from the Cooper ratings associated with the lead values presented on this figure. In addition, it was decided not to examine run number 671011-5 (K_B/s) in further detail since the the computed values of ω_c, ϕ_M and τ_e are all quite compatible with the measured data. This is also true for this configuration for the values of ω_c and ϕ_M that were obtained from the Nichols charts technique previously presented. The following table presents the values of pilot gain (K_p), pilot lead equalization (T_L) and pilot-induced time delay for the specific configurations of interest. In addition the $Y_p Y_c$ transfer function obtain using regression analysis is compared to the expression that is implied by the data of Reference 11. (Run 29-15 was selected for K_B/s^2, and Run 9-7 for $K_B/s(s+1)$.)

Run Number	Configuration	K_p	T_L	τ	$Y_p Y_c$	$Y_p Y_c$ (REF. 11)
671129-3	$\frac{2.15}{s(s+4)}$	6.44	.331	.276	$\frac{4.58(s+3.02)e^{-.276s}}{s(s+4)}$	$\frac{4.2}{s}e^{-.25s}$
671129-1	$\frac{2.15}{s(s+2)}$	2.44	.89	.284	$\frac{4.67(s+1.12)e^{-.284s}}{s(s+2)}$	$\frac{4.2}{s}e^{-.264s}$
671009-7	$\frac{2.15}{s(s+1)}$	2.41	.626	.280	$\frac{3.24(s+1.6)e^{-.28s}}{s(s+1)}$	$\frac{3.4}{s}e^{-.294s}$
671129-15	$\frac{1.17}{s^2}$	1.500	1.81	.316	$\frac{1.76(1.81s+1)e^{-.316s}}{s^2}$	$\frac{.66}{s^2}(5s+1)e^{-.3s}$*

*Based on the inferred values in Reference 11 of T_L = 5.0 seconds.

The following table presents a comparison of the crossover frequency and phase margin that were obtained from the linear regression analysis with the data presented in Reference 11 for the configurations analyzed:

		REGRESSION ANALYSIS		REFERENCE 11		
λ	Run Number	ω_c (rad/sec)	ϕ_M (deg)	ω_c (rad/sec)	ϕ_M (deg)	ϕ_M^* (deg)
4	671129-3	4.07	33.3	4.2	26	29.8
2	671129-1	4.38	29.0	4.2	24	26.5
1	671009-7	3.44	26.0	3.4	16	32.7
0	671129-15	3.22	22.0	3.3	20	29.8

ϕ_M^* is the value of phase margin previously computed using the "measured" values of τ_L , τ and ω_c of Reference 11. Thus although the values of ω_c , τ and phase margin are reasonably similar (using the regression analysis techniques) to those presented in Reference 11, the values of τ_L are significantly different. This data has been examined to indicate that it is quite difficult to correlate pilot rating with lead equalization due to the values of lead that can be otbained from "measured" data. Thus, measurement techniques and the identification of pertinent pilot parameters obviously require more refinement then the techniques possibly used in Reference 11, although representative values of crossover frequency and phase margin were obtained. The results of this analysis are similar to those published in other references (e.g. Reference 13). That is, there is a band of rating decrement with pilot lead equalization. If we just select the $K_\theta/s(s+\lambda)$ configurations evaluated for the task (1.88 rad/sec, 1.0 cm/sec), the following table summarizes the results of the various lead values measured and computed:

		REF. 11			PILOT RATING	
Run Number	λ (1/sec)	τ_L (sec)	τ_L^* (sec)	τ_L^{**} (sec)	C	CH
671129-3	4	.25	.219	.331	4	A4.5
671129-1	2	.50	.449	.89	4	A4.5
671129-13	1	1.0	1.280	--	5.5	A5.5
671009-7	1	1.0	.451	.626	5.0	A5.5

NOTE: τ_L^* as previously computed using PM equation and "measured" values for PM, ω_c , τ ; while τ_L^{**} are values computed by regression analysis.

Figure 64 presents the data obtained from the regression analysis procedures in the closed-loop parameter plane (M_p , $\tan^{-1}(T_L \omega_B)$). Included with the analyzed configurations is run number 11-5 (K_B/s), with T_L = 0. The required values of bandwidth were obtained from the regression functions previously presented on the table on page 146. In addition, the bandwidth associated with the fit that is implied by Reference 11 for $Y_p Y_c$ is also shown. Comparison to figures obtained from the simplified Nichols chart analysis previously presented in this section can be made by examination of the data presented on Figure 64 with the data for the appropriate configuration on Figures 58 and 59, and in the tables previously presented in this section. Essentially, Figure 64 indicates that Level 1 pilot ratings for the task used in Reference 11 could be obtained for $M_p \leq 5.0$, T_L = 0.0. The remaining data (that was analyzed) indicates that for $M_p > 7.0$ and $\tan^{-1}(T_L \omega_B) > 50^\circ$, the best that could be expected is Level 2 pilot ratings for the task used. This analysis has been presented to illustrate some of the difficulties that occur when attempting to specifically correlate pilot rating with lead equalization. Figure 64 indicates that these difficulties can be somewhat overcome, especially when a region in the parameter plane of M_p and $\tan^{-1}(T_L \omega_B)$ can be associated with a pilot rating, and that the regions appear to be relatively self-contained regardless of computational problems in the determination of the exact value of lead equalization. In addition, this last figure indicates that with sufficient "measured" pilot data and appropriate tasks it may be possible to determine the appropriate regions in the closed-loop parameter plane (M_p , $\tan^{-1}(T_L \omega_B)$) that can be related directly to levels of flying qualities. Sufficient time and money were not available to analyze the remaining configurations of Reference 11 by regression techniques.

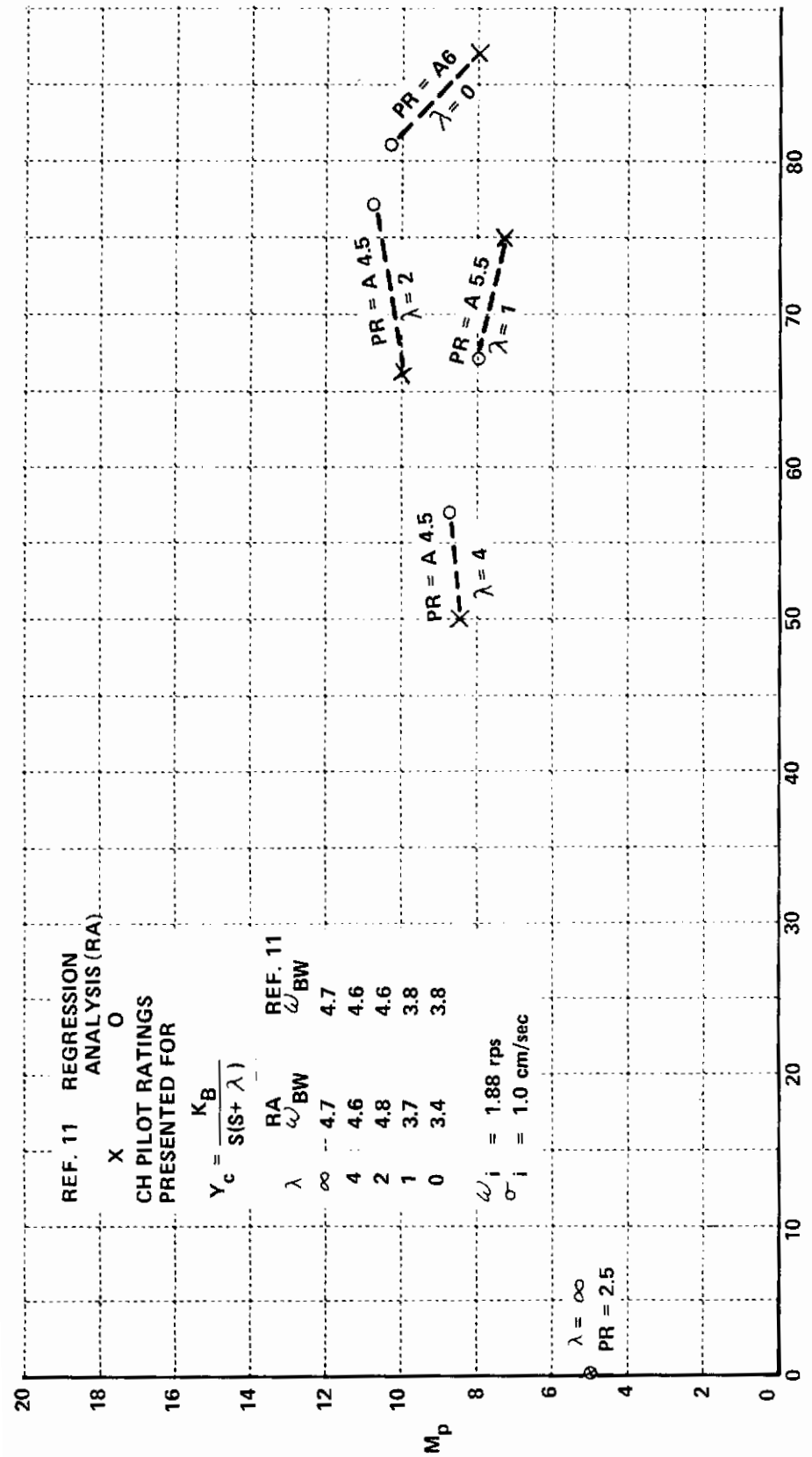

Figure 64 PILOT RATING AS A FUNCTION OF CLOSED-LOOP PARAMETERS FROM "MEASURED" PILOT LEAD EQUALIZATION

3.5 CONCLUSIONS AND RECOMMENDATIONS FROM HOVER AND LOW SPEED EXPERIMENT AND ANALYSIS

(1) In general, the results of the recent UARL investigation tend to substantiate the present hover and low-speed flight requirements of MIL-F-83300.

(2) Attempts to correlate "open-loop" parameters (ω_{BEF} and $\Delta\phi$) with pilot ratings for tasks and transfer functions associated with hover and low speed flight were quite satisfactory.

(3) Further investigations and correlation studies are warranted to examine the influence of control power, task, displays, and turbulence effects on the "open-loop" parameters associated with the transfer functions appropriate to hover and low-speed flight.

(4) Additional investigations are required to systematically examine the transfer functions which are representative of VTOL, STOL and V/STOL aircraft, including possibly higher-order augmentation and control systems, using open-loop parameters.

(5) The effects of transition from hover and low speed to forward flight should be investigated using the open-loop parameters as correlation parameters. This examination should be performed to formulate the redefinition of MIL-F-83300 and the transition of requirements from MIL-F-83300 to MIL-F-8785B(ASG).

(6) Since open-loop parameters are not necessarily unique, investigations should be performed to determine the "optimum" parameters that should be used for specifications (e.g. phase margin as opposed to $\Delta \phi$).

(7) The influence of closed-loop parameters using simple pilot-models should be investigated systematically using the techniques illustrated in this report for more complex transfer functions.

(8) The data examined in this report indicates that unrealistic task requirements can impose constraints which increase pilot workload with an associated degradation in task performance and pilot rating, for systems which are in general acceptable for the mission.

(9) The closed-loop analysis performed indicates that pilot lead equalization to achieve pole-zero cancellation is not necessarily a "best" choice, and that pilot equalization strategy can be severely compromised by imposing unrealistic tasks in the experiment.

(10) The open-loop phase margin of the pilot-aircraft system is directly indicative of closed-loop resonance amplitude for the low order controlled elements examined.

(11) Attempts to determine pilot closed-loop equalization parameters from regression techniques indicate that further work is required to measure and identify properly such parameters as T_L , τ and K_p .

(12) The data examined in this report indicates that it is questionable to attempt to correlate pilot rating directly with lead equalization. However, the use of the closed-loop parameter plane (M_p, $\tan^{-1}(\tau_L \omega_B)$) tends to minimize some of the computational problems in the measurement of pilot-model parameters for correlation with pilot ratings.

(13) Further investigations should be performed to systematically develop the relationships between open-loop parameters (e.g. ω_{REF} and $\Delta\phi$) and closed-loop parameters (e.g. M_p and $\tan^{-1}(\tau_L \omega_B)$) that correlate with pilot ratings for the appropriate tasks and transfer functions. In addition, the results of these correlation studies should be compared to other analytical pilot rating techniques (e.g. "paper-pilot") prior to recommending revisions to MIL-F-83300.

LIST OF REFERENCES

1. Anon.: "Military Specification -- Flying Qualities of Piloted V/STOL Aircraft" , MIL-F-83300, December 1970.

2. Chalk, C.R., D.L. Key, J.Kroll, Jr., R. Wasserman and R.C. Radford: "Background Information and User Guide for MIL-F-83300 -- Military Specification -- Flying Qualities of Piloted V/STOL Aircraft," AFFDL-TR-70-88, February 1971.

3. Key, D.L. and R.C. Radford: "CAL Test Plan for STOL Landing Approach Simulation at AFFDL", Calspan VTOL H.Q. Technical Memorandum No. 31, 11 February 1971.

4. Key, D.L. and J. Kroll, Jr.: "Calspan Experiment Design for NRC In-Flight Simulation of STOL Longitudinal Characteristics in Landing Approach", Calspan VTOL H.Q. Technical Memorandum No. 35, 22 January 1973.

5. Kroll, John Jr.: "Calspan Experimental Design of NRC In-Flight Simulation of STOL Longitudinal Characteristics in Landing Approach", Calspan VTOL H.Q. Technical Memorandum No. 35, Addendum A, 8 March 1973.

6. Doetsch, K-H. and D.W. Laurie-Lean: "The Flight Investigation and Analysis of Longitudinal Handling Qualities of STOL Aircraft on Landing Approach", AFFDL-TR-74-18, March 1974.

7. Vinje, E.W. and D.P. Miller: "Flight Simulator Experiments and Analysis in Support of Further Development of MIL-F-83300 -- V/STOL Flying Qualities Specification", AFFDL-TR-73-74, July 1973.

8. Key, D.L. , R.C. Radford and R.T.C. Chen: "First Interim Report on Program to Improve MIL-F-83300", Calspan Report No. AD-5013-F-1, May 1972.

9. Anon.: "Military Specification -- Flying Qualities of Piloted Airplanes", MIL-F-8785B(ASG), August 1969.

10. Smith, R.E., J.V. Lebacqz, and J.M. Schuler: "Flight Investigation of Various Longitudinal Short-Term Dynamics for STOL Landing Approach Using the X-22A Variable Stability Airplane", Calspan Report No. TB-3011-F-2, January 1973.

11. McDonnell, J.D.: "Pilot Rating Techniques for the Estimation and Evaluation of Handling Qualities", AFFDL-TR-68-76, December 1968.

12. McRuer, D. and D. Graham: "Human Pilot Dynamics in Compensatory Systems", AFFDL-TR-65-15, July 1965.

13. McRuer, D.T. and H.R. Jex: "Effects of Task Variables on Pilot Models for Manually Controlled Vehicles", Paper presented at AGARD Meeting, Cambridge, England, September 1966.

14. Neal, T.P. and R.E. Smith: "An In-Flight Investigation to Develop Control System Design Criteria for Fighter Airplanes", AFFDL-TR-70-14, June 1970.

15. Chalk, C.R., D.A. Di Franco, J.V. Lebacqz and T.P. Neal: "Revisions to MIL-F-8785B(ASG) Proposed by Cornell Aeronautical Laboratory Under Contract F33615-71-C-1254", AFFDL-TR-72-41, April 1973.

16. Di Carlo, Daniel J., James R. Kelly and Robert W. Sommer: "Flight Investigation to Determine the Effect of Longitudinal Characteristics on Low-Speed Instrument Operation", NASA TN D-4364, March 1968.

17. Wasserman, R. et al.: "In-Flight Simulation of Minimum Longitudinal Stability for Large Delta-Wing Transports in Landing Approach and Touchdowns", AFFDL-TR-72-143, Vol. I and II, February 1973.

18. Vinje, Edward W. and David P. Miller: "Analytical and Flight Simulator Studies to Develop Design Criteria for VTOL Aircraft Control Systems", AFFDL-TR-68-165, April 1969.

19. Anon.: "Recommendations for V/STOL Handling Qualities", AGARD Report No. 408A, 1962.

20. Chen, Chih-Fan and I. John Haas: "Elements of Control Systems Analysis: Classical and Modern Approaches", Prentice-Hall Publishing Company, Inc. 1968.

21. Melsa, James L. and Donald G. Schultz: "Linear Control Systems", McGraw-Hill Book Company, 1969.

22. Wasserman, Richard and Paul R. Motyka: "In-Flight Investigation of the B-1 Control System", AFFDL-TR-73-139, December 1973.

$d\gamma/dV$	ratio of steady state flight path angle change with velocity in response to an elevator control input, degrees/knot
F_{ES}	cockpit elevator control force, pounds
g	acceleration due to gravity, feet/second^2
$\|G\|$	amplitude ratio of open-loop transfer function
h	altitude, feet
$\dot{h}$	rate of change of altitude, feet/second^2
$(\dot{h}/u)_{\delta_{ES}}$	ratio of altitude rate to velocity in response to cockpit elevator control command
$\|H\|$	amplitude ratio of closed-loop transfer function
$H(s)$	closed-loop transfer function
i	imaginary part, $= \sqrt{-1}$, input task
K	crossover gain, system gain
L_p	change in body axes roll acceleration with roll rate, sec^{-1}-rad^{-1}
L_{δ_a}	change in body axis roll acceleration with aileron control input, sec^{-2} rad^{-1}
L_ϕ	change in body axis roll acceleration with roll attitude, sec^{-1} rad^{-1}
M_p	magnitude of closed-loop resonant peak dB

M_q change in body axis pitch acceleration with pitch rate, sec^{-1} rad^{-1}

M_w change in body axis pitch acceleration with vertical velocity, sec^{-1} ft^{-1}

M_{δ_c} change in body axis pitch acceleration with collective control input, sec^{-2}-in. rad^{-1}

M_{δ_e} change in body axis pitch acceleration with elevator surface deflection, sec^{-2} rad^{-1}

M_{δ_T} change in body axis pitch acceleration with thrust control input, sec^{-2} $in.^{-1}$

M_θ change in body axis pitch acceleration with pitch attitude, sec^{-2}

n_z/α steady state normal acceleration change per unit change in angle of attack for an incremental elevator control deflection at constant speed, g/rad

N_r change in body axis yaw acceleration with yaw rate, sec^{-1} rad^{-1}

N_{δ_r} change in body axis yaw acceleration with rudder surface deflection, sec^{-2} rad^{-1}

s Laplace operator

T_I pilot control lag compensation time constant, sec

$1/T_{h_1}$ the lowest frequency zero in the altitude to elevator transfer function numerator, sec^{-1}

T_L pilot control lead compensation time constant, sec

T/W thrust to weight ratio

u_g longitudinal velocity component of atmospheric turbulence, ft/sec

$(u/\dot{h})_{\delta_T}$ transfer function of longitudinal speed change with rate of change of altitude in response to thrust magnitude control input

u/θ transfer function of longitudinal speed change with altitude in response to elevator control input, ft/rad-sec

v_g lateral velocity component of atmospheric turbulence, ft/sec

V airspeed, ft/sec

V_{con} the speed which determines the upper limit of applicability of the requirements of MIL-F-83300 and the lower limit of applicability of the requirements of MIL-F-8785, ft/sec

X component of aerodynamic forces along the x-body axis, lb

X_u change in body axis X -acceleration with longitudinal velocity, sec^{-1}

X_w change in body axis X -acceleration with vertical velocity, sec^{-1}

Y_c controlled element transfer function

Y_p pilot model transfer function

$|Y_pY_c|$ magnitude of open-loop pilot and controlled element transfer functions

$Y_{p_{\dot{h}}}$ transfer function representation of pilot generated attitude command in response to perceived altitude rate error, $rad/ft\text{-}sec^{-1}$

Y_{p_u} transfer function representation of pilot generated attitude command in response to perceived velocity error, rad/ft-sec^{-1}

Y_{p_v} transfer function representation of pilot's collective control input in response to perceived longitudinal velocity error, in.-sec/ft

Y_{p_θ} transfer function representation of force applied by pilot to cockpit elevator control in response to perceived attitude error, lb/rad

Y_v change in body axis Y -acceleration with lateral velocity, sec^{-1}

Z component of aerodynamic forces along the z -body axis, lb

Z_u change in body axis Z -force with longitudinal velocity, sec^{-1}

Z_w change in body axis Z -force with vertical velocity, sec^{-1}

Z_{δ_e} change in body axis Z -force with elevator surface deflection sec^{-2} rad^{-1}

Z_{δ_T} change in body axis Z -force with cockpit thrust magnitude control, ft/sec^{-2}-in.

γ_g glide slope angle with respect to the ground, rad

δ first order root of longitudinal characteristic equation, sec^{-1}

δ_c cockpit collective control input, in.

ζ damping ratio

θ pitch attitude, rad

θ/δ_{ES} transfer function representation of attitude response to cockpit elevator control input, rad/in.

ϕ_M open-loop phase margin (PM), deg

ϕ/δ_a transfer function of roll angle to aileron

$\phi(\omega)$ phase angle of open-loop transfer function, deg

ω_B closed-loop bandwidth frequency, rad/sec

ω_c open-loop gain crossover frequency, rad/sec

ω_i forcing function input bandwidth, rad/sec

ω_n undamped natural frequency, rad/sec

ω_p closed-loop resonant frequency, rad/sec

ω_{REF} reference frequency, rad/sec

λ_i first order root of the transfer function of i, i = w, θ, ϕ, ψ, sec^{-1}

σ root mean square value

τ numerator or denominator time constant, or pilot-induced time delay, sec

Subscripts

c	command or controlled element
CL	closed-loop
h	altitude
i	input forcing function
m	model
p	pilot
SAS	stability augmentation system
SP	short period
SS	steady state
ϵ	error between commanded response and actual response

Abbreviations

C	Cooper Rating Scale
C-H	Cooper-Harper Rating Scale
GM	gain margin
IFR	instrument flight rules
ILS	instrument landing system
IVSI	instantaneous vertical speed indicator
NRC	National Research Council of Canada
PM	phase margin
PR	pilot rating
VFR	visual flight rules
VSI	vertical

☆U.S.Government Printing Office: 1974 — 657-015/197